THE ROLE AND MOLECULAR MECHANISM OF HMGN PROTEINS IN GLOBAL GENOME REPAIR AFTER UV IRRADIATION

A DISSERTATION

SUBMITTED IN PARTIAL FULFILLMENT OF REQUIREMENTS FOR THE

DEGREE OF DOCTOR OF PHILOSOPHY

IN THE GRADUATE SCHOOL OF THE

TEXAS WOMAN'S UNIVERSITY

COLLEGE OF ARTS AND SCIENCES

BY

MANGALAM SUBRAMANIAN, B. Sc., M. Sc.

DENTON, TEXAS

DECEMBER 2009

TEXAS WOMAN'S UNIVERSITY

DENTON, TEXAS

November 13, 2009

To the Dean of the Graduate School:

I am submitting herewith a dissertation written by Mangalam Subramanian entitled "The Role and Molecular Mechanism of HMGN Proteins in Global Genome Repair After UV Irradiation." I have examined this dissertation for form and content and recommend that it be accepted in partial fulfillment of the requirements for the degree of Doctor of Philosophy with a major in Molecular Biology.

Michael Bergel, Ph. D., Major Professor

We have read this dissertation and recommend its acceptance:

Heather Conrad-Webb

Pamela Padilla

Nathaniel Mills

Sarah A. McIntire

Department Chair

Accepted:

Jennifer Martin

Dean of the Graduate School

ACKNOWLEDGEMENTS

It will be apt to start with expressing my sincere and heartfelt gratitude to Dr. Michael Bergel who has been my mentor, guide, constant source of inspiration and a pillar of strength throughout my Ph.D. journey. I had the privilege to be his first Ph.D. student and had the rare opportunity of setting up the lab right from its inception. He has provided me with many helpful suggestions, important advice and constant encouragement during the course of this work. He was instrumental in grooming me into a young scientific investigator.

I express my sincere gratitude to Dr. Sarah McIntire, Chair of the Department of Biology, for many valuable suggestions and constructive advice, especially for encouraging me to take up leadership roles and nominating me for some of the most prestigious scholarships.

I am indebted to all my committee members, Dr. Heather C. Webb, Dr. DiAnna Hynds, Dr. Nathaniel Mills and Dr. Pam Padilla for taking out their valuable time and efforts to give their critical inputs. They have supported me in all my endeavors.

I wish to express my sincere gratitude to Ms. Reta (Smiddy) Foreman for her continuous support during my teaching assignments.

I want to express my appreciation to Dr. Rene Paulson (Biostatistician, TWU) for her advice and assistance in my doctoral work.

This journey could not have been completed but for the continuous support and cooperation of my colleagues in the laboratory. I like to thank my graduate colleagues in the lab; Ms. Rhiannon W. Gonzalez, Ms. Hemangi Patil, Ms. LaTondra Lawrence, Mr. Sudheer Dhanireddy, and Ms. Carrie Wilks. I also extend my sincere appreciation for the efforts put in by Ms. Sheba John and Ms. Leah BeCoats, the undergraduate students who worked under my supervision. I must express my sincere appreciation to Ms. Rhiannon W. Gonzalez, Ms. Hemangi Patil and Mr. Sudheer Dhanireddy for their contribution towards publication of my first article in FEBS J., 2009. Special thanks to Ms. Gunisha Sagar for her invaluable friendship and advice.

My sincere gratitude to the Former Student's Association and the Board of Regents, TWU for their scholarships provided during my educational career.

My sincere thanks to Ms. Petrucci for arranging timely supply of materials required for the lab.

My special thanks to my older brother Mr. Raman Subramanian and my sister-in-law Ms. Lakshmi Raman for their support.

Finally, I would express special thanks to my mother Mrs. Mythili Subramanian, father Mr. V. R. Subramanian and my other older brother, Mr. Jambunathan Subramanian for their active support, encouragement and help, without which, this study would not have been completed.

ABSTRACT

MANGALAM SUBRAMANIAN

THE ROLE AND MOLECULAR MECHANISM OF HMGN PROTEINS IN GLOBAL GENOME REPAIR AFTER UV IRRADIATION

DECEMBER 2009

High Mobility Group Nucleosomal Binding proteins (HMGNs) are a family of non-histone proteins that unfold chromatin by interacting with histone tails, competing with histone H1, and modulating post-translational modification of histones. By virtue of these architectural chromatin changes, HMGNs regulate transcription, replication and DNA repair. Nucleotide excision repair is a major DNA repair pathway that removes bulky DNA adducts caused by ultraviolet (UV) irradiation. The chromatin structure restricts the access of repair complexes to DNA lesions, and, therefore, remodeling and unfolding the chromatin is essential. We found that HMGN null cells (derived from DT40 chicken cells) were sensitive to UV irradiation. These cells also had a high apoptotic rate and a prolonged arrest in the G_2/M and mitotic phases following UV irradiation. Moreover, UV-hypersensitive HMGN null cells showed low cyclobutane pyrimidine dimers (CPD) removal rates as compared to the wild-type cells. These results demonstrate the functional significance of HMGN proteins in nucleotide excision repair– global genome repair (NER-GGR). A global wave of core histone deacetylation peaking 4 hours after UV irradiation was observed in chicken and

human cell lines. Following the nadir of acetylation, the acetylation levels gradually returned to the pre-UV steady state levels. We demonstrated that the wild-type cells but not HMGN1a/N2 null cells had a global increase in acetylation of histones H4K5 and H3K9 48 hours after UV irradiation. At 72 hours after UV irradiation H3K14 acetylation increased, a phenomenon that happened also in HeLa cells 24 hours after UV irradiation. Immunoprecipitations of HMGN1 from HeLa cells followed by histone acetyltransferase (HAT) assays demonstrated an associated HAT activity before UV irradiation and at 10 hours and 24 hours after UV irradiation. By co-immunoprecipitation assays, we showed that before UV irradiation and 2 minutes after UV irradiation, HMGN1 associated with p300, and 10 minutes and 24 hours following UV irradiation, HMGN1 associated with CBP. These results showed that HMGNs are involved in NER-GGR, but the association of HMGNs to p300/CBP and to the HAT-activity did not correlate with the peak of the CPD removal, indicating that HMGNs are involved in NER-GGR by HAT-dependent and independent pathways.

TABLE OF CONTENTS

Page

ACKNLOWLEDGEMENTS iii

ABSTRACT vi

LIST OF TABLES xi

LIST OF FIGURES xii

Chapters

I. INTRODUCTION 1

The Cellular Response to UV Irradiation 1
Signaling Pathways Activated Upon UV Irradiation 1
Apoptosis versus DNA Repair 2
ATM/ATR Response 3
DNA Repair Mechanisms and Focus on NER-GGR 4
Causes of DNA Damage 4
Types of DNA Damage 5
Subpathways and Various Components of NER 6
Impairment in NER 9
Chromatin 10
Chromatin Structure 10
NER Meets Chromatin 10
Rearrangement of Chromatin Structure During NER Repair 12
ATP-dependent Chromatin Modifying Enzymes 12
HATs/HDACs 13
HATs 13
Acetylation of Histones and Non-histones by HATs 13
Deacetylation of Histones 15
Role of HMGNs in NER 16
HMG Chromatin Proteins-HMGA, HMGB, and HMGN 16
Functional Significance of HMGNs 16
Our Research Questions and Research Hypotheses 18

HMGN Null Cells – a Tool Used for the Study 19
HMGN1a and HMGN2 Null Cells are Viable 20

II. MATERIALS AND METHODS 21

Maintenance of Chicken HMGN Null Cell Lines 21
Derivation of HeLa HMGN1 Tag Cell Lines 21
Maintenance of HeLa HMGN Tag Cell Lines 22
UV Survival Assay 22
Growth Curve of DT40 and DT40 Derivative Chicken Cells 23
Southwestern Analysis of Photoproduct Levels 23
Apoptosis Studies in Chicken HMGN Null Cells 24
Cell Cycle Analysis 25
Western Blot Assays for Cell Cycle Analysis 26
Histone Post-translational Modifications in Chicken Lymphoblasts, Post-UV Irradiation 27
Histone Post-translational Modifications in UV Irradiated HeLa Cells 28
Analysis of HeLa HMGN Clones 28
HAT Assay of HMGN1 Immunoprecipitate Following UV Irradiation 29
Co-Immunoprecipitation Assay 30
CPD Removal Rate of HMGN Null cells With and Without Trichostatin A 32

III. RESULTS 34

Experiment 1: HMGN1a and HMGN2 Null Mutants are Hypersensitive to UV Irradiation 34
Experiment 2: Growth Curve of Chicken HMGN1a and HMGN2 Mono Knockout and Double Knockout Cells at 37°C 38
Experiment 3: Decreased Rate of Cyclobutane Pyrimidine Dimers Removal in Cells Lacking Either HMGN2 or Both HMGN1a and HMGN2 Proteins 43
Experiment 4: UV-Hypersensitive HMGN2 and HMGN1a/N2 Null Cells Have a Higher Apoptosis Rate Than the Wild-type Cells 46
Experiment 5: Loss of HMGN2 or HMGN1a and HMGN2 Increases G_2/M Checkpoint Arrest Following UV Irradiation 50
Experiment 6: Cells Lacking HMGN2 or Both HMGN1a and HMGN2 Show Prolonged G_2/M Arrest and Early Mitotic Arrest in HMGN1a and HMGN2 Double Null Cells 53

Experiment 7: Study of Core Histone Post-translational Modifications in Chicken HMGN1a-/-; N2-/- Cells Following UV Irradiation 58
Experiment 8: Core Histone Post-translational Modifications in HeLa Cells Following UV Irradiation 65
Experiment 9: Isolation of HMGN1 Overexpressing Clones for Co-immunoprecipitation 69
Experiment 10: HAT Assay of HMGN1-Immunoprecipitate Following UV Irradiation 71
Experiment 11: Co-immunoprecipitation Assay of HAT and HMGN1 Proteins 75
Experiment 12: HMGN Null Cells Remove CPDs from DNA in a HAT-Independent Manner 80

IV. DISCUSSION 84

HMGN1a and HMGN2 are in the Same Pathway in UV-induced DNA Damage Response 85
HMGN1a/N2 are Involved in Global Genome Repair 87
HMGNs Modulate PTMs After UV Irradiation 89
HMGN1 Associates With HAT Proteins 94
HMGN1 is Involved in NER-GGR in HAT-independent Manner 96
Mechanism of HMGN1 Involvement in NER-GGR 97

REFERENCES 100
APPENDIX 111
LIST OF ABBREVIATIONS 112

LIST OF TABLES

Table Page

1. LD_{50} of UV irradiated wild-type DT40 cells and DT40 derived null HMGN cell lines 36
2. Saturation density and doubling time of wild-type and HMGN1a/N2 null cells grown at 37°C 40
3. Represents statistically significant doubling time and saturation densities of HMGN null chicken cells from the growth curve analysis 42
4. Higher UV-induced apoptosis rate in HMGN2-/- and HMGN1a-/-; N2-/- cells 49
5. Expression levels of HMGN1-HA protein in stably transfected HeLa cells 71
6. Folds of acetylation of H4K5ac relatively to non-Immune IgG (control1) 74

LIST OF FIGURES

Figure Page

1. Two major types of DNA damages caused by UV irradiation 6
2. Two subpathways of mammalian NER..... 7
3. HMGN1a/N2 null cell lines derived from the DT40 lymphoblastoid chicken cells 20
4. Chicken cells that lack HMGN1a, HMGN2 or both HMGN1a and HMGN2 are hypersensitive to UV irradiation..... 36
5. Growth curves of DT40 and DT40 derived HMGN1a or HMGN2 null cell lines at 37°C 39
6. A decreased rate of cyclobutane pyrimidine dimers removal in cells lacking HMGN proteins 44
7. Higher UV-induced apoptosis rate in HMGN2-/- and HMGN1a-/-;N2-/- cells..... 48
8. UVC-induced G_2/M or mitotic arrest in HMGN2-/- and HMGN1a-/-;N2-/- cells..... 51
9. Prolonged G_2/M checkpoint arrest and high mitotic arrest in HMGN1a-/-;HMGN2-/- cells..... 55
10. Quantification of G_2/M checkpoint arrest in chicken HMGN null cells..... 56
11. Quantification of mitotic checkpoint arrest in chicken HMGN null cells..... 57
12. The effect of UV irradiation on post-translational modifications of histones H3 and H4 in wild-type and HMGN1a/N2 null chicken cells 60
13. Kinetics of acetylation of histone H4 lysine 5 (H4K5ac) post-UV irradiation in wild-type DT40 and HMGN1a/N2 null chicken cells 61
14. Kinetics of acetylation of histone H3 lysine 9 (H3K9ac) post-UV irradiation in wild-type DT40 and HMGN1a/N2 null chicken cells 62
15. Kinetics of acetylation of histone H3 lysine 14 (H3K14ac) post-UV irradiation in wild-type DT40 and HMGN1a/N2 null 3 chicken cells 63
16. Kinetics of histone H3 lysine 9 trimethylation (H3K9me3) post-UV irradiation in wild-type DT40 and HMGN1a/N2 null chicken cells 64

17. UV irradiation induces a rapid and global wave of deacetylation of core histones in HeLa cells 66
18. UV irradiation induces a rapid global wave of deacetylation of core histones H3 and H4 in HeLa cells (quantification) 67
19. Analysis of the expression levels of HMGN1-HA in various stably transfected HeLa cell clones 70
20. HAT activity is associated with immunoprecipitated HMGN1 74
21. Goat- and rabbit-antibodies against human HMGN1 can efficiently precipitate HMGN1 in IP experiments 76
22. p300 and HMGN1 are associated with each other before and after UV irradiation in HeLa cells 77
23. CBP and HMGN1 are associated with each other after UV irradiation in HeLa cells 78
24. p400 and HMGN1 do not associate with each other before or after UV irradiation 79
25. TSA treated HMGN null chicken cells show slow DNA repair rate similar to the untreated cells 82
26. Proposed model for HMGN1's involvement in NER-GGR 99

CHAPTER I

INTRODUCTION

The Cellular Response to UV Irradiation

Signaling Pathways Activated Upon UV Irradiation.

A major adverse effect of ultraviolet (UV) radiation on cells is damage to DNA caused primarily by pyrimidine dimers, leading to either cell death or somatic mutations, which are thought to be one of the initial steps of neoplastic transformation. However, UV irradiation not only leads to the destruction of cellular integrity, but also induces specific cellular reactions. This induction response, known as the "mammalian UV response", is characterized by transcriptional activation or repression of a specific set of genes, gene amplification, an increase in the rate of recombination and the induction of endogenous viruses (Ronai *et al.*, 1990; Herrlich *et al.*, 1992). Among the first gene products that are activated via increased transcription and or post-translational modification (PTM) are the tumor suppressor protein p53 and several transcription factors encoded by the class of immediate early genes, such as c-*myc*, *egr*-1, NF-κB, $p62^{TCF}$/*elk*-1, and c-*fos* and c-*jun*, components of the dimeric transcription factor AP-1 (Herrlich *et al.*, 1992). Mammalian UV response is mediated by AP-1 which is involved in a protective function other

than the repair (Devary *et al.*, 1992; Engelberg *et al.*, 1994). Most DNA damaging agents, including UV radiation, are known to damage other cellular components such as the membrane lipids, proteins, RNAs and ribosomes. Schreiber and others showed that the transcription factor c-Fos is an essential component of the cellular defense mechanism against the cytotoxic effects of UVC irradiation (Schreiber *et al.*, 1995). Cells lacking c-Fos are hypersensitive to UV irradiation, but are fully capable of repairing UV-damaged DNA, demonstrating that functions of the UV response other than DNA repair are indeed relevant to the survival of mammalian cells (Schreiber *et al.*, 1995).

Apoptosis Versus DNA Repair.

In addition to cellular response to UV, other pathways are activated upon UV irradiation which occurs in the nucleus (Schreiber *et al.*, 1995). Damage to DNA induces several cellular responses that enable the cell either to eliminate or cope with the damage, or to activate a programmed cell death process, presumably to eliminate cells with potentially catastrophic mutations. These DNA damage response reactions include: (a) removal of the DNA damage and restoration of the continuity of the DNA duplex; (b) activation of a DNA damage checkpoint, which arrests cell cycle progression to allow the repair and prevent the transmission of damaged or incompletely replicated chromosomes; (c) transcriptional response, which causes changes in the transcription profile that may be beneficial to the cell; and (d) apoptosis, which eliminates heavily

damaged or seriously deregulated cells (Sancar *et al.*, 2004). DNA repair mechanisms include direct repair, base excision repair, nucleotide excision repair, double-strand break repair, and cross-link repair (Sancar *et al.*, 2004).

ATM/ATR Response.

DNA-damage checkpoints block progression through the cell cycle until the damage is repaired. ATM/ATR and Chk1/2 are tumor-suppressor proteins that normally function in the DNA damage checkpoints (Lodish, 2007). People with mutations in both copies of ATM and Chk2 develop cancers far more frequently than normal people (Lodish, 2007). Double-strand break formation resulting from collapse of replication forks is responsible for the activation of ATM and DNA- dependent protein kinases (DNA-PKcs kinases) catalytic subunit, which phosphorylate Chk2, thereby activating its kinase activity (Yajima *et al.*, 2009). Activated Chk2 then phosphorylates the Cdc25A phosphatase, marking it for polyubiquitination (Niida and Nakanishi, 2006). Degradation of Cdc25A leads to arrest in G_1 or S, by inactivation of cyclin-dependent kinases (Cdks) (Lodish, 2007).

Another tumor suppressor protein, p53, is essential for the G_1 checkpoint arrests, when the cells are exposed to DNA-damaging irradiation (Lodish, 2007). Unlike other cell-cycle proteins, p53 is present at very low levels in normal cells because it is extremely unstable and is rapidly degraded by Mdm2, an ubiquitin ligase (Lodish, 2007). Expression of p53 gene is heightened only in stressful

situations, such as UV or gamma irradiation, heat or low oxygen levels. DNA damage by gamma irradiation or by other stresses leads to the activation of ATM or ATR, resulting in phosphorylation, stabilization and marked increase in the concentration of p53 (Lodish, 2007). This leads to increase in p21, which inhibits all mammalian cyclin-CDKs (Lodish, 2007). If the DNA damage is limited and repairable, phosphorylation of p53 occurs at certain sites and the modified p53 activates genes related to cell cycle arrest and eventually DNA repair; for example p21, GADD45, and p53R2 (Nakamura, 2004). Under some circumstances, when cells suffer from extensive DNA damage, p53 also activates expression of pro-apoptotic proteins like Bax that leads to apoptosis, the process of programmed cell death (Nakamura, 2004).

DNA Repair Mechanisms and Focus on NER-GGR

Causes of DNA Damage.

The DNA is frequently damaged by a variety of environmental and endogenous agents produced as products or byproducts of physiological reactions (Ames *et al.*, 1993). DNA damage can be subdivided into two main types:

(1) endogenous damage such as attack by reactive oxygen radicals produced from normal metabolic byproducts. Reactive oxygen species (ROS) including H_2O_2, the $O_2^{-\cdot}$ radical and $OH^{\cdot}$ radical, which is widely believed to play a

critical role in the etiology of aging, many degenerative diseases and cancer (Ames *et al.*, 2003).

(2) exogenous damage includes external agents such as ultraviolet (UV 200-300 nm) radiation from the sun, other radiation frequencies including x-rays and gamma rays, hydrolysis or thermal disruption, certain plant toxins, human-made mutagenic chemicals such as hydrocarbons from cigarette smoke, and cancer chemotherapy and radiotherapy (Ura and Hayes, 2002).

Types of DNA Damage.

Some types of DNA damages are (Lodish, 2007; Watson, 2007):

(1) oxidation of bases [e.g. 8-oxo-7,8-dihydroguanine (8-oxoG)] and generation of DNA strand interruptions from reactive oxygen species.

(2) alkylation of bases (usually methylation) such as formation of 7-methylguanine.

(3) hydrolysis of bases such as depurination and depyrimidination.

(4) mismatch of bases due to DNA replication errors in which the wrong DNA base is added in the newly formed DNA strand.

Since repair systems must be capable of recognizing and dealing with each type of damage, it is not surprising that there are a number of different types of repair systems. Our research focuses on one such type of repair mechanism, nucleotide excision repair (NER). This repair mechanism enables the removal of a variety of bulky, DNA-distorting lesions, including UV-induced

cis-*syn* cyclobutane pyrimidine dimers (CPDs) and pyrimidine (6-4) pyrimidone photoproducts (6-4PPs) that induces a DNA bend or kink of 7-9° and 44°, respectively (Figure 1) (Kim and Choi, 1995; van Steeg and Kraemer, 1999; Ura and Hayes, 2002).

A. cyclobutane pyrimidine dimers (CPDs)

B. pyrimidine (6-4) pyrimidone photoproducts (6-4 PPs)

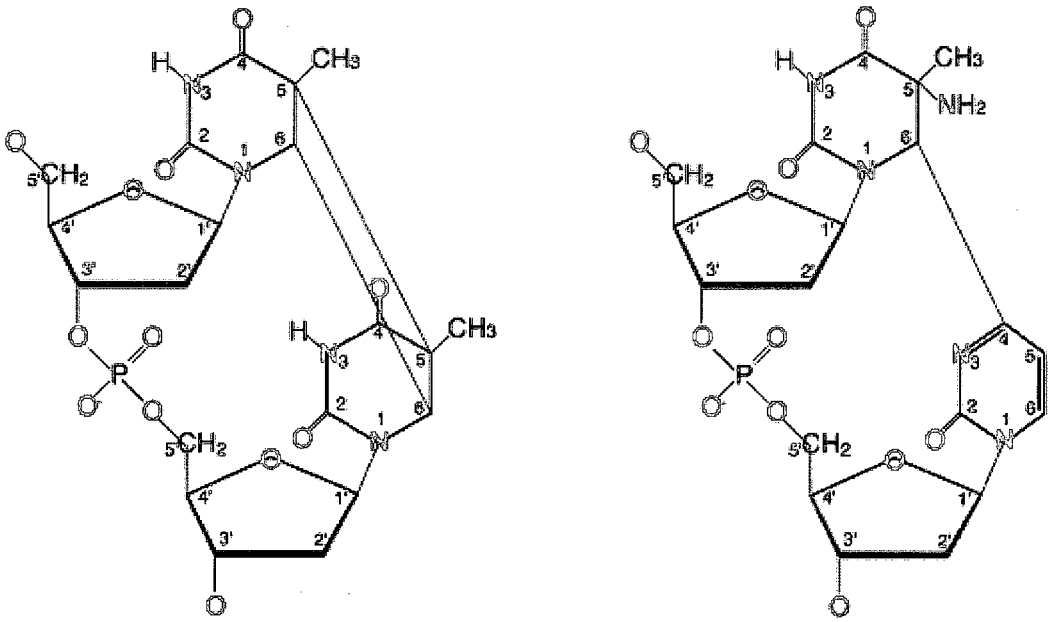

Figure 1. Two major types of DNA damages caused by UV irradiation. (http://asajj.roswellpark.org/huberman/DNA_Repair/damage_types.html)

Subpathways and Various Components of NER.

The process of NER incorporates two subpathways, transcription coupled repair (TCR) and global genome repair (GGR) (see Figure 2). TCR, as its name suggests, is a mechanism by which transcriptionally active genes are repaired.

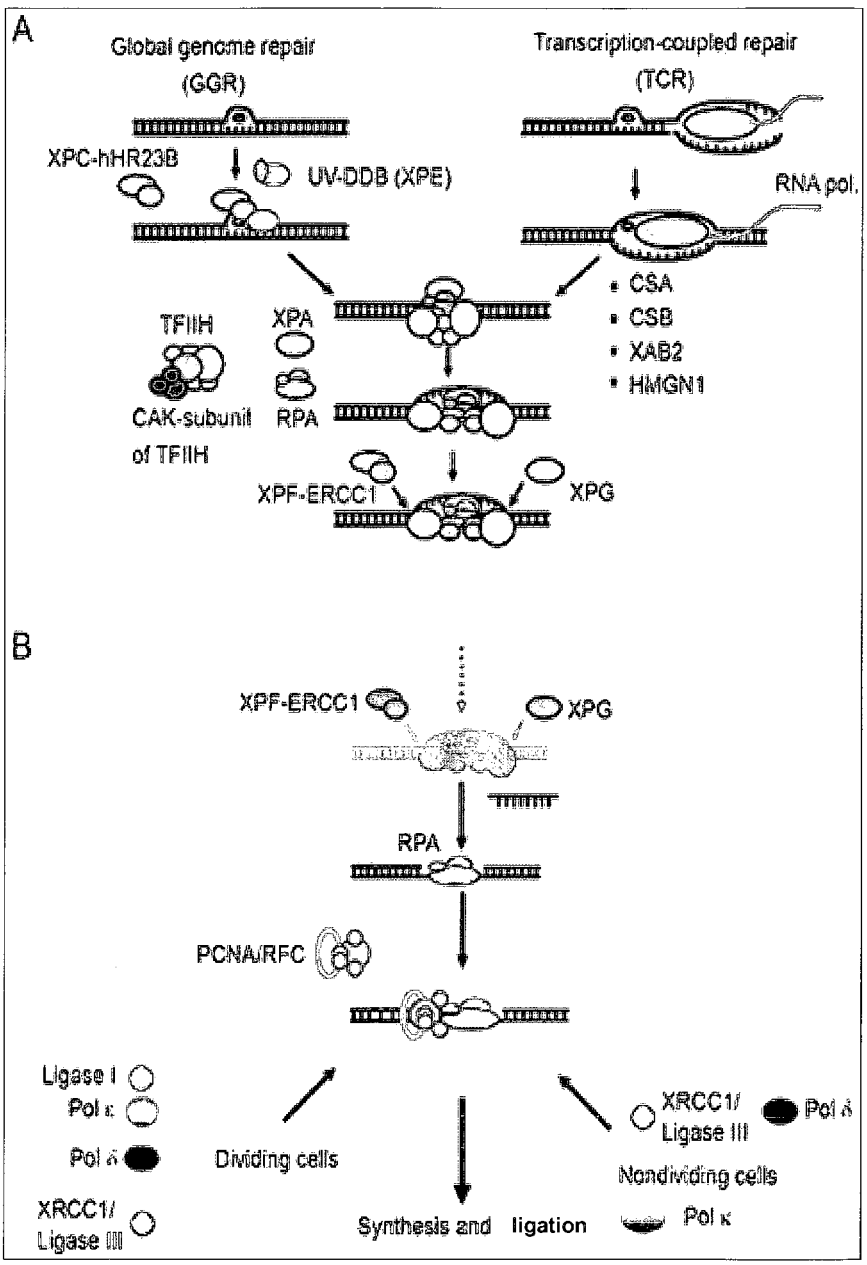

Figure 2. Two subpathways of mammalian NER (Fousteri and Mullenders, 2008). (A) Damage/distortion recognition in GGR-NER and TCR-NER. (B) Gap filling and ligation.

TCR removes 6-4PPs and CPDs efficiently from the transcribed strand of expressed genes (van Hoffen *et al.*, 1995; Ura and Hayes, 2002). On the other hand, GGR is transcription independent and removes lesions from the entire genome including the non-transcribed DNA strand genes (Ura and Hayes, 2002).

A major difference between the two modes of NER is in the damage recognition step. In transcription-coupled NER, damage recognition is mediated by RNA polymerase II (pol II) stalling at damage sites (Tornaletti and Hanawalt, 1999). In GGR-NER, the XPC along with hHR23b protein, play a key role in the recognition of DNA lesions (Sugasawa *et al.*, 1998; Riedl *et al.*, 2003). Even though the initial damage recognition step differs, both the pathways follow the same method of removing the bulky adduct.

NER works in the following manner, which is highly conserved in eukaryotes (Figure 2):

(1) Duplex DNA around the damaged site is unwound by helicase activities of transcription factor II H (TFIIH) in the presence of xeroderma pigmentosum proteins such as XPA, XPB, XPD and replication protein A (RPA) (Evans *et al.*, 1997a; Evans *et al.*, 1997b); (2) This open complex formation is a prerequisite for dual incision by two structure-specific endonucleases, xeroderma pigmentosum-Excision repair cross complementing protein 1 (XPF-ERCC1) and xeroderma pigmentosum G (XPG), at sites 5′ and 3′ of the lesion, respectively (O'Donovan *et al.*, 1994; Park *et al.*, 1995; Sijbers *et al.*, 1996); (3) The resulting

gap is filled by DNA polymerase (δ or ε), and the nick in the repaired DNA strand is rejoined by DNA ligase I.

There are more than 30 recognized proteins which participate in NER, some of which are proteins that also participate in transcription and replication (Aboussekhra *et al.*, 1995).

Impairment in NER.

Impairment in NER activity has been associated with at least three rare human autosomal recessive genetic disorders: xeroderma pigmentosum (XP), Cockayne syndrome (CS), and trichothiodystrophy (TTD). So far, seven NER-deficient XP complementation groups (XPA through XPG), two CS groups (CSA and CSB), and one TTD group (TTD-A) have been identified, and in all cases the responsible genes have been cloned (Nishi *et al.*, 2005). Other DNA repair disorders include Werner's syndrome (which is associated with premature aging and retarded growth), Bloom's syndrome (sunlight hypersensitivity, high incidence of malignancies especially leukemias) and ataxia telangiectasia (sensitivity to ionizing radiation and some chemical agents). All of the above diseases are often called "segmental progerias" (accelerated aging diseases), because their victims appear elderly and suffer from aging-related diseases at an abnormally young age (Ellis, 1997).

Chromatin

Chromatin Structure.

DNA is compacted and organized in chromatin in the eukaryotic nucleus. Organization of DNA into chromatin and chromosomal structures plays a central role in many aspects of cell biology and development in eukaryotes (Ehrenhofer-Murray, 2004). Folding of DNA in the chromatin structure is important, since it enables compression of 2-meter long DNA strand into a 10-micrometer size cell. The repeat unit of chromatin is the core nucleosome in which 146 base pairs of DNA are wrapped around the histone octamer that consists of two molecules each of the core histones H2A, H2B, H3 and H4 (Luger *et al.*, 1997; Ehrenhofer-Murray, 2004). Nucleosomal arrays along the DNA fold into a 30 nm fiber, upon incorporation of the linker histone H1. There are two kinds of chromatin structures: heterochromatin and euchromatin. The most common form of silencing of genes is associated with a dense form of chromatin called heterochromatin (e.g. telomeres, centromeres) and euchromatin is the region, which is unfolded and active in transcription (Watson, 2007).

NER Meets Chromatin.

In eukaryotic cells, the inheritance of both the DNA sequence and its organization into chromatin is critical to maintain genome stability. This maintenance is challenged by DNA damage (Green and Almouzni, 2002). Early work of Smerdon and colleagues demonstrated that chromatin structure is

altered during NER repair of UV-induced DNA lesions (Smerdon and Lieberman, 1978). As mentioned before, UV radiation induces the formation of CPDs and 6-4PPs, which form bulky lesions in chromatin (Aboussekhra and Thoma, 1999; Peterson and Cote, 2004). Their yield and distribution depend on DNA sequence, the local DNA structure and the association of DNA with chromosomal proteins (Pfeifer, 1997; Peterson and Cote, 2004). Specifically, the chromatin environment has been shown to affect UV-induced damage distribution in nucleosomes isolated from UV irradiated cells (Gale *et al.*, 1987; Pehrson, 1995). The CPD distribution shows a striking 10.3-bp periodicity with a strong preference for sites where the minor groove is oriented away from the histone surface (Gale *et al.*, 1987; Pehrson, 1995). On the other hand, 6-4PPs are distributed relatively uniformly within nucleosome cores and preferentially formed in linker DNA of bulk chromatin from UV irradiated cells (Mitchell *et al.*, 1990).

In order to investigate the effects of nucleosome structure on the formation of UV-induced DNA lesions, several groups have used reconstituted model nucleosomes containing a defined DNA sequence (Suquet and Smerdon, 1993; Liu *et al.*, 2000; Ura *et al.*, 2001). The use of a dinucleosome as a substrate further demonstrated that excision of 6-4 photoproducts by purified factors is strongly inhibited by this chromatin structure even when the lesion was located within the linker DNA (Ura *et al.*, 2001). Proteins required before excision include XPC-hHR23B (homologous to yeast RAD23p) complex, XPA, and the replication

protein A (RPA) (Volker *et al.*, 2001). Consistent with inhibition occurring at this stage, the affinities of both XPC and XPA for DNA are decreased 5-fold on nucleosomal DNA compared with naked DNA (Hara *et al.*, 2000).

From the above findings, it is apparent that the chromatin structure restricts the access of proteins or protein complexes to their respective DNA binding sites. This clearly indicates that there should be a step before repair, which is "Chromatin Remodeling". ATP-dependent remodeling enzymes, histone-modifying enzymes, chromosomal architectural factors, or post-translational modifications of histones achieve chromatin remodeling individually or in combination, and is discussed in detail in the following sections.

Rearrangement of Chromatin Structure During NER Repair

ATP-dependent Chromatin Modifying Enzymes.

SWI/SNF chromatin remodeling enzymes are multi-subunit complexes that hydrolyze ATP to alter chromatin structure and allow the binding of regulatory factors to nucleosomal DNA (Ura and Hayes, 2002). SWI/SNF enzymes have been shown to activate and repress a subset of genes in both yeast and higher eukaryotes (Hill *et al.*, 2005). These chromatin-remodeling complexes of the SNF2 super family are classified into one of three distinct groups: SWI/SNF-like (e.g. SWI/SNF, RSC and BRM), ISWI-like (e.g. NURF, CHRAC, ACF, yISWI complexes and RSF), and CHD-like (e.g. Mi-2/NURD) proteins (Ura and Hayes, 2002). The recent purification of a complex containing

SNF2-related ATPase that may be linked to DNA repair underscores a connection between repair and chromatin remodeling activities specifically. Recombinant ACF facilitates the excision of 6-4PP lesions by the NER core factors, in particular those situated in the linker DNA (Ura *et al.*, 2001). This was the first biological evidence to indicate a direct connection between ATP-dependent chromatin remodeling and NER (Ura *et al.*, 2001).

HATs/HDACs

HATs.

Another set of chromatin remodeling enzymes are histone acetyl transferases (HATs) that are usually involved in unfolding the chromatin. Addition of an acetyl group to the core histones by the HATs neutralizes the positive charges of the histones, thus alleviating the strong interaction between the negative charged DNA and the less positively charged histones (Gray and Teh, 2001). There are two types of HATs, the cytosolic (type-B) HATs and the nuclear (type-A) HATs (Gray and Teh, 2001). We will be concentrating on nuclear HAT proteins, type-A.

Acetylation of Histones and Non-histones by HATs.

UV irradiation stimulates histone acetylation (histone H3 and H4) and chromatin remodeling at a repressed yeast locus, *MFA2* (Yu *et al.*, 2005). This is brought about by Gcn5p (HAT in yeast) and partially by Swi2p. The deletion of

GCN5 but not of *SWI2*, impairs repair of DNA damage at the *MFA2* promoter (Yu *et al.*, 2005).

The HAT protein, p300 is not only found to be linked in NER, but also with other DNA repair mechanisms. p300 is found to be associated with newly synthesized DNA at UV-damaged sites, especially with PCNA, which is a key protein in DNA synthesis (Hasan *et al.*, 2001). In addition, p300 is found to interact and acetylate other proteins, which are essential elements in the DNA repair machinery of the cell. These proteins include: p53 – a very important stress response and DNA repair protein (Rubbi and Milner, 2003), p127 – a part of a UV-DNA binding protein (UV-DDB) heterodimer (Rapic-Otrin *et al.*, 2002) and NEIL 2 – a recently discovered glycosylase (Bhakat *et al.*, 2004). Further, histone acetylation by an essential Sas2-related acetyltransferase 1 (Esa1) is linked to the double strand break repair (DSB) repair protein Ku70 especially during non-homologous end joining repair (NHEJ), where histone H4 gets hyperacetylated (Bird *et al.*, 2002).

Histone acetyl transferases CREB binding protein (CBP) and p300 interact with the small subunit of the XP-E damage-specific DNA binding protein (DDB). The human SPT3–TAF_{II}31–GCN5L acetylase complex (STAGA) interacts with the large subunit of DDB (Datta *et al.*, 2001; Martinez *et al.*, 2001). Recently, Bhakat and others found that human 8-oxoguanine-DNA glycosylase 1 (OGG1) is acetylated by p300 *in vivo* predominantly at Lys338/Lys341 in HeLa cells. The

OGG1 is the major DNA glycosylase responsible for repair of 7, 8-dihydro-8-oxoguanine (8-oxoG) and ring-opened fapy-guanine, critical mutagenic DNA lesions that are induced by reactive oxygen species (Bhakat *et al.*, 2006). Recent studies showed the interaction of p300 with CSB protein following UV irradiation in NER-TCR subpathway (Fousteri *et al.*, 2006).

In addition, p300 is known to serve as co-activator of many transcription factors (Chen *et al.*, 2002). One study showed p300 served as a co-activator of cardiac–specific transcription factors like GATA-4. Their findings demonstrated that acetylation of GATA-4 and other histones by p300 was involved in the differentiation of ES cells into cardiac myocytes (Kawamura *et al.*, 2005). p300 associates with cyclooxygenase 2 (*COX-2*) promoter, which increases COX-2 mRNA expression. Defective histone acetylation due to reduced recruitment of HATs to the *COX-2* promoter results in diminished *COX-2* gene transcription in idiopathic pulmonary fibrosis (IPF) (Coward *et al.*, 2009).

Deacetylation of Histones.

The histone deacetylases (HDACs) are class of enzymes that remove the acetyl groups from an ε-N terminal amino acid on a histone. Deacetylation of histones is important for compaction of chromatin after DNA repair is completed. Sin3p/Rpd3p deacetylase complex is required for efficient repair by NHEJ in *Saccharomyces cerevisiae* (Fernandez-Capetillo *et al.*, 2004; Fernandez-Capetillo and Nussenzweig, 2004). In another study, researchers showed role of

HDACs in DNA repair after reactive oxygen species (ROS) damage. In this case, OGG1 interacts with class I histone deacetylases (Bhakat *et al.*, 2006).

Role of HMGNs in NER

HMG Chromatin Proteins – HMGA, HMGB and HMGN.

The HMG proteins are among the largest and best characterized group of non-histone chromosomal proteins (Bustin and Reeves, 1996; Bustin, 1999; Bustin, 2001). There are three families of HMG proteins that are classified according to their functional DNA interaction motifs: HMGA, HMGB, and HMGN. The DNA binding motif for the HMGA family is called the "AT hook", the "HMG-box" defines the HMGB family, and the HMGN family is known for its nucleosome-binding domain (Bustin and Reeves, 1996; Bustin, 1999; Bustin, 2001). Members of the HMGN family include HMGN1, HMGN2, HMGN3, HMGN4 (Birger *et al.*, 2001), and HMGN5 (Rochman *et al.*, 2009). The binding of HMGN to nucleosome reduces the compaction of the chromatin fiber by competing with linker histone H1, by interacting with N-terminal tails of histone H3 and H2A and by modulating the post-translational modification of core histones, thereby promoting overall accessibility to nucleosomes (Lim *et al.*, 2005; Postnikov *et al.*, 2006).

Functional Significance of HMGNs.

Traditionally, HMGNs were thought to be factors that enhance the rate of transcriptional initiation (Paranjape *et al.*, 1995), transcription elongation (Ding *et*

al., 1997) and replication (Ding *et al.*, 1994; Ding *et al.*, 1997). In recent years, HMGNs were found to participate in stress responses and DNA repair. Birger and colleagues found that loss of HMGN1 protein increased the cellular sensitivity to ionizing radiation and the tumor burden of mice (Birger *et al.*, 2005). HMGNs are also known to participate in the response for various stresses such as heat shock (Belova *et al.*, 2008). Studies with mice embryonic fibroblast lacking HMGN1 suggested a role of HMGN1 in TCR, but this system did not provide information about GGR since this repair is not efficient in mice cells (Birger *et al.*, 2003). A study by another group showed that HMGN1 is associated with Cockayne syndrome A (CSA) protein in the NER-TCR subpathway (Fousteri *et al.*, 2006). There are only a few proteins known to associate with HMGN1. For instance, 14.3.3 protein was shown to interact with HMGN1. This interaction impedes the reentry of the HMGNs into the nucleus until the end of telophase (Prymakowska-Bosak *et al.*, 2002). Hansen and colleagues showed HMGN1 interacts specifically with both estrogen receptor α (ERα) and serum response factor (SRF), which regulate the responses of Trefoil factor 1(*TFF1*) and *FOS* to estrogen (Zhu and Hansen, 2007). The latter work indicates the role of HMGN1 in regulating the expression of particular genes via specific protein-protein interactions with transcription factors at target gene regulatory regions (Zhu and Hansen, 2007).

It has been shown that HMGN1 elevates the levels of histone H3 lysine 14 (H3K14ac) based in knockout mice studies (Lim *et al.*, 2005). *In vitro*, HMGN1 enhances the ability of p300/CBP-associated factor (PCAF) to acetylate nucleosomal, but not free histone H3. Thus, HMGN1 modulates the levels of H3K14ac by binding to chromatin (Lim *et al.*, 2005). HMGN1 also enhances the rate of heat shock-induced H3K14 acetylation in the *Hsp70* promoter, thereby enhancing the rate of chromatin remodeling and the subsequent transcription during the early rounds of *Hsp70* activation when the gene is still associated with histones in a nucleosomal conformation (Belova *et al.*, 2008).

Our Research Questions and Research Hypotheses.

The above studies indicate that HMGN proteins are involved in various stress responses, but they do not indicate the role of HMGN proteins in the NER-GGR subpathway. Therefore, our main research goal is to identify the role of HMGN proteins in NER-GGR. The second aim of our research is to elucidate the potential of HMGN-HATs' association that might be involved in HMGNs response to UV irradiation, via NER-GGR subpathway. It has been shown that the HAT-p300, and HAT-PCAF acetylate HMGN1 and HMGN2 (Herrera *et al.*, 1999; Bergel *et al.*, 2000). Other studies suggest that p300 not only acetylates non-histone proteins, but also interacts with some of them, such as in the case of p53 (Iyer *et al.*, 2004). Therefore, our hypothesis was that the HMGNs tether HATs to the chromatin to facilitate acetylation of core histones. We further postulated that

the p300 or other HATs complex is recruited to the DNA damage site by HMGNs, as part of the repair process in NER-GGR.

HMGN Null Cells – a Tool Used for the Study.

HMGN1a/N2 null cells were derived from DT40 chicken B-lymphoblastoid cell lines at Dr. Jerry Dodgson's lab (Li and Dodgson, 1995; Li *et al.*, 1997). DT40 chicken cells have a high homologous recombination rate making them a favorable system for targeted disruption of various genes. The HMGN1a null cell line was named 8/bsr8 and HMGN2 null cell lines were named D98-7 and D108-1. Double null cell lines (quadruple disruptions) were generated by two independent pathways and were named Nh43, Nh52, Bp39, and Bp5 respectively (as shown in Figure 3). Two *HMGN2* vectors were used to target the endogenous gene and these were designed to replace the majority of the promoter sequence and exon 1 (which contains the translation initiation codon and four additional highly conserved codons) with drug-selectable cassettes; therefore, the null mutants were not expressing any *HMGN2* mRNA. Two *HMGN1a* vectors were used to target the endogenous gene and these were designed to replace four of the six *HMGN1a* exons with drug-selectable markers. Therefore, the *HMGN1a* doubly disrupted cell line 8/bsr8 and the quadruply disrupted *HMGN1a/HMGN2* mutant cell lines were not expressing any *HMGN1a* mRNA.

Generation of HMGN1a, HMGN2 and Double Null Mutants

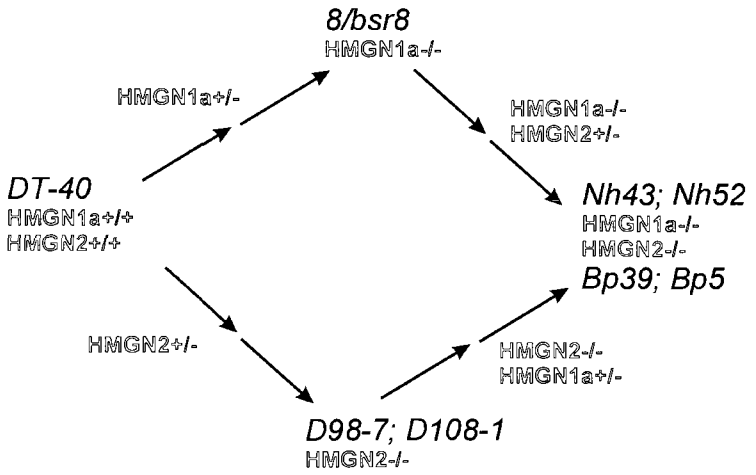

Figure 3. HMGN1a/N2 null cell lines derived from the DT40 lymphoblastoid chicken cells.The names of the cell lines are presented in italics. The smaller blue and red fonts are describing the allele which was disrupted in each selection step (gift of Dr. Jerry Dodgson, Michigan State University).

HMGN1a and HMGN2 Null Cells are Viable.

Preliminary results indicated that deletion of *HMGN1a* and *HMGN2* genes were not lethal and the cells could grow in tissue culture (Li and Dodgson, 1995; Li *et al.*, 1997). Our scientific goal was to test whether the HMGN null cells will be sensitive to the UV irradiation and to study if and how HMGNs facilitate the DNA repair after UV irradiation with respect to GGR.

CHAPTER II

MATERIALS AND METHODS

Maintenance of Chicken HMGN Null Cell Lines

The DT40 derived cell lines; null for HMGN1a, HMGN2 or for both HMGN1a and HMGN2 were generated by targeted gene disruption in Dr. Jerry Dodgson's laboratory (Li and Dodgson, 1995; Li *et al.*, 1997). Cells were cultured at 37°C under 7.5% CO_2 in Dulbeco's modified Eagle's medium containing high glucose or 4 mM L-glutamine (Gibco BRL, catalog number 11960-044) supplemented with 10% fetal bovine serum (Gemini Bioproducts), 5% chicken serum (Gibco BRL), 10 μg/ml gentamicin (Gibco BRL), 0.5 μg/ml amphotericin B (Fungizone, Gibco BRL) and 50 μM 2-mercaptoethanol. The above serums were inactivated for 30 minutes at 56°C.

Derivation of HeLa HMGN1 Tag Cell Lines

HeLa cells were established to express stably HMGN1or HMGN2 tagged at the carboxyl terminus with both FLAG and HA peptide tags by retroviral transduction (Ogryzko *et al.*, 1998; Lim *et al.*, 2002). A wild-type HeLa cells were stably tranduced with co-cistronic retroviral construct containing a CMV promoter with HMGN1, HA-tag, FLAG-tag and IL2 receptor. Similarly empty plasmid was stably transfected in HeLa cells which served as control for the experiments and named by us HeLa wild-type tag.

Maintenance of HeLa HMGN Tag Cell Lines

HeLa HMGN1 tag and wild-type tag cell lines were maintained at 37°C under 5% CO_2 in Dulbeco's modified Eagle's medium (Gibco BRL, catalog number 11960-044) supplemented with 10% fetal bovine serum and 0.1 mg/ml of streptomycin and penicillin.

UV Survival Assay

Exponentially growing DT40 derived cell lines with a concentration of 0.5 x 10^6 cells/2 ml of 1X PBS were plated in 60 mm petri dishes. The cells were irradiated with UVC (254 nm) at various joulages- 0, 3, 6, 9 and 12 J/m^2. The irradiated cells were centrifuged in 15 ml test tubes and fresh medium was added to the cell pellet. Then the cells were transferred to 60 mm petri dishes and incubated at 37°C, 7.5% CO_2 for 72 hours. For testing the cells viability we used Trypan blue exclusion assay (0.2%). The cells that are colorless were determined alive and cells which stained blue as dead. The survival curves were plotted where survival is expressed as percentage of survived/untreated cells (0 J/m^2). All experiments were conducted in triplicate and were repeated at least twice. To test the reliability of results, statistical analysis was performed with non-parametric Mann-Whitney U tests, two-tailed, $p \leq 0.1$. Due to small sample sizes and use of non-parametric testing the alpha error is set at 0.1.

Growth Curve of DT40 and DT40 Derivative Chicken Cells

Exponentially growing DT40 derived chicken lymphoblastoid cell lines with concentration of 0.1 x 10^6 per 4.5 ml of media containing cells were plated in 60 mm petri dishes in triplicate. These cells were maintained at 7.5% CO_2 at 37°C. These cells were counted on hemocytometer slide using Trypan blue exclusion assay (0.2%), every 24 hours. Nine to twelve counts were made for every time point. The graph was plotted as concentration of cells (cells/ml) versus time (hours). All the doubling time of the HMGN null derivative cell lines were calculated from the slope of the exponential phase, except for D98-7 cell line which showed a trimodal curve, the doubling time was calculated by combining the three peaks of saturation densities and calculated from the slope of the exponential phase. Standard errors were calculated for each point and added to the graph. The results were analyzed by Mann-Whitney U test, two tailed, $p \leq 0.1$. All experiments were done in triplicate. Due to small sample sizes and use of non-parametric testing the alpha error is set at 0.1.

Southwestern Analysis of Photoproduct Levels

DNA was extracted from cells at various times after UV irradiation with a dose of 12 J/m^2 and slot-blotted onto Hybond-N+ membrane (Amersham Pharmacia). The DNA was cross-linked by 15-minute incubation in an 80°C vacuum-oven. The relative levels of CPD dimers were assessed using mouse anti-cyclobutane pyrimidine dimer (CPD) monoclonal antibody, TDM-2 (gift from

Dr. Taketsugu Tadokoro, Department of Dermatology, Osaka University, Japan). The relative level of DNA loaded on each blot was determined by staining with 0.5 μg/ml ethidium bromide, in 1X TAE (40 mM Tris acetate; 2 mM disodium EDTA). The CPD/DNA ratio was determined using spot densitometry of the CPD blot and ImageQuant software (Molecular Dynamics). The tests were done in a linear range according to the calibration curve. The results were analyzed by Kruskal-Wallis test, two tailed, $p \leq 0.1$. Due to small sample sizes and use of non-parametric testing the alpha error is set at 0.1.

Apoptosis Studies in Chicken HMGN Null Cells

Exponentially growing DT40 and DT40 derived HMGN cells were irradiated with a UVC dose of 6 J/m^2 with a concentration of 0.5 x 10^6 cells/2ml PBS in triplicate. The irradiated cells were centrifuged and media were added to the pellet. The cells were maintained in the petriplates for 48 hours in the incubator at 7.5% CO_2 and 100% humidity. Briefly, 48 hours following irradiation the cells were rinsed twice with chilled 1X PBS and centrifuged at room temperature at 1000 rpm for 8 minutes and the pellet was resuspended in 500 μl (1x10^6 cells/ml) 1X Annexin V Binding Buffer. Non-irradiated cells were used as control. The cells were labeled using the Annexin V-FITC Apoptosis Detection Kit I (BD Pharmingen), according to the manufacturer recommendations with slight modifications. Then 200 μl cells were stained with 10 μl propidium iodide and 5 μl of Annexin V-FITC and incubated for 15 minutes at room temperature in the dark.

The samples were brought to a volume of 800 ml with Binding Buffer and run on a FACS Calibur (BD Biosciences). A minimum of 10,000 cells was acquired for each sample. Cell Quest Pro software was used for both acquisition and analysis. All experiments were done in triplicate. The results were analyzed by independent *t*-test and paired *t*-test, two-tailed, $p \leq 0.05$. Due to small sample sizes and use of parametric testing the alpha error is set at 0.05.

Cell Cycle Analysis

Cells grown at 5 x10^6 cells/ml in 90 mm petri dishes were UV irradiated at 12 J/m^2. Forty-eight hours after irradiation the cells were pulsed with 20 μM BrdU for 30 minutes. Cells were washed with 1X PBS, resuspended, fixed with chilled 70% ethanol, and stored in –20°C. For analysis, the cells were incubated with 3 ml 2N HCl for 30 minutes and then 6 ml of 0.1 M sodium borate (pH 8.5) was added. The cells were washed twice with PBS containing 0.5% Tween and 0.5% BSA (PBS/T). The cells were stained with anti BrdU-FITC conjugated antibody for 60 minutes at room temperature. This was followed by a 20 minute treatment with 200 g/ml RNase A, and an overnight incubation with 20 g/ml propidium iodide. Samples were run on a FACS Calibur (BD Biosciences). A minimum of 20,000 cells was acquired for each sample. CellQuest software was used for both acquisition and analysis. The results were analyzed by independent *t*-test and paired *t*-test, one-tailed, $p \leq 0.05$. Due to small sample sizes and use of parametric testing the alpha error is set at 0.05.

Western Blot Assays for Cell Cycle Analysis

Whole cell lysates were prepared from irradiated chicken cells at 12 J/m^2 at various time intervals after irradiation: 30 minutes, 4 hours, 10 hours, 24 hours, 48 hours and 72 hours and non-irradiated cells being the control. The lysates were run on 15% SDS-PAGE gels and transferred to Immobilon PVDF membrane (Millipore, Temecula, CA) by semi-dry transfer cell (BIO-RAD). The membranes were then subjected to antibodies against phosphorylated-Chk1 Ser345 (0.1 μg/ml, Cell Signaling) and phospho-H3 Ser 10 (0.04 μg/ml, Upstate Biotech). The membranes were incubated overnight at 4°C on a rotary shaker at a low speed. The membranes were rinsed twice with 1X PBS and washed three times for 10, 5, and 5 minutes with 0.1% Tween-20 (1X PBS-T) before incubation at room temperature with horse radish peroxidase (HRP)-conjugated secondary antibody (goat-anti rabbit, 2 x 10^{-6} μg/ μl ; Thermo Scientific, Rockford, IL). Following incubation, membranes were rinsed twice with 1X PBS and washed three times with 0.1% PBS-T. Blots were then incubated with ECL chemiluminiscent reagent (Amersham, Piscataway, NJ) for 5 minutes. The membranes were then exposed to X-ray films (Immobilon, Amersham), developed with Kodak developer and fixer solutions. Densitometric analysis (Alpha Innotech, San Leandro, CA) was carried out to determine the levels of phosphorylation relatively to protein levels as determined by Coomassie staining technique. All experiments were done in triplicate. The results were analyzed by

non-parametric, Kruskal-Wallis test analysis and Mann-Whitney U with a significance level of two-tailed, $p \leq 0.1$. Due to small sample sizes and use of non-parametric testing the alpha error is set at 0.1.

Histone Post-translational Modifications in Chicken Lymphoblasts, Post-UV Irradiation

Both wild-type and double null chicken cells (6×10^7 cells/ml), were irradiated with UVC (254 nm) while gently agitated, at a dose of 12 J/m^2, whole cell lysates were prepared at various time intervals post-UV irradiation: 30 minutes, 4 h, 10 h, 24 h, 48 h and 72 h in 150 mm petri dishes. The proteins were resolved on a 15% SDS-PAGE criterion gels. Non-irradiated cells were used as a negative control. The cell treatment after irradiation is explained in the above procedure (see UV survival assay). Whole cell extracts were prepared from the respective time intervals using 1X SDS Laemmli buffer (1.0 M Tris-HCl, pH 6.8, glycerol, 10% (w/v) SDS, 0.1% (w/v) bromophenol blue). The proteins were resolved on a 15% SDS-PAGE gel. The extracts were subjected to Western blot analysis (as explained above, see assaying for checkpoint arrest) using the following antibodies against: H3K9ac (1×10^{-3} μg/ml, Upstate), H4K5ac (4×10^{-5} μg/ml, Santa Cruz Biotech), H3K14ac (2×10^{-5} μg/ml, Upstate), and H3K9me3 (2×10^{-5} μg/ml, Upstate). Spot densitometric analysis was used for determining the standardized levels of acetylation and methylation by Alpha Innotech software. All experiments were repeated five times. The results were analyzed by non-parametric, Kruskal-Wallis test analysis and Mann-Whitney U with a significance

level of two-tailed, $p \leq 0.1$. Due to small sample sizes and use of non-parametric testing the alpha error is set at 0.1.

Histone Post-translational Modifications in UV Irradiated HeLa Cells

HeLa wild-type cells were grown to 80% confluency in 100 mm tissue culture petri dishes, in triplicate. The cells were incubated at 37°C, 5% CO_2, and 100% humidity. These cells were UV irradiated at 30 J/m^2 and whole cell lysates were extracted after 30 min, 4 hours, 10 hours, 24 hours, 48 hours and 72 hours using 1X Laemmli buffer. Non-irradiated cells were used as control. The proteins were resolved on a 15% SDS-PAGE. These lysates were subjected to Western blot analysis (as explained above) using specific antibodies against H3K9ac (1 x 10^{-3} μg/ml, Upstate), H3K14ac (2 x 10^{-5} μg/ml, Upstate), and H4K5ac (4 x 10^{-5} μg/ml, Santa Cruz Biotech). The protein loading was standardized using Coomassie staining technique. ECL treated membranes were exposed to X-ray films, and then spot densitometric analysis (Alpha Innotech) was performed to measure the levels of acetylation. The protein levels and the relative modifications rate were calculated based on the optical densities of three experiments.

Analysis of HeLa HMGN Clones

We wanted to explore the possibility that HMGNs and HATs interact during UV-induced DNA damage repair. Co-immunoprecipitations of HA-tagged

HMGNs could be a useful tool for this purpose. HeLa cells stably transfected with recombinant HA-tagged HMGN1 or HMGN2 genes (Ogryzko *et al.*, 1998; Lim *et al.*, 2002) were cloned in 96 and 24 well-plates, and were analyzed to identify high level HMGN expressing clones, using antibodies against HMGN1 with a concentration of 4.21×10^{-2} μg/ml and HMGN2 with concentration of 0.51 μg/ml (gifts by Dr. Bustin) and against HA antibody (Upstate Biotech) with a concentration of 0.001 μg/ml. The proteins were resolved on 18% SDS-PAGE. The blots were incubated with secondary antibody with goat-anti-rabbit (PIERCE) horse radish peroxidase. The blots were stained with ECL (Amersham) were exposed to X-rays (Immobilon). Equal loading was determined by Coomassie staining. Spot densitometric analysis (Quantity One image software, FX) was carried out to determine the levels of HMGN expression. Clones which expressed high levels of HMGNs were used for Co-IP assays.

HAT Assay of HMGN1 Immunoprecipitate Following UV Irradiation

Protein extracts were prepared from HeLa overexpressing HMGN1 tag and wild-type tag cells using RIPA buffer of total volume of 25 ml (containing sterile 1X PBS buffer (Biosource), 100 mM sodium othovanadate, 0.5 M sodium fluoride, 500 μM Nonidet p-40, 2 μM trichostatin A), complete Mini was added as the protease inhibitor (Roche Diagnostics). The protein concentration was determined by Bradford Assay. These whole cell lysates were prepared from UV irradiating HeLa cells (30 J/m^2) at various time intervals. The immunoprecipitation

assay was performed following the protocol given in Santa Cruz Biotechnology with slight modification.

The immunoprecipitate was added to 1 X HAT buffer (2 X Tris borate, 1mM DTT) containing free core histones (0.25 M sulfuric acid extraction from DT40 chicken cells) and 72 μM Ac-CoA (Sigma) in a final volume (50 μl). The reaction mixtures were incubated at 37°C for 40 minutes with constant agitation. The reactions were stopped by the addition of an equal volume of 2X SDS-gel sample buffer (100 mM Tris-HCl (pH 6.8), 200 mM DTT, 2% SDS, 0.1% bromophenol blue, 20% glycerol). The mixtures were boiled for 5 minutes, and the proteins were resolved on a 15% SDS-polyacrylamide gel. The reaction mixtures were subjected to Western blot with antibodies against H4K5ac and H3K14ac, to test for HAT activity. The electrophoresis was performed at 15 V/cm^2 and stopped when the bromophenol blue reached the bottom of the gel. Non-parametric Wilcoxon-Signed Ranks test was used to test the significance in acetylation of HMGN1 immunoprecipitates, one-tailed, $p \leq 0.1$. Due to small sample sizes and use of non-parametric testing the alpha error is set at 0.1.

Co-Immunoprecipitation Assay

Whole cell protein extracts were prepared from HeLa overexpressing HMGN1 tag (C10 clone, table 5) and wild-type tag cells using RIPA buffer of total volume of 25 ml (containing sterile 1X PBS buffer (Biosource), 100 mM sodium othovanadate, 0.5 M sodium fluoride, 500 μM Nonidet p-40, 2 μM trichostatin A),

complete Mini was added as the protease inhibitor (Roche Diagnostics). The protein concentration was determined by Bradford Assay. These whole cell protein extracts were prepared from UV irradiating HeLa cells (30 J/m^2) at various time intervals after UV irradiation. The immunoprecipitation assay was performed following the protocol given by Santa Cruz Biotechnology with slight modification. Protein extracts (2 mg - 4 mg) were precleared with 0.25 μg of IgG (normal mouse, rabbit, or goat IgG) corresponding to the host species of the primary antibody, together with 20 μl of resuspended volume of the appropriate agarose conjugate (protein A/G agarose). They were incubated at 4°C for 1 hour. Post-preclearing, the supernatant was collected by centrifugation at 2,500 rpm for 5 minutes at 4°C. The protein extracts (2 mg or 4 mg) were incubated with 2 μg of one of the following antibodies against HMGN1 (gift from Dr. Bustin), against p300 (Upstate Biotech, Santa Cruz biotech), against p400 (Santa Cruz Biotech) or against CBP (Upstate Biotech). Twenty μl of protein A/G- Agarose conjugate was added to the supernatant. A negative control was prepared by immunoprecipitating the protein extracts using antibody against non-immune IgG. The tubes were incubated at 4°C on a rollordrum overnight. After incubation, the pellet was collected by centrifugation at 2,500 rpm for 5 minutes at 4°C. The pellet was washed 3 times with RIPA buffer, each time repeating centrifugation step above. 30μl of 1X SDS Laemmli loading buffer was added and boiled for 5 minutes. These were then subjected to 15% or 5% SDS-PAGE gels. Western

blot analysis detected the protein bound to the immunoprecipitate (for details see above in the section of histone post-translational modifications in UV irradiated HeLa cells).

CPD Removal Rate of HMGN Null Cells With and Without Trichostatin A

Wild-type chicken and HMGN null cells were plated with a concentration of 0.88 x 10^6 cells/ml in 260 mm tissue culture petri dishes. The cells were incubated in the given conditions: at 37°C, 7.5% CO_2, and 100% humidity. Prior to UV irradiation, the cells were treated with 2 μM TSA, an HDAC inhibitor, for 15 hours. The cells were then subjected to UVC irradiation at 12 J/m^2. Cells were incubated with DMEM medium for time intervals of 7 hours and 20 hours. Cells were extracted using cell scrapper and digestion buffer. DNA was purified immediately after UV irradiation (time 0) & 7 h and 20 h after UV irradiation. Non-irradiated cells were used as control. Repair rates of each cell line were detected by Southwestern blot analysis. One μg of DNA per treatment group was loaded on a slot blot membrane and incubated with antibodies against mouse anti-cyclobutane pyrimidine dimer (CPD) monoclonal antibody, TDM-2 (gift of Dr. Taketsugu Tadokoro, Department of Dermatology, Osaka University, Japan). Standard Western blot protocol was followed after incubation. ECL treated membranes were exposed to X-ray films. The DNA loading was quantified using ethidium bromide staining technique. Spot densitometric analysis was performed to calculate the CPD/DNA ratio, DNA levels, and their repair rates. The

experiments were repeated three times independently. The results were analyzed by non-parametric, Mann-Whitney U test and Wilcoxon Signed Rank test with a significance level of two-tailed, $p \leq 0.1$. Due to small sample sizes and use of non-parametric testing the alpha error is set at 0.1.

CHAPTER III

RESULTS

Experiment 1: HMGN1a and HMGN2 Null Mutants are Hypersensitive to UV Irradiation

The functional significance of proteins can be studied by "knocking out" their gene. Previous studies have shown that mice lacking the HMGN1 gene were more sensitive to UV and gamma irradiations and had a lower capacity to repair UV-induced DNA-damage by TCR (Birger *et al.*, 2003). Recent studies showed that MEF cells lacking HMGN1 were also sensitive to heat shock (Belova *et al.*, 2008). However, HMGN1 knockout mice could not be used to study the involvement of HMGNs in NER-GGR since mice cells do not have an efficient NER-GGR. Chicken cells, like human cells but unlike mouse cells, have efficient global genome repair (GGR). Dodgson and his colleagues (Li *et al.*, 1997) generated HMGN1a and HMGN2 null cells from DT40 chicken B-lymphoblastoid cell line (Figure 3). These cells enabled us to test whether HMGNs are involved in NER-GGR. Since deletion of HMGN1a and HMGN2 genes were not lethal and the cells could grow in tissue culture (Li and Dodgson, 1995; Li *et al.*, 1997), we could test if HMGN null cells would be sensitive to UV irradiation. Wild-type and mutant DT40 cells (Figure 3) were irradiated with UVC doses ranging from 3 to12 J/m^2. The four HMGN knockout strains were: (1) HMGN1 mono knockout; (2) HMGN2 mono knockout; (3) HMGN double knockout cells, first disrupted for

HMGN1a followed by HMGN2 and (4) HMGN double knockout first for HMGN2 followed by HMGN1a. Seventy-two hours after the irradiation, the viability of cells was measured by Trypan blue exclusion assay.

All the HMGN null mutant cells were significantly more UV-sensitive as compared to wild-type DT40 control cells (Figure 4, Table 1). The LD_{50} (UV dose resulting in 50% lethality) for the wild-type cells was 9.4 ± 2.33 J/m^2, while the LD_{50} for the cell variants lacking HMGN was in the range of 2.63 ± 0.51 to 3.69 ± 0.83 J/m^2. These differences in the LD_{50} values between the wild-type cells and all the HMGN null cells were found to be significant (Mann-Whitney U Tests, two tailed, $p \leq 0.1$). The level of UV sensitivity of HMGN2-/- cells (D108-1) (3.69 ± 0.83 J/m^2) was somewhat lower than that of the other null cells but analysis showed that D108-1 cells were statistically similar to the other HMGN null cells (non-parametric Mann-Whitney U, $p > 0.127$). Interestingly, the levels of UV sensitivity of HMGN2-/- cells (D108-1) and HMGN1a-/- cells (8/bsr8) were similar to each other and similar to the two doubly disrupted cell lines Nh43 and Bp5. No apparent additive or synergistic effects were observed in the sensitivity of the doubly disrupted cell lines. Thus, cells lacking HMGN showed increased sensitivity to UV irradiation.

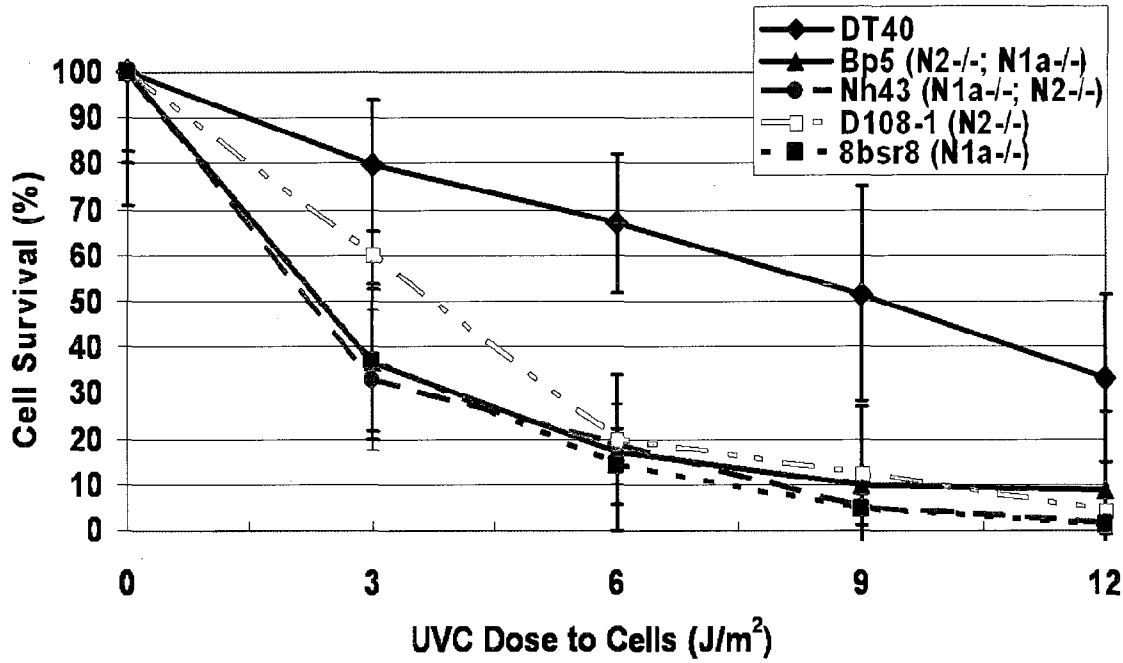

Figure 4. Chicken cells that lack HMGN1a, HMGN2 or both HMGN1a and HMGN2 are hypersensitive to UV irradiation. Shown are survival curves of wild-type and null mutant HMGN DT40 cells, 72 hours after irradiation with various doses of UVC in the range of 0-12J/m^2. Each data point represents the mean of three independent measurements (±SE), as measured by Trypan blue exclusion assay.

Table1. LD_{50} of UV irradiated wild-type DT40 cells and DT40 derived null HMGN cell lines.

DT40	D108-1	8/bsr8	Bp5	Nh43
9.40±2.33 J/m^2	3.69±0.83 J/m^2 *	2.83±0.35 J/m^2 *	3.03±0.80 J/m^2 *	2.63±0.51 J/m^2 *

The LD_{50} values (in J/m^2 ± SD) of the wild-type DT40 cells, the derived null HMGN2 cells (D108-1), null HMGN1a cells (8/bsr8), and two double null cells HMGN1a-/-;N2-/- (Bp5 and Nh43) were calculated based on the experiments presented in Figure 4 ($n \geq 3$) .
Note: * - indicates a significant difference of HMGN null cells from the wild-type cells as determined by non-parametric Mann-Whitney U tests ($p \leq 0.1$).

The hypersensitivity of HMGN null cells could be explained by three possible ways:

(1) There is a growth advantage of wild-type cells relatively to the HMGN null cells;

(2) HMGN null cells are repairing damage slower; therefore, it may lead to slower recuperation from DNA damage and massive death from apoptosis; or

(3) HMGNs are involved in some of the survival pathways which are induced by cellular targets that are not related to DNA damage.

Experiment 2: Growth Curve of Chicken HMGN1a and HMGN2 Mono Knockout and Double Knockout Cells at 37°C

We wanted to test whether the hypersensitivity to UV irradiation by HMGN null cells is because of growth rate advantage of wild-type cells over HMGN null cells. Such a phenomenon was found, for example, with cells lacking the *FOS* gene (Schreiber *et al.*, 1995). In order to test this possibility, the growth rates of wild-type DT40 cell line and the derived chicken HMGN null cell lines were studied at 37°C. The cells were diluted to a concentration of 0.1×10^6 cells/ml and grown in the same growth medium (see Materials and Methods) and were counted every 24 hours by Trypan blue exclusion assays. These experiments were carried out in triplicate and the cell counts were taken until the cells reached their death phase.

Based on previous studies, we hypothesized, that there would be no differences in the growth rates between the HMGN null cells and wild-type cells (Li *et al.*, 1997). However, based on our detailed analysis there were some cell lines that showed significant differences either in their saturation density, or their growth rate [(Mann-Whitney U test, $p \leq 0.1$) (Figure 5, Tables 2 and 3)]. The differences were between the wild-type DT40 cells and the HMGN null cells or differences were between the various cell lines.

Based on the results shown in from Figure 5 and Tables 2 and 3; overall there were no significant differences observed between the wild-type DT40 cells and the HMGN null cells in their doubling time and saturation density (Mann-

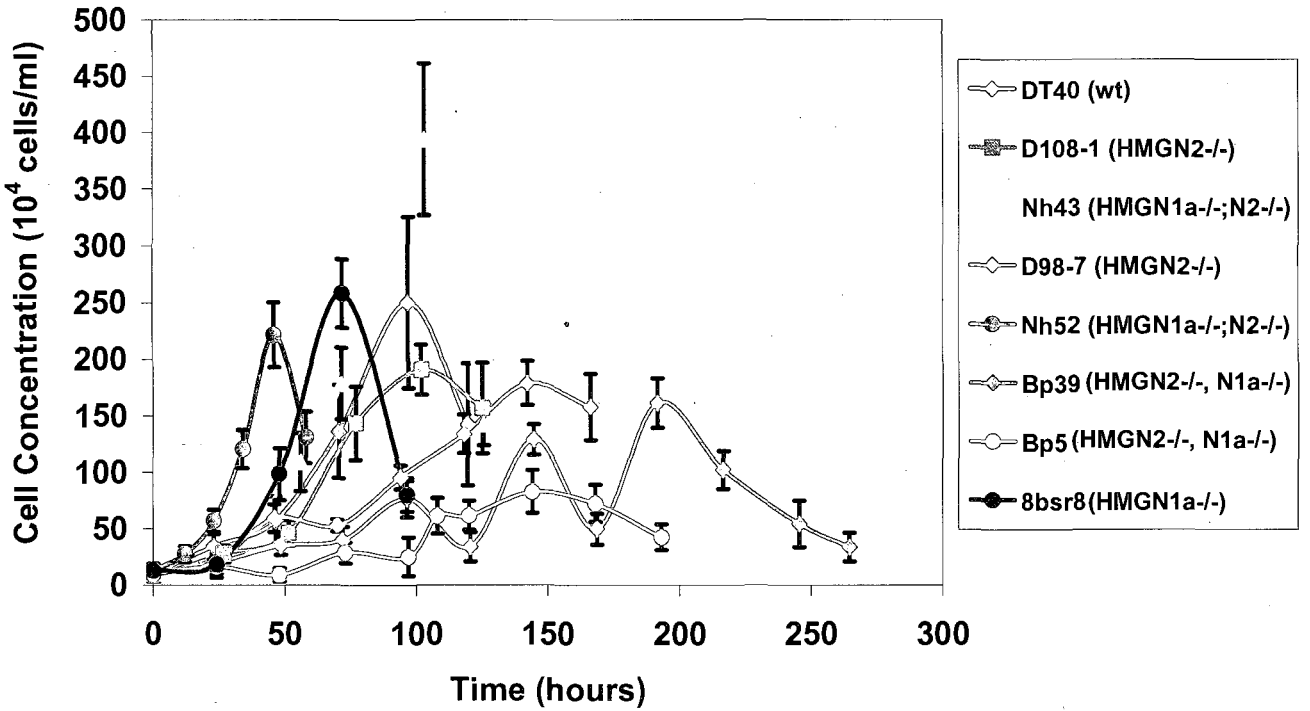

Figure 5. Growth curves of DT40 and DT40 derived HMGN1a or HMGN2 null cell lines at 37°C. HMGN null cells derived from knocking out HMGN1a first (yellow, green and dark blue) grow faster than cells derived from knocking out HMGN2 first (purple, light blue and pink). Trypan blue exclusion assay was used to count the cells. Each data point represents the mean of three independent experiments (±SE).

Table 2. Saturation density and doubling time of wild-type and HMGN1a/N2 null cells grown at 37°C.

Cell lines	Genotype	Saturation density ± SD (10^6 cells/ml)	Doubling time (hours)
DT40	(WT)	2.50 ± 0.75	29.11 ± 4.56
8/bsr-8	(HMGN1a-/-)	2.58 ± 0.31	19.7 ± 2.05
D108-1	(HMGN2-/-)	1.90 ± 0.22	37.24 ± 6.29
D98-7	(HMGN2-/-)	1.60± 0.15	61.70± 6.22*
Nh43	(HMGN1a-/-;N2-/-)	3.96 ± 0.67*	28.27 ± 1.59
Nh52	(HMGN1a-/-;N2-/-)	2.21 ± 0.29	26.9 ± 1.58
Bp39	(HMGN2-/-;N1a-/-)	1.80 ± 0.19	53.9 ± 3.85*
Bp5	(HMGN2-/-;N1a-/-)	0.83 ± 0.19*	46.44 ± 8.76

The numbers are calculated from Figure 5, based on three independent experiments. Saturation density is the maximal concentration the cells reach. Doubling time is the time it takes for the cells to duplicate their concentration at the logarithmic phase of the curve (i.e. at their maximal growing rate).

Note: * - significantly different from wild-type by non-parametric Mann-Whitney U test, two-tailed, $p \leq 0.1$.

Whitney U test, two-tailed, $p \leq 0.1$). However, chicken cells derived from disrupting HMGN1a first followed by disrupting HMGN2 (Nh43, 3.96 ± 0.67 cells/ml) showed significantly higher saturation density, as compared to cells derived from disrupting HMGN2 first followed by HMGN1a (Bp5, 0.83 ± 0.19 cells/ml). Chicken cells disrupted for HMGN1a alone, 8bsr/8 showed significantly higher saturation density and doubling time (2.58 ± 0.31 cells/ml; 19.7 ± 2.05 hours) as compared to cells derived by disrupting both HMGN2 alone (D98-7, 1.60 ± 0.15 cells/ml; 61.70 ± 6.22 hours) or disrupting HMGN2 first followed by HMGN1a (Bp5, 0.83 ± 0.19 cells/ml; 46.44 ± 8.76 hours). Based on the doubling time, D98-7 (61.7 ± 6.22 hours) and Bp39 (53.9 ± 3.85 hours), cells derived from disrupting HMGN2 alone, grew significantly slower compared to the wild-type and HMGN1a null cells. Since D98-7 cell line showed a trimodal curve, the doubling time was calculated by combining the three peaks of saturation densities and calculated from the slope of the exponential phase.

Thus, the growth curves of the HMGN null knockout first for HMGN1a had faster growth rate as well as high saturation density in comparison with those of the wild-type cells and the HMGN2 null cells (Figure 5). In spite of the differences in the growth pattern of HMGN null cells their UV sensitivity was similar, and therefore, we concluded that UV-hypersensitivity of HMGN null cells is not due to growth rate advantage of the wild-type or HMGN1a -/- cells. Therefore, we wanted to test other possible causes for the UV-hypersensitivity of HMGN null

cells. One such possibility is that the HMGN null cells repair damage slower than the wild-type cells, which may lead to a slower recuperation from DNA damage and a massive death from apoptosis.

D.T / S. D	DT40	8/bsr8	D108-1	D98-7	Nh43	Bp5	Bp39
DT40							
8/bsr8	N.S. / N.S.						
D108-1	N.S. / N.S.	N.S. / *					
D98-7	N.S. / N.S	N.S. / *	N.S. / *				
Nh43	N.S. / *	* / *	N.S. / *	* / *			
Bp5	N.S. / *	* / *	N.S. / *	* / *	N.S. / *		
Bp39	* / N.S.	* / *	N.S. / N.S.	* / N.S.	* / *	N.S. / *	
Nh52	N.S. / N.S.	* / *	N.S. / *	* / *	* / *	N.S. / *	* / *

Table 3. Represents statistically significant doubling time and saturation densities of HMGN null chicken cells from the growth curve analysis shown in Figure 5 and Table 2, using non-parametric Mann-Whitney U test, $p \leq 0.1$.
D.T – doubling time
S.D – saturation density
Note: * - indicates significant differences in the doubling time and saturation density between the cell lines. This difference was using non-parametric Mann-Whitney U test, and was shown to be significant, two-tailed, $p \leq 0.1$
N.S. – indicates there are no significant differences between the saturation density and doubling time across the cell lines.

Experiment 3: Decreased Rate of Cyclobutane Pyrimidine Dimers Removal in Cells Lacking Either HMGN2 or Both HMGN1a and HMGN2 Proteins

Since the wild-type cells, DT40, did not have a growth advantage over the HMGN null cells, we tested whether the increased mortality rate after UV irradiation was due to slow DNA repair rate in the null cells. To test this hypothesis, we analyzed the kinetics of cyclobutane pyrimidine dimers (CPDs) removal in HMGN null and wild-type cells following UV irradiation (in collaboration with Ms. R.W. Gonzalez). DNA was purified from cells immediately after UV irradiation (time 0) and at 7 h and at 20 h after UV irradiation. The DNA was slot blotted onto nylon membrane and probed with antibodies directed against CPDs (Figure 6A). To measure the amount of DNA loaded, the nylon membrane was stained with ethidium bromide. Following UV irradiation there was a gradual decrease in the CPD content of the DNA of all the cells, an indication of active repair of the damaged DNA. However, the removal of CPDs from the chromatin of the HMGN2-/- and HMGN1a-/-; N2-/- cells was significantly slower in comparison to the removal of CPDs from the chromatin of the wild-type cells (by non-parametric Kruskal-Wallis test, $p \leq 0.1$). Seven hours, after irradiation 60% of CPDs were removed from wild-type DT40 cells but less than 20% were removed from cells lacking HMGN variants (Figure 6B).

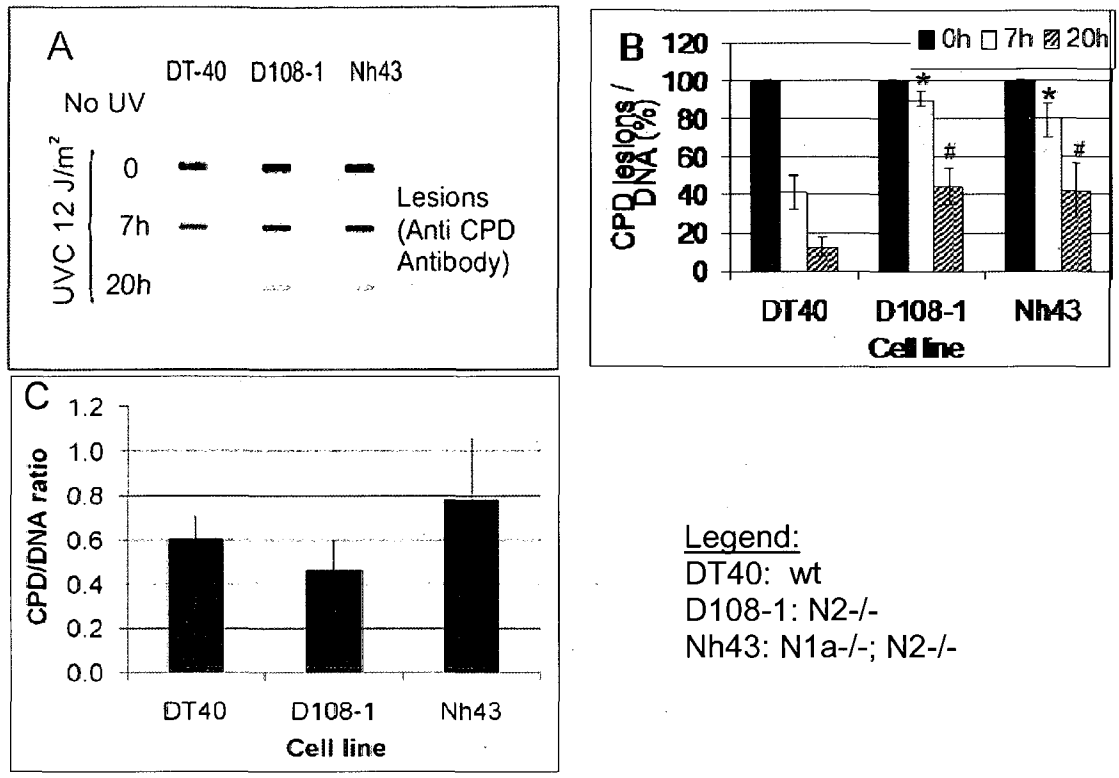

Figure 6. A decreased rate of cyclobutane pyrimidine dimers removal in cells lacking HMGN proteins. (A) Shown is southwestern analysis of the CPD removal rates in cells lacking HMGN2 (D108-1) or both HMGN2 and HMGN1a (Nh43) compared to that of wild-type DT40 cells. DNA was extracted from cells at 0, 7 and 20 hours after UVC irradiation with a dose of 12 J/m^2. Two μg of DNA were loaded per slot in a Slot Blot system and transferred to Hybond-N+ membrane. The membrane was incubated with CPD monoclonal antibody. The CPD values were normalized against the DNA levels by staining the membranes with ethidium bromide. The CPD/DNA ratio was determined using spot densitometry of the CPD and DNA blots. (B) Quantification of the experiment represented in panel A. The bar graph represents the kinetics of removal of photoproducts. The percent CPD is the percentage of CPD levels at the time interval after UV irradiation relatively to the levels of CPDs after 0 h. The graph represents the means (± SE) from three independent experiments. (C) A bar graph presenting the averages (± SE) of the CPDs/DNA at time 0 after UV irradiation of three repetitions of the experiment described in panels A and B. Note: *, # - HMGN null cells have a significantly slower CPD removal rate, 7 h and 20 h following UV irradiation as compared to the wild-type DT40 cells (Kruskal-Wallis test, $p \leq 0.1$). The wild-type DT40 cells and the null D108-1 and Nh43 cells were not statistically different from each other (Kruskal-Wallis test, $p > 0.275$).

Twenty hours following the amount of CPDs present in wild-type cells was approximately 10% of the initial content, while in the HMGN null cells approximately 40% of the original damage still remained in the DNA. These results indicate that loss of HMGNs decreases the removal rate of CPD photoproducts from the chromatin, suggesting that HMGNs affect the rate of repair of the DNA damage induced by UVC irradiation. In addition, we analyzed the CPD/DNA ratio at time zero after UV irradiation in the wild-type DT40 cells and in the null HMGN cells, without standardizing these values to 100% (Figure 6C). The data indicate that though there are small differences between the wild-type DT40 cells and the null cells, these differences are not consistent between the null cell lines, and they are not statistically significant, neither between the HMGN null cells to DT40 cells, nor between the null D108-1 cells and Nh43 cells (non-parametric Kruskal-Wallis test, all $p > 0.275$). These results therefore, suggest that HMGNs affect the repair rate of DNA damage induced by UV irradiation and not the initial rate of CPDs caused by UV. The repair kinetics in cells lacking only HMGN2 was similar to those of cells lacking both HMGN1a and HMGN2.

It is known that increased rate of mortality in UV irradiated cells is linked to the activation of the apoptotic pathway (Martin *et al.*, 1991; Aseeta *et al.*, 2005). Therefore, we wanted to test if the UV-hypersensitive HMGN null cells have a higher apoptosis rate than the wild-type.

Experiment 4: UV-Hypersensitive HMGN2 and HMGN1a/N2 Null Cells Have a Higher Apoptosis Rate Than the Wild-type Cells

Since the HMGN null cells died at a higher rate after UV exposure (see Figure 4), we wanted to test if HMGN null cells have a higher apoptosis rate as compared to the wild-type cells, after UV irradiation. HMGN2-/- cells, HMGN1a-/-; N2-/- cells and wild-type DT40 cells were UV irradiated with 6 J/m^2 and 48 hours following irradiation the cells were tested for their apoptosis levels. The reason for choosing 6 J/m^2 was that at this dosage we observed the largest differences between the survival of wild-type and the HMGN null cells in the UV survival curve (Figure 4 and Table 1).

The apoptosis assay was conducted by staining control and UV irradiated unfixed cells with Annexin V and propidium iodide. FITC-conjugated Annexin V detects translocation of phosphatidylserine from the inner leaflet of the membrane to the outer leaflet of the membrane, an early apoptotic event. Propidium iodide is used to detect the permeabilization of the plasma membrane, an event that occurs late in apoptosis. The levels of fluorescence were measured by flow cytometry using a fluorescent activated cell sorter (FACS). Using quadrant analysis on a dot plot images from these experiments provided a quantitative measure of the percentage of cells in early and late apoptosis.

The quadrant analysis of the FACS results demonstrated that, post-UV irradiation, the late and total apoptosis rates were higher in both HMGN2-/- cells (D108-1), as well as in the HMGN1a-/-;N2-/- double knockout clones (Nh43 and

Bp5), as compared to the wild-type DT40 cells (Figure 7 and Table 4) by independent group *t*-test, $p \leq 0.05$. The sum total of both early and late apoptotic cells were: 33.7% for the wild-type DT40 cells, 41.7% for the D108-1 cells, 47.9% for Nh43 cells, and 58.6% for Bp5 cells (Table 4). In contrast to that, the early apoptotic rates were lower in the HMGN null cell lines in comparison to the wild-type DT40 cells (independent group *t*-test, $p \leq 0.05$).

These results all together indicate that cells lacking HMGN proteins had a higher apoptosis rate following UV irradiation as well as activated the apoptotic pathway faster, and therefore moved faster from early to late apoptosis.

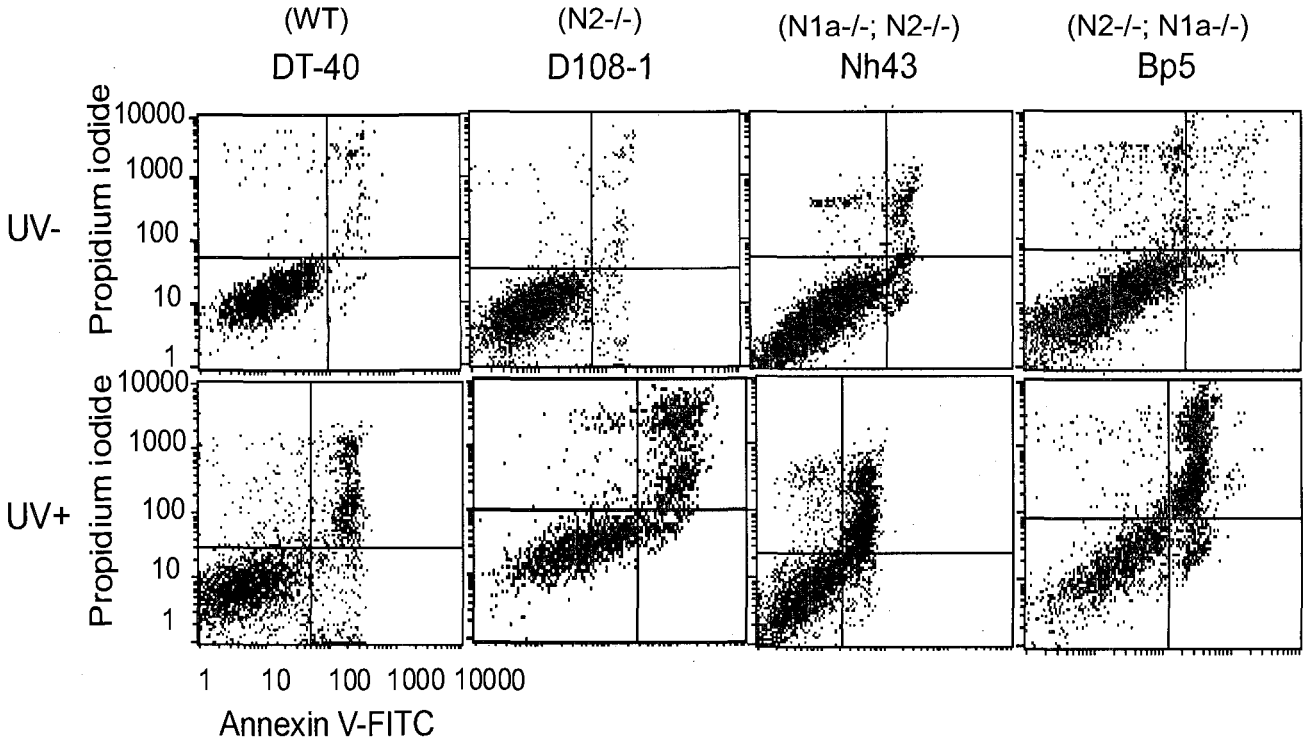

Figure 7. Higher UV-induced apoptosis rate in HMGN2-/- and HMGN1a-/-; N2-/- cells. Wild-type DT40 cells, knockout HMGN2-/- cells (D1081-1) and double knockout HMGN1a-/-; N2-/- cells (Nh43 and Bp5), were irradiated with UVC at 6 J/m^2. Early and late apoptosis rates were measured 48 hours after UV irradiation by Annexin V and propidium iodide double stain. Shown is a dot plot of the cell population as detected by FACS and analyzed by quadrant statistics. The lower left quadrant represents live and non-apoptotic cells, which are negative for both Annexin and propidium iodide, the lower right quadrant represents early apoptotic cells, which are Annexin positive, but propidium iodide negative. The upper right quadrant (PI positive and Annexin V positive) represents late apoptotic cells; the upper left quadrant includes dead cells (only PI positive). The percentage of cells in both early and late apoptosis (bottom right and top right rectangles) is shown in Table 4.

Table 4. Higher UV-induced apoptosis rate in HMGN2-/- and HMGN1a-/-; N2-/- cells.

Cell line	Early before UV	Early after UV	Late before UV	Late after UV	Total before UV	Total after UV
DT-40	2.91 ± 0.75	10.40 ± 0.95*	2.20 ± 0.44	23.30 ± 3.27*	5.11 ± 1.18	33.70 ± 3.62*
D108-1	1.26 ± 0.15	5.21 ± 1.46$^{*\xi}$	3.28 ± 0.55	36.48 ± 1.07$^{*\xi}$	4.54 ± 0.47	41.69 ± 2.43$^{*\xi}$
Nh43	2.07 ± 0.51	5.39 ± 0.70$^{*\xi}$	6.48 ± 3.42	42.55 ± 2.54$^{*\xi}$	8.55 ± 3.91	47.94 ± 3.15$^{*\xi}$
Bp5	1.35 ± 0.32	6.72 ± 0.44$^{*\xi}$	2.54 ± 0.57	51.86 ± 1.98$^{*\xi}$	3.90 ± 0.88	58.58 ± 2.02$^{*\xi}$

Apoptosis levels following UV irradiation of cell lacking HMGNs. The wild-type and null HMGN cells were irradiated at 6 J/m^2 and 48 hours later were double labeled with propidium iodide and Annexin V (see explanations in the legend of Figure 7 and Materials and Methods). The labeled cells were then subjected to FACS analysis, and quadrant analysis was carried out to detect apoptotic rates.
Note: * - There is a significant difference in apoptotic levels (both early and late) between the UV irradiated and the non-irradiated cells within each cell line. This difference was tested using paired *t* test, and was shown to be significant, $p \leq 0.05$. ξ - There is a significant difference between wild-type and null HMGN cell line in early and late phases post-UV irradiation. This difference was tested using independent group *t* test, and was shown to be significant, $p \leq 0.05$.

Experiment 5: Loss of HMGN2 or HMGN1a and HMGN2 Increases G_2/M Checkpoint Arrest Following UV Irradiation

The cellular response to UV irradiation is known to involve not only apoptosis but also cell cycle arrest, mainly at the G_1/S and the G_2/M checkpoints (Saka *et al.*, 1997). Therefore, our next goal was to explore whether the UV-hypersensitivity involves an increased activation of one of these checkpoints.

The cells lacking HMGNs were UV irradiated (12 J/m^2) and 48 hours after irradiation their cell cycle distribution was measured as follows. The cells were pulsed for 30 minutes with BrdU, fixed in 70% ethanol, and double stained with anti-BrdU antibodies and propidium iodide.

In FACS analysis, a dot plot of BrdU levels against propidium iodide (PI) levels produces a typical "horse shoe" shape (Figure 8A) in which the G_1 and G_0 cells are represented in the lower left corner of the plot while the G_2-M cells are depicted by the right side of the plot. All the cells that are in between these two groups, in the arch of the "horse shoe", which are high in BrdU, are cells in S–phase (Figure 8A).

The results revealed that UV irradiation of cells lacking either HMGN2 (D108-1 cells), or lacking both HMGN1a and HMGN2 (Nh43 cells), decreased the relative amount of cells in S-phase as compared to the more moderate decrease in the wild-type DT40 cells. The S-phase population significantly decreased in D108-1 cells from 40.7% to 21.1%, and in Nh43 cells from 48.2% to

14.0% (paired *t*-test. $p \leq 0.05$), as opposed to an insignificant decrease in the wild-type cells from 38.7% to 30.3% (Figure 8B).

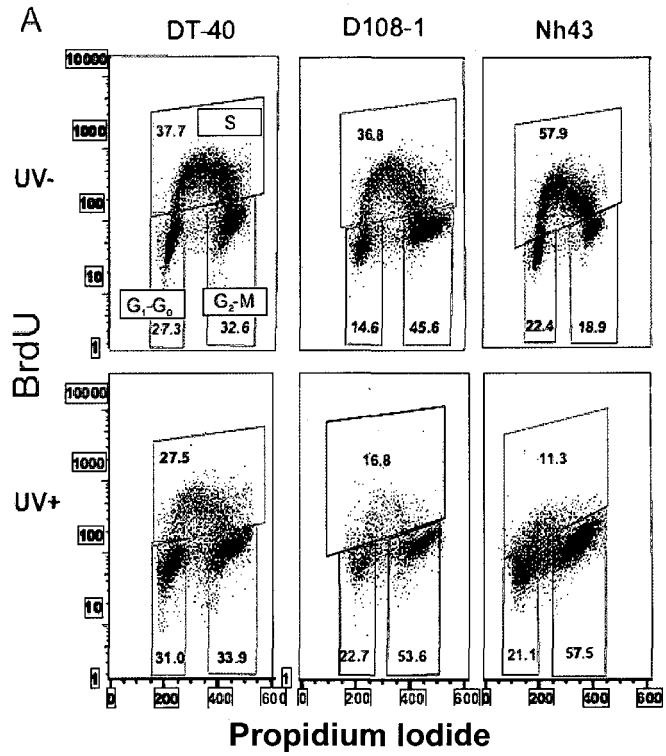

Legend:
DT40: wt
D108-1: N2-/-
Nh43: N1a-/-; N2-/-

Figure 8. UVC-induced G_2/M or mitotic arrest in HMGN2-/- and HMGN1a-/-; N2-/- cells. This Figure shows the UV-induced cell cycle arrest in wild-type DT40 cells, HMGN2-/- disrupted clone, D108-1, and double disrupted HMGN1a-/-;N2-/- cells, Nh43. Cells at a concentration of $1x10^6$ cells/ml were irradiated with a joulage of 12 J/m^2. Forty-eight hours later the cells were labeled with BrdU, fixed and incubated with anti BrdU-FITC antibody, propidium iodide stained, and analyzed by FACS. The results indicate that cells lacking HMGN2, and even further, cells lacking both HMGN1a and HMGN2, have a higher accumulation rate at G_2/M or M, and a much lower rate of S-phase cells (continued on the next page).

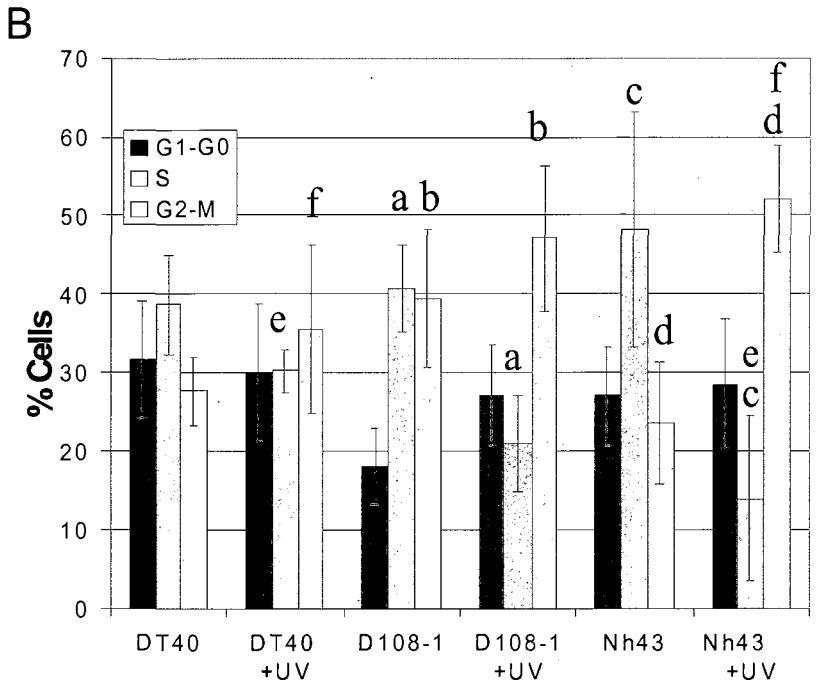

Figure 8 continued. Quantification of UVC-induced G_2/M or mitotic arrest in HMGN2-/- and HMGN1a-/-; N2-/- cells. Quantification of the experiment represented in Figure 8A, n = 3. Overall there is a significantly higher G_2/M or M arrest in N1a-/-; N2-/- as compared to wild-type after UV irradiation using independent t-test, one-tailed, $p \leq 0.05$. The letters a–d indicate the columns with significant statistical differences as determined by paired t-test (one-tailed, $p < 0.05$). The letters e and f indicate the columns with significant statistical differences as determined by independent t-test (one-tailed, $p \leq 0.05$).

The decrease of cells in the S-phase after UV irradiation is associated with a concomitant increase in the population of G_2-M cells in the null mutants as compared to non-irradiated cells, (paired *t*-test, one-tailed, $p \leq 0.05$), and a significant increase of the G_2-M population of irradiated Nh43 cells also in comparison to the irradiated wild-type cells (independent *t*-test, one-tailed, $p \leq 0.05$). This increase in the G_2/M population could be the result of an activation of either the G_2/M checkpoint arrest, one of the mitotic checkpoints or activation of

both. However, there were no significant differences in G_1/S arrest in HMGN null cells after UV irradiation by paired *t*-test, one-tailed, $p \leq 0.05$, (Figure 8, A and B).

Experiment 6: Cells Lacking HMGN2 or Both HMGN1a and HMGN2 Show Prolonged G_2/M Arrest and Early Mitotic Arrest in HMGN1a and HMGN2 Double Null Cells

Studies in Dr. Bustin's lab showed that HMGN1-/- mice had lower G_2/M arrest upon ionizing-irradiation (Birger *et al.*, 2005). The previous experiment (Figure 8, A and B) showed that both HMGN2-/- and HMGN1a-/-; N2-/- cells showed high G_2/M or mitotic arrest as compared to the wild-type. This experiment, however, did not distinguish between the two types of cell cycle arrest: G_2/M or mitotic arrest.

Therefore, we wanted to test whether the HMGN null cells are involved in increased activation of the G_2/M or the mitotic checkpoints after UV irradiation. We extracted proteins following UV irradiation at 12 J/m^2 from mono knockout, double knockout and wild-type cells at various time intervals (see Materials and Methods) and subjected them to Western blot analysis using respective antibodies. We used two checkpoint markers: phosphorylated Chk1 Ser345 for G_2/M checkpoint arrest; and phosphorylation of H3 Ser 10 (H3S10p) for mitotic arrest.

The Western blot analysis (Figure 9) indicated that the cells lacking HMGN2, and furthermore, the double null cells lacking HMGN1a and HMGN2, had longer arrest time in G_2/M checkpoint. In the wild-type DT40 cells there is a sharp drop in the phosphorylation of Chk1 Ser345 10 hours after UV irradiation.

In contrast, in the D108-1 cell-line the high levels of Chk1 phosphorylation continued to the 24 hour point, and in the double null Nh43 cells the high level of phosphorylation remained even 48 hours after UV irradiation. The rates of mitotic cells were also higher after UV irradiation in the double null cells, indicating activation of mitotic checkpoints as well. Figure 10 demonstrates that 24 hours after UV irradiation, HMGN1a-/-; N2-/- cells showed prolonged G_2/M arrest as compared to the wild-type and HMGN2-/- cells (Kruskal-Wallis test, $p \leq 0.1$). Figure 11 demonstrates that, 4 hours and 72 hours post-UV irradiation, HMGN1a-/-; HMGN2-/- cells showed high mitotic arrest relatively to wild-type and HMGN2-/- cells (Kruskal-Wallis test, $p \leq 0.1$). However, HMGN2-/- and the wild-type cells did not show any significant differences in mitotic arrest after UV irradiation (Figure 11) (Kruskal-Wallis test, $p \leq 0.1$). These results explain the significantly higher levels of G_2 and M cells in the HMGN1a-/-; N2-/- cells, Nh43, which were observed in the propidium iodide and BrdU double staining (Figure 8A). It is important to note that the differences between the null cell lines, D108-1 and Nh43, and the wild-type DT40 cells, cannot be attributed to random mutations that may have accumulated in these cells, but only to the lack of HMGN proteins. The reason for excluding this possibility is that the two null cell lines were independently derived from DT40; Nh43 cells were first disrupted for HMGN1a alleles and then for the two HMGN2 alleles, so they were not derived from the D108-1 (HMGN2-/-) cells (see Figure 3 on page 20).

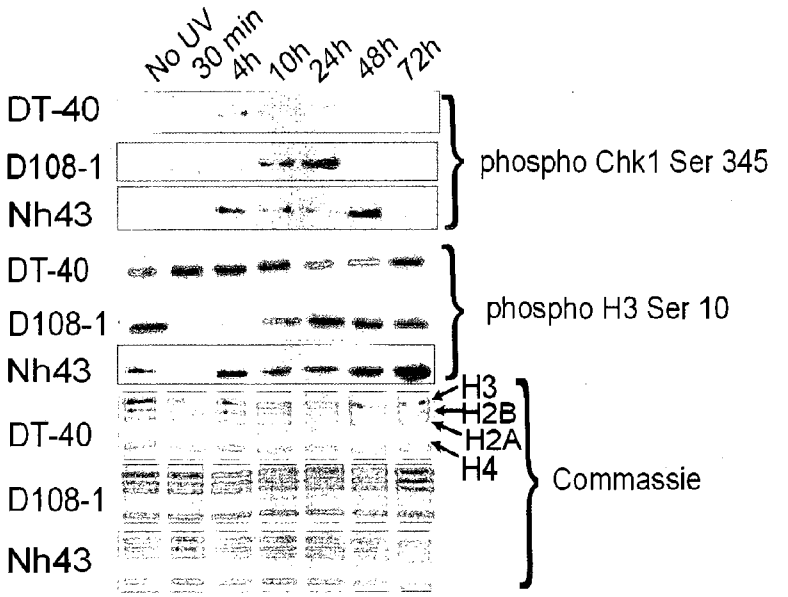

Legend:
DT40: wt
D108-1: N2-/-
Nh43: N1a-/-; N2-/-

Figure 9. Prolonged G_2/M checkpoint arrest and high mitotic arrest in HMGN1a-/-; HMGN2-/- cells. UV irradiated cell lines DT40, Nh43 and D108-1 were lysed at different time intervals. The proteins were resolved on a 15% SDS-PAGE. The whole cell lysates were subjected to Western blot analysis against phosphorylated Chk1 Ser345 and H3S10p. Equal loading of proteins was determined by Coomassie staining of a similar gel. The Western blot analysis indicated that D108-1 and Nh43 cells have high G_2/M arrest after 24 h and even 48 h as opposed to the wild-type cells, thus indication of prolonged G_2/M arrest. Nh43 has an early and increased mitotic arrest which is evidenced especially 4 hours and 72 hours after UV irradiation.

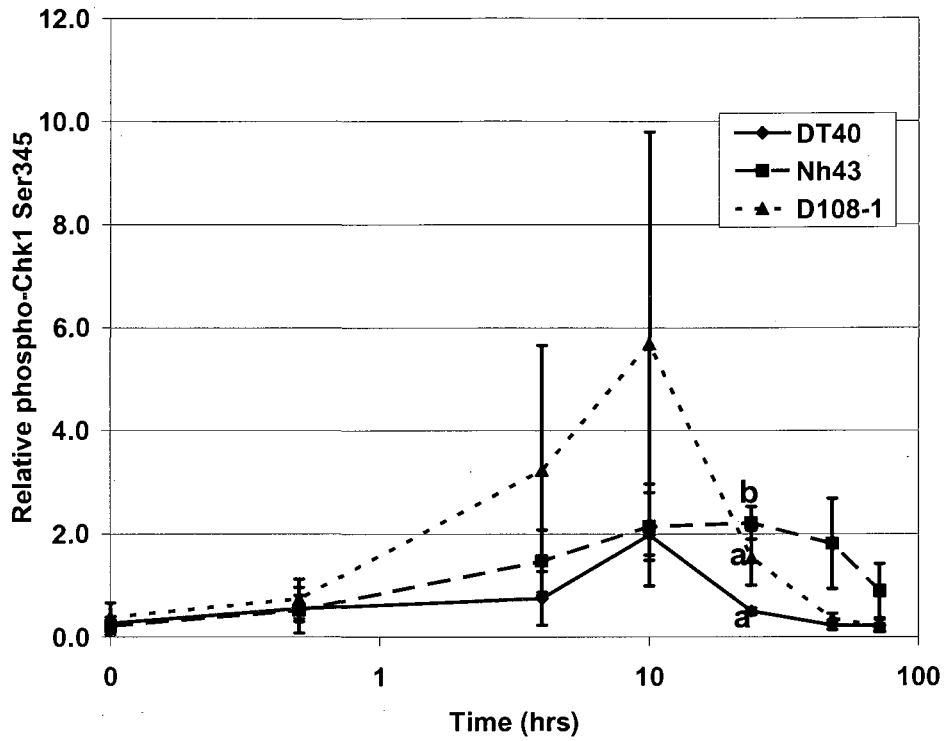

Legend:
DT40: wt
D108-1: N2-/-
Nh43: N1a-/-; N2-/-

Figure 10. Quantification of G_2/M checkpoint arrest in chicken HMGN null cells. The graph shows that HMGN1a-/-; N2-/- cells have a prolonged G_2/M arrest as compared to the wild-type and HMGN2-/- cells, 24 hours after UV irradiation (Kruskal-Wallis, $p \leq 0.1$). The relative phosphorylation of Chk1-Ser 345 is calculated as the ratio between the spot densitometric values of Ph-Chk1 (from Western blot) and the values of histone H3 or H4 (from Coomassie staining). Each data point represents the mean of three independent measurements (± SE) such as the one presented in Figure 9. Different letters (a and b) indicate cell lines with significant differences at the specific time point (Kruskal-Wallis, two-tailed, $p \leq 0.1$). Post-hoc analysis shows statistical differences between a and b.

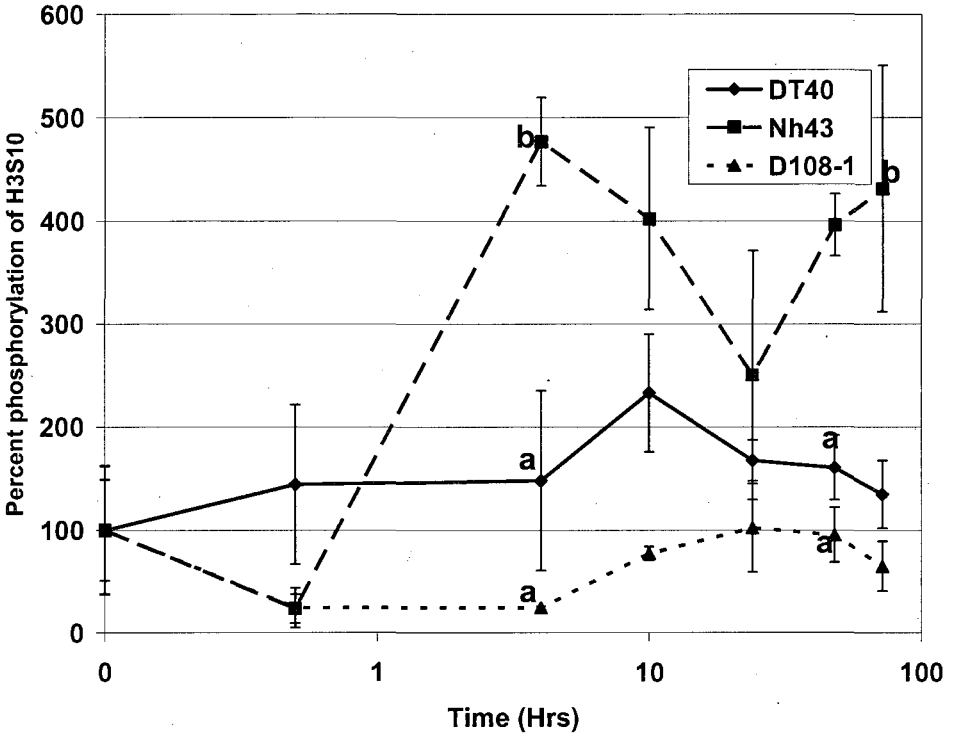

Legend:
DT40: wt
D108-1: N2-/-
Nh43: N1a-/-; N2-/-

Figure 11. Quantification of mitotic checkpoint arrest in chicken HMGN null cells. The graph shows that HMGN1a-/-; N2 cells have high mitotic arrest as compared to the wild-type and HMGN2-/- cells, 4 hours and 72 hours post-UV irradiation (Kruskal-Wallis, two-tailed, $p \leq 0.1$). The percent phosphorylation is calculated based on the ratio between the spot densitometric values of H3S10p (from the Western blot) and the levels of the histone H3 or H4 from Coomassie staining. Each data point represents the mean of three independent measurements (± SE) such as the one presented in Figure 9. Different letters (a and b) indicate cell lines with significant differences at the specific time point. The same letters indicate cell lines with no significant differences between each other at the specific time points. Post-hoc analysis shows statistical differences between a and b.

From the above experiments we concluded that, the UV-hypersensitivity of HMGN null cells, the high apoptosis and increased G_2/M checkpoint arrest are due to slow DNA repair rate. We therefore wanted to investigate the molecular mechanism by which HMGN1 protein is involved in the DNA repair pathway post-UV irradiation.

Experiment 7: Study of Core Histone Post-translational Modifications in Chicken HMGN1a-/-; N2-/- Cells Following UV Irradiation

There is ample evidence that acetylation of core histones is mechanistically important for DNA repair (Ramanathan and Smerdon, 1989). Recently, HMGNs were shown to modulate core histones post-translational modifications (Lim *et al.*, 2005). Therefore, the inability of HMGN null cells to repair DNA efficiently may be due to their deregulated core histone post-translational modifications.

We hypothesized that HMGNs are involved in the regulation of histone modifications after UV irradiation. Therefore, we compared the acetylation and methylation levels of several lysine residues in histones H3 and H4, in HMGN double null chicken cells and wild-type cells, as a function of time after UV irradiation. The reason we chose to continue this experiment on the HMGN1a/N2 double null cells and not on the mono null cells for HMGN1a or HMGN2 were that the double null cells showed a stronger effect in the cell cycle arrest experiments. HMGN double null cells and wild-type chicken cells were UV irradiated at 12 J/m^2 and cell lysates were prepared before UV irradiation and at

various time intervals post-UV irradiation: 0 minutes (non-irradiated), 30 minutes, 4 hours, 10 hours, 24 hours, 48 hours, and 72 hours. Here, no UV served as the basal line. The protein extracts were subjected to Western blot analysis using antibodies against acetylated histone H3 lysine 9 (H3K9ac), acetylated histone H3 lysine 14 (H3K14ac), acetylated histone H4 lysine 5 (H4K5ac) and trimethylated histone H3 lysine 9 (H3K9me3). Figure 12 represents Western blots of post-translational modifications of histones at different time points after UV irradiation. Accompanied with Figure 12, are the graphical representations of post-translational modifications of the histones obtained by five independent experiments (Figures 13–16).

Acetylation of histone H4 lysine 5, 48 hours post-UV irradiation was significantly higher in DT40 as compared to Nh43 and Bp5 (Figure 13) (non-parametric Kruskal-Wallis test, $p \leq 0.1$). Acetylation of histone H3 lysine 9 (H3K9ac), 48 hours after UV irradiation was significantly higher in DT40 as compared to Nh43 and Bp5 cells (Figure 14) (Kruskal-Wallis test, $p \leq 0.1$). The percent of acetylation of histone H3 lysine 14 (H3K14ac), 72 hours after UV irradiation was significantly higher in DT40 cells as compared to Nh43 and Bp5 cells (Figure 15) (Kruskal-Wallis test, $p \leq 0.1$).

This phenomenon of returning to the pre-UV acetylation steady state levels was observed only in the DT40 wild-type chicken cells but was lacking in the HMGN null cells. However, H3K9me3 (Figure 16) did not show any significant differences across the cell lines (Kruskal-Wallis test, $p > 0.1$).

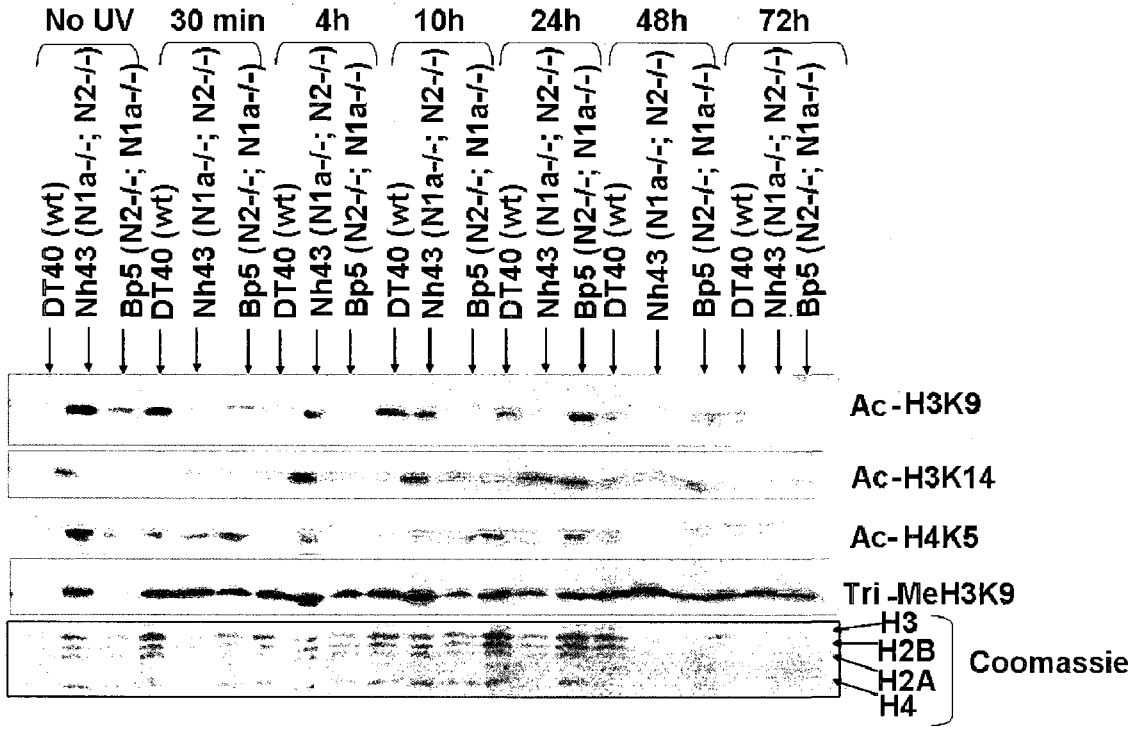

Figure 12. The effect of UV irradiation on post-translational modifications of histones H3 and H4 in wild-type and HMGN1a/N2 null chicken cells. Wild-type DT40 cells and HMGN double null cells were UV irradiated at 12 J/m^2 and whole cell lysates were obtained using 1X Laemelli buffer, at various times post-UV irradiation. The proteins were resolved on a 15% criterion SDS-PAGE (BIO-RAD). Post-translational modifications of these proteins were detected by Western blot analysis using specific antibodies against the various post-translational modifications as indicated in the figure (top four rows). The protein loading was quantified using Coomassie staining technique (bottom panel).

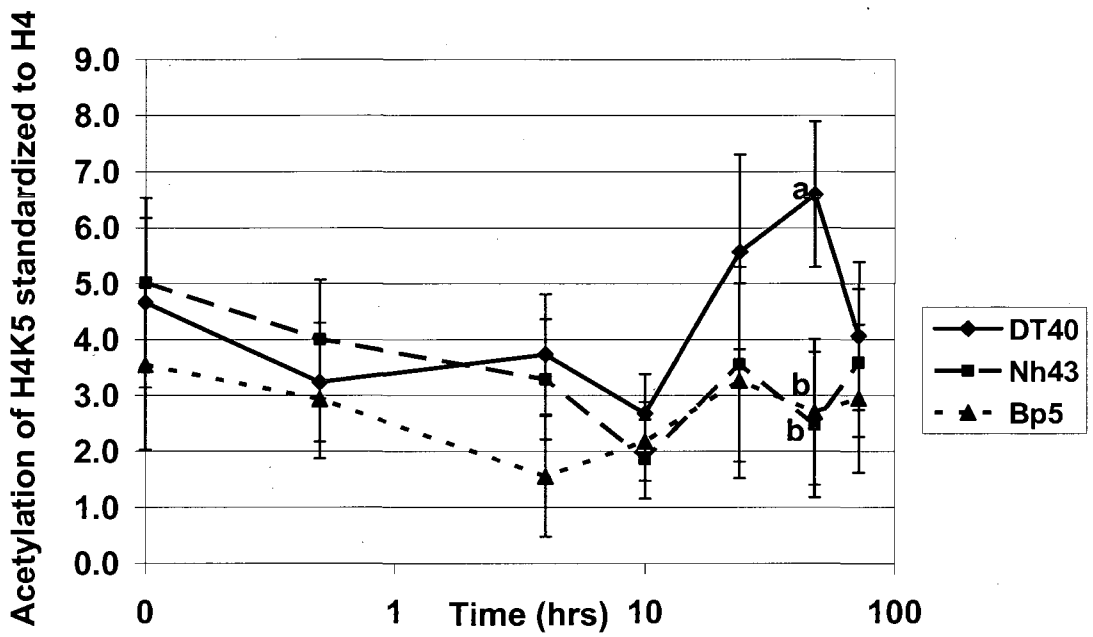

Figure 13. Kinetics of acetylation of histone H4 lysine 5 (H4K5ac) post-UV irradiation in wild-type DT40 and HMGN1a/N2 null chicken cells. The graph represents the effect of time after UV irradiation on the levels of H4K5ac as detected by Western blots on whole cell lysates, such as the one presented in Figure 12. Acetylation of histone H4 lysine 5, 48 hours post-UV irradiation was significantly higher in DT40 as compared to Nh43 and Bp5, (Kruskal-Wallis, $p \leq 0.1$). The standardized levels of acetylation were calculated as the ratio between the levels of H4K5ac obtained from the Western blot to the levels of histone H4 obtained from Coomassie staining. Spot densitometric analysis is carried out using Alpha Innotech software program. Each data point represents the mean of five independent experiments (± SE). Different letters (a and b) represent cell lines with significant differences in the specific time point. The same letters indicate cell lines with no significant differences between each other in the specific time point. Post-hoc analysis shows statistical differences between a and b.

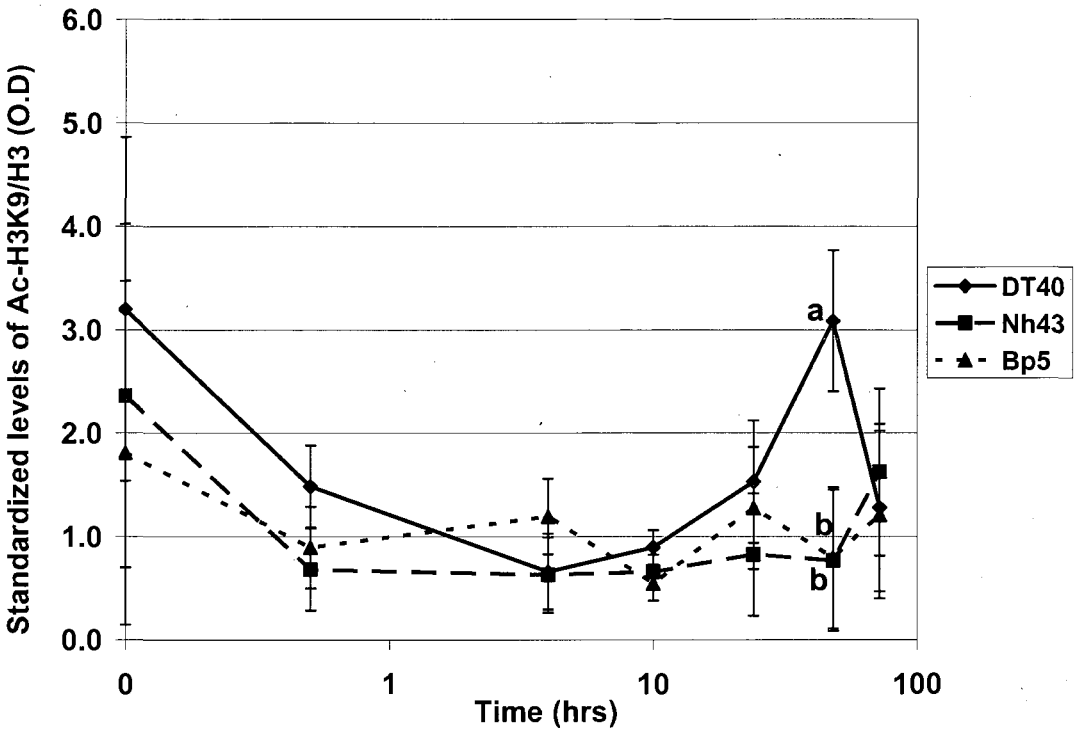

Figure 14. Kinetics of acetylation of histone H3 lysine 9 (H3K9ac) post-UV irradiation in wild-type DT40 and HMGN1a/N2 null chicken cells. The graph represents the effect of time after UV irradiation on the levels of H3K9ac as detected by Western blots on whole cell lysates, such as the one presented in Figure 12. Acetylation of histone H3 lysine 9, 48 hours post-UV irradiation was significantly higher in DT40 as compared to Nh43 and Bp5, (Kruskal-Wallis, $p \leq 0.1$). The standardized levels of acetylation were calculated as the ratio between the levels of H3K9ac obtained from the Western blot to the levels of histone H3 obtained from Coomassie staining. Spot densitometric analysis is carried out using Alpha Innotech software program. Each data point represents the mean of five independent experiments (± SE). Different letters (a and b) represent cell lines with significant differences in the specific time point. The same letters indicate cell lines with no significant differences between each other in the specific time point. Post-hoc analysis shows statistical differences between a and b.

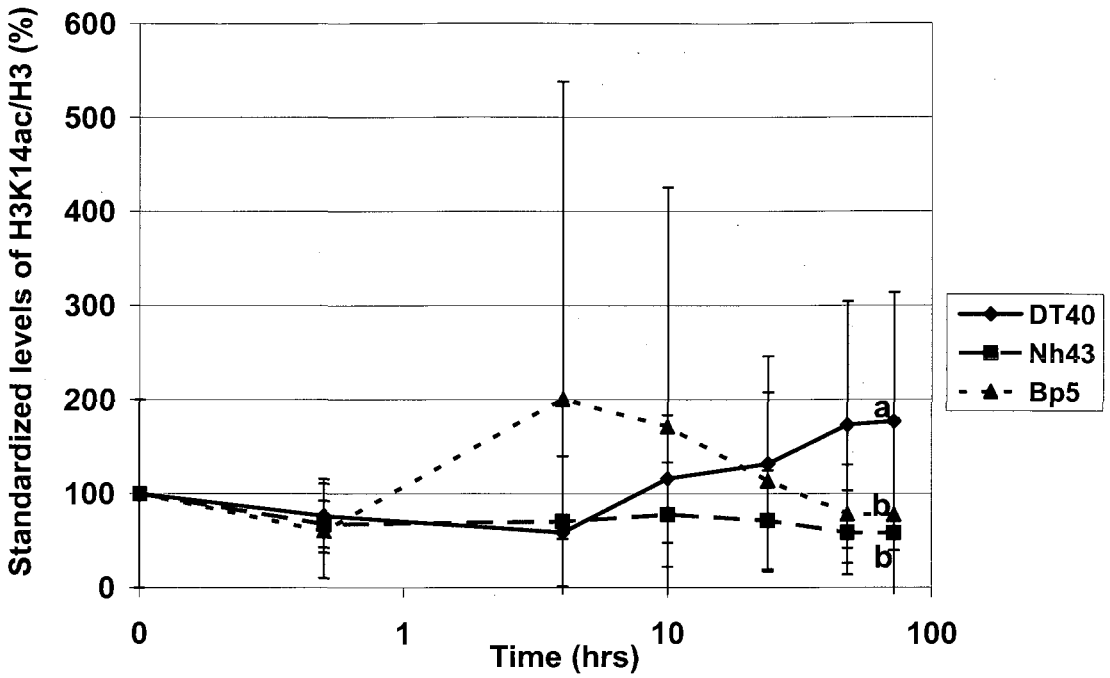

Figure 15. Kinetics of acetylation of histone H3 lysine 14 (H3K14ac) post-UV irradiation in wild-type DT40 and HMGN1a/N2 null chicken cells. The graph represents the effect of time after UV irradiation on the levels of H3K14ac as detected by Western blots on whole cell lysates, such as the one presented in Figure 12. Acetylation of histone H3 lysine 14, 72 hours post-UV irradiation was significantly higher in DT40 as compared to Nh43 and Bp5, (Kruskal-Wallis, $p \leq 0.1$). The percent acetylation is calculated as the ratio of the levels of H3K14ac obtained from the Western blot to the levels of histone H3 obtained from Coomassie staining. Spot densitometric analysis is carried out using Alpha Innotech software program. Each data point represents the mean of five independent experiments (± SE). Different letters (a and b) represent cell lines with significant differences in the specific time point. The same letters indicate cell lines with no significant differences between each other in the specific time point. Post-hoc analysis shows statistical differences between a and b.

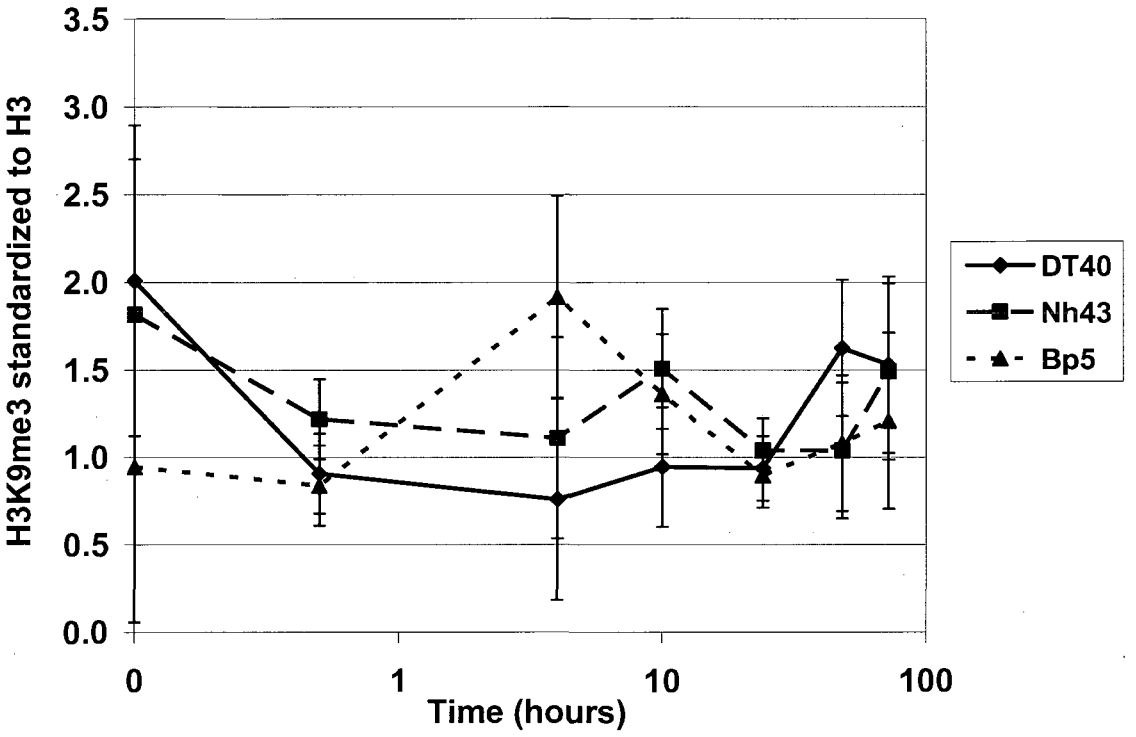

Figure 16. Kinetics of histone H3 lysine 9 trimethylation (H3K9me3) post-UV irradiation in wild-type DT40 and HMGN1a/N2 null chicken cells. The graph represents the relative levels of histone H3 lysine 9 trimethylation (H3K9me3) over the period of time. There were no significant differences in H3K9me3 across the cell lines over the period of time after UV irradiation, by non-parametric Kruskal-Wallis test, $p > 0.1$. The standardized levels of trimethylation were calculated as the ratio between the levels of H3K9me3 obtained from the Western blot to the levels of histone H3 obtained from Coomassie staining. Spot densitometric analysis is carried out using Alpha Innotech software program. Each data point represents the mean of five independent experiments (± SE).

Experiment 8: Core Histone Post-translational Modifications in HeLa Cells Following UV Irradiation

Since chicken cells demonstrated significantly a slower recovery in the acetylation levels of histones H3 and H4 after UV irradiation as a function of the presence of HMGN1a/N2 in the cells, we suggested that HMGNs may be involved in recruiting HATs to the chromatin following UV irradiation. Given that most commercially available antibodies are directed against human proteins, we decided to test our hypothesis in HeLa cells. To this end, we wanted to first test whether the human cells showed similar kinetics of PTMs to chicken cells following UV irradiation.

HeLa wild-type tag cells (containing empty vector plasmid) were UV irradiated at 30 J/m^2 and whole cell lysates were prepared at various time intervals after the irradiation. The lysates were then subjected to Western blot analysis using the following antibodies: anti-H3K9ac, anti-H3K14ac, and anti-H4K5ac (see Materials and Methods).

The Western blot analysis (Figure 17) and the graphical presentation (Figure 18) revealed a global wave of deacetylation reaching its maximum 4 h after UV irradiation in the respective sites: H4K5ac, H3K9ac and H3K14ac, in HeLa cells. After the 4 h point, there is a gradual increase in the acetylation of these residues back to pre-UV steady state levels. This phenomenon of returning to the pre-UV acetylation steady state levels was also observed in the DT40 wild-type chicken cells but was lacking in the HMGN null cells (Figures 13–15).

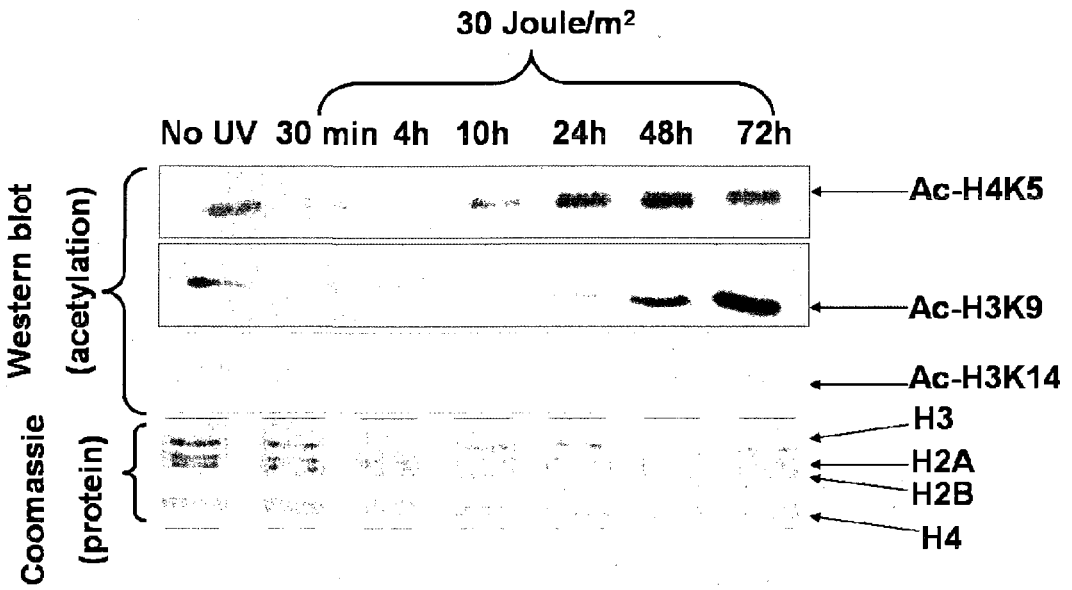

Figure 17. UV irradiation induces a rapid and global wave of deacetylation of core histones in HeLa cells. The top three rows represent Western blots displaying levels of three different acetyl lysines in histones H3 and H4 (as indicated). The bottom panel with the Coomassie staining demonstrates equal loading of proteins. The proteins were resolved on a 15% SDS-PAGE. The cells were irradiated at 30 J/m^2 and extracted at various time intervals post-UV irradiation. The proteins were resolved on the blots and were subjected to antibodies against: H3K9ac, H4K5ac and H3K14ac. UV irradiation induces a rapid and global wave of deacetylation of core histones in HeLa cells. Each experiment was repeated three independent times and the graphical presentation of the averages is shown in Figure 18.

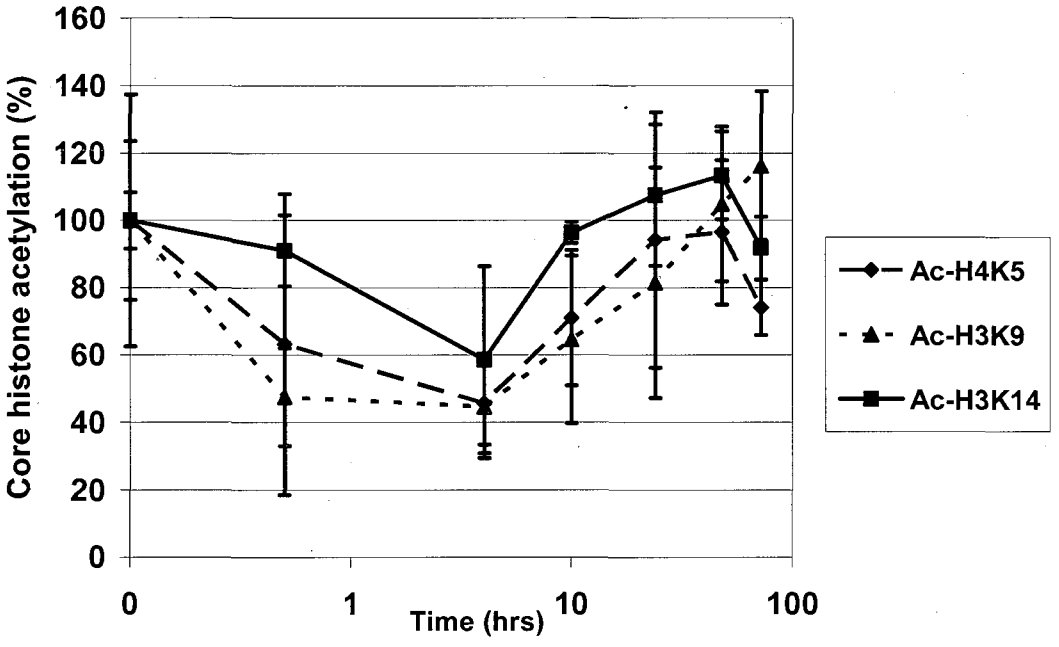

Figure 18. UV irradiation induces a rapid global wave of deacetylation of core histones H3 and H4 in HeLa cells (quantification). The graph represents percent acetylation over time (hours) post-UV irradiation. The cells were irradiated at 30 J/m^2 at different time intervals. The deacetylation reached its maximum at 4 hours in the respective residues: H3K9, H3K14 and H4K5. Each data point represents the mean of three independent repetitions (± SE) of the experiments show in Figure17. The levels of acetylation were measured by spot densitometry and standardized against the levels of H3 and H4.

Both chicken and human cells have similar post-translational modifications. They both have a wave of global deacetylation followed with an increase in the acetylation reaching to pre-UV steady state acetylation levels after UV irradiation (Figures 13–15). Since both cell lines had a phase of increased acetylation, we were able to test whether p300 or other HATs are associated with HMGN1 at these times (we tested no UV, 4 h, 10 h and 24 h after UV irradiation).

Experiment 9: Isolation of HMGN1 Overexpressing Clones for Co-immunoprecipitation

Since we observed change in the levels of histone acetylation after UV irradiation in HeLa cells, we decided to explore the possibility that HMGNs and HATs interact following UV irradiation and that HMGN recruit HATs to chromatin. Co-immunoprecipitations of HA-tagged HMGNs can be a useful tool for this purpose. HeLa cells previously stably transfected with recombinant HA-tagged *HMGN1* or *HMGN2* genes (Ogryzko *et al.*, 1998; Lim *et al.*, 2002) were cloned by limited dilution in 96 and 24 well-plates. The clones were analyzed to identify those that highly expressed HMGN proteins, using antibodies against HMGN1 and HMGN2 (gifts by Dr. Bustin) and against HA (Upstate Biotech). Equal loading was determined by Coomassie staining. Spot densitometric analysis was carried out to determine various HMGN expression levels. Clones that were determined to express high level of HMGNs were used for the subsequently described Co-IP assays. The clone C10 overexpressing HMGN1-HA tag was used for the following co-immunoprecipitation assay (Figure 19, Table 5).

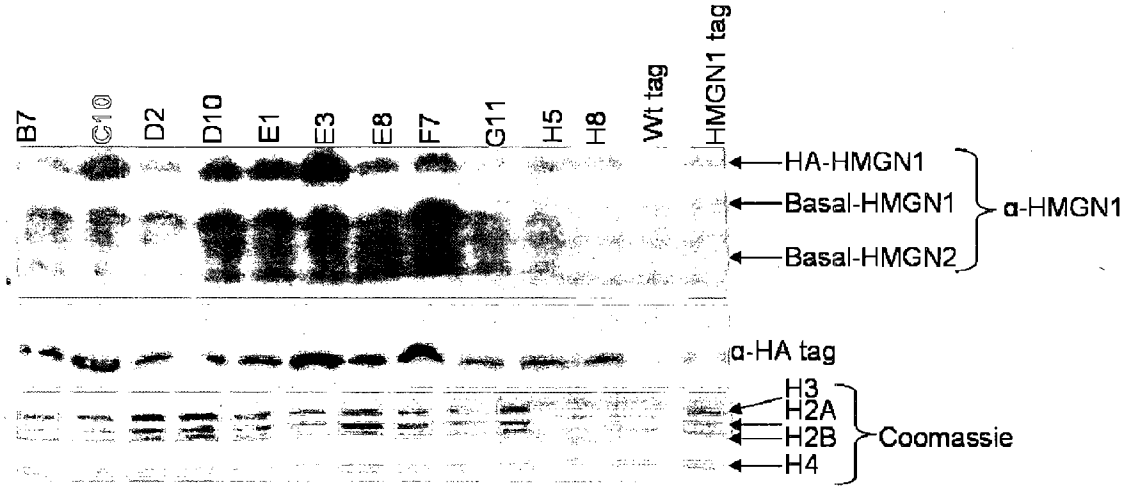

Figure 19. Analysis of the expression levels of HMGN1-HA in various stably transfected HeLa cell clones. (A) Western blot analysis of HMGN1 clones using antibodies against HMGN1 and against HA. The proteins were resolved on an 18% SDS-PAGE. HeLa cells stably transfected with recombinant HA-tagged HMGN1 genes were cloned by limited dilution and the clones were analyzed to identify high level HMGN-HA expressers. The bottom panel shows equal loading of protein lysates by Coomassie staining. Densitometric analysis was carried out to determine various levels of HMGN expression.

Table 5. Expression levels of HMGN1-HA protein in stably transfected HeLa cells.

Clones / Blots	B7	C10	D2	D10	E1	E3	E8	F7	G11	H5	H8
α-HMGN1	+	+++	+	++	++	+++	+	+++	+	++	+
α-HA	++	+++	++	++	++	+++	++	++	+	++	+
Expression level	L-M	H	L-M	M	M	H	L-M	M	L	M	L

Summarizes the levels of HMGN1-HA expression based on the Western blots shown in Figure 19.

Experiment 10: HAT Assay of HMGN1-immunoprecipitate Following UV Irradiation

We have demonstrated that in chicken cells the loss of HMGN1a and HMGN2 is associated with impaired NER-GGR and with decreased acetylation of H3K9, H3K14 and H4K5 after UV irradiation. Therefore, we suggested that in the later stages after UV irradiation HMGN may associate with HATs and tether them to the chromatin to increase the acetylation of these histone residues and consequently increase the repair efficiency.

Histone acetyltransferase p300 was reported to specifically acetylate but not associate with HMGN1 (Bergel *et al.*, 2000; Lim *et al.*, 2005). p300 has been found to interact with and acetylate non-histone proteins, like p53 (Iyer *et al.*, 1998) - a very important stress response protein and DNA repair protein (Iyer *et al.*, 1998). p300 was also found to be associated with newly synthesized DNA at UV-damaged sites, especially with PCNA (Hasan *et al.*, 2001), which is a key protein in DNA synthesis. Specific acetylation of HMGN1 by p300 weakens its

interaction with nucleosome cores (Bergel *et al.*, 2000.). HMGN1 elevates the levels of H3K14ac and H3K9ac by enhancing the action of HAT (Lim *et al.*, 2005; Belova *et al.*, 2008). However, an association between HMGNs and HATs was never reported.

To test for the possible association between HMGN1 and a HAT, we decided to test HMGN1 precipitates for HAT activity. The HAT activity in HMGN1 immunoprecipitates was determined by the following HAT assay. Whole cell protein extracts from HeLa C10 cells were immunoprecipitated with anti-HA antibody. The immunoprecipitate complexes were incubated in a HAT reaction buffer with core histones and Ac-CoA (72 μM) at 37°C, with constant agitation, for 40 minutes. The complex was then subjected to Western blot analysis using antibodies against H4K5ac and H3K14ac.

The HAT assay showed that HMGN1 immunoprecipitates are associated with acetylation activity of H4K5 for the most part before UV irradiation and 10 hours and 24 hours after UV irradiation (Figure 20, A and B). But a lower level HAT activity was also observed 4 h after UV irradiation. HMGN1 immunoprecipitates, both before and after UV irradiation, showed significantly higher acetylation activity of H4K5 as compared to the control, by non-parametric Wilcoxon-Signed Ranks test, $p \leq 0.1$ (Table 6). However, the HMGN1 immunoprecipitates did not associate with acetylation of H3K14ac before or after UV irradiation (Figure 20, A and B). The increase in acetylation of H4K5 10 hours and 24 hours post-UV irradiation observed in HeLa cells (Figure 18), especially

H4K5 correlates with the HMGN1 immunoprecipitated HAT activity in those time intervals (Figure 20B and Table 6). Nevertheless, these results indicated that HMGN1 is associated with a certain HAT and we wanted to identify this HAT by co-immunoprecipitation assays.

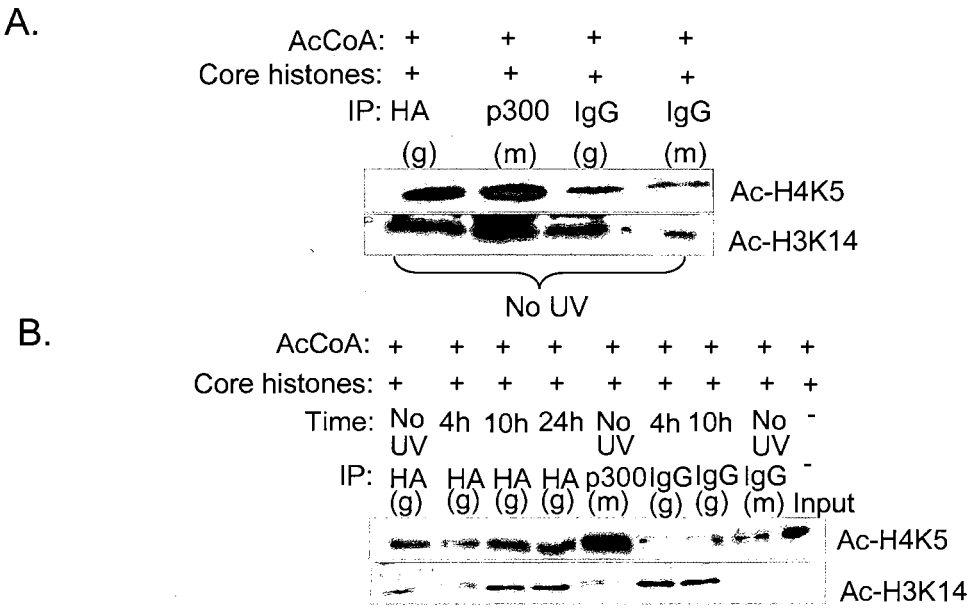

Figure 20. HAT activity is associated with immunoprecipitated HMGN1. (A) HAT assay in which non-irradiated whole cell lysates from HeLa cells were immunoprecipitated with anti-HA antibody and acetylation of free core histones (isolated from DT40 chicken cells) was detected using anti H4K5ac and anti H3K14ac antibodies. Cold 72 μM Ac-CoA was used for the reaction mixture and the mixture was incubated at 37°C for 40 minutes with constant agitation. (B) HMGN1 immunoprecipitates are associated with H4K5 acetylation especially before UV irradiation and 10 hours and 24 hours after UV irradiation, when immunoprecipitated with anti-HA antibody. The proteins were resolved on a 15% SDS-PAGE for both the experiments.

Table 6. Folds of acetylation of H4K5ac relatively to non-Immune IgG (control1).

control	No UV	4h	10h	24h	p300 (No UV)
1	2.28±0.70*	1.61±0.37*	2.38±0.89*	2.11±0.36*	5.32±2.75*

Represents the folds of acetylation of H4K5 in anti-HA immunoprecipitates relatively to non-Immune IgG shown in Figure 20B. The HMGN1 immunoprecipitates, both before and after UV irradiation, have significantly higher acetylation of H4K5 activity as compared to the control non- Immune IgG precipitates in HeLa overexpressing HMGN1 tag cells. These experiments were repeated three times independently. Note: * - significant differences by Wilcoxon-Signed Ranks test, one-tailed, $p \leq 0.1$.

Experiment 11: Co-immunoprecipitation Assay of HAT and HMGN1 Proteins

HMGN null cells showed slower recovery of acetylation of histones H3 and H4 after UV irradiation, we therefore suggested that HMGNs may be involved in recruiting HATs to the chromatin. Moreover, we have shown that HMGN1 immunoprecipitates were associated with HAT activity, we wanted to explore the specific HAT associated with HMGN1. Since the previous reports have shown that p300 is involved in NER, we hypothesized that HMGN1-p300 dimerization is induced by DNA damage after UV irradiation. The potential association of p300, and the p300 family HATs, p400 and CBP, with HMGN1 was explored by co-immunoprecipitation assay.

HMGN1-HA tag overexpressing HeLa cells (clone C10) were used for the co-immunoprecipitation assay. These cells were UV irradiated at 30 J/m^2 and whole cell and protein extracts were prepared at various time intervals after UV irradiation. The protein extracts were then subjected to immunoprecipitation with anti-HA or anti-HMGN1 antibodies and following Western blot with anti-p300, anti-p400, or anti-CBP (CREB - binding protein) antibodies.

Figure 21 is a control immunoprecipitation that shows goat- and rabbit-antibodies against human HMGN1 can efficiently precipitate HMGN1 in IP experiments. The association between p300 and HMGN1 was observed before UV irradiation and 2 minutes after UV irradiation (Figure 22D). The association between CBP and HMGN1 was observed 10 minutes and 24 hours after UV

irradiation (Figure 23, A and B). However, association between p400 and HMGN1 could not be observed before or after UV irradiation (Figure 24).

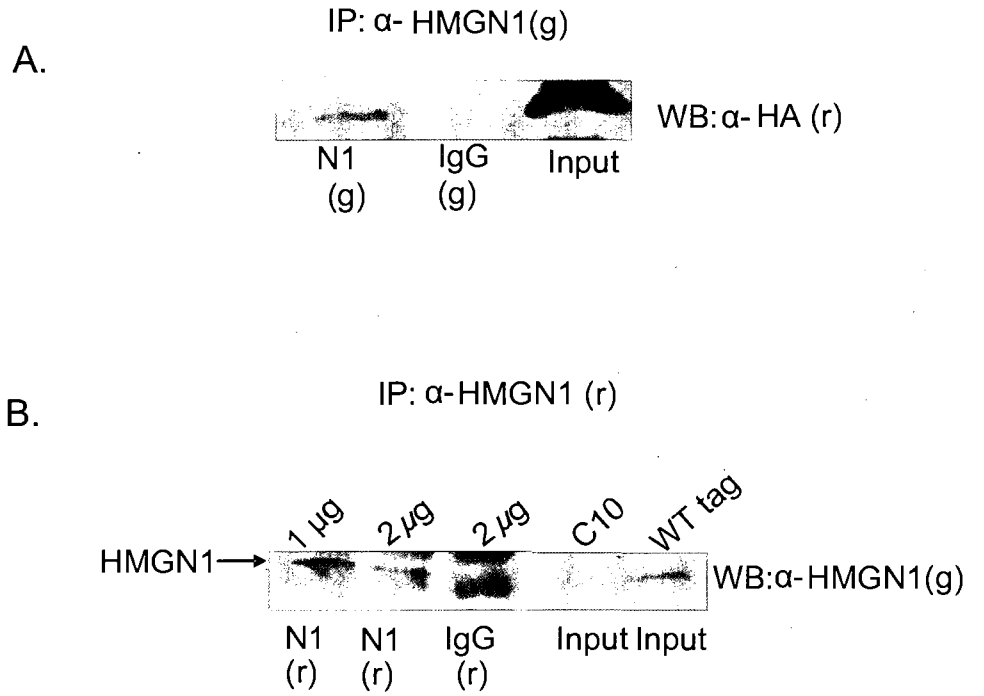

Figure 21. Goat- and rabbit-antibodies against human HMGN1 can efficiently precipitate HMGN1 in IP experiments. (A) Demonstrates that goat anti-HMGN1 immunoprecipitates HMGN1. (B) Demonstrates that rabbit anti-HMGN1 immunoprecipitates HMGN1. The proteins were resolved on a 15% SDS-PAGE.

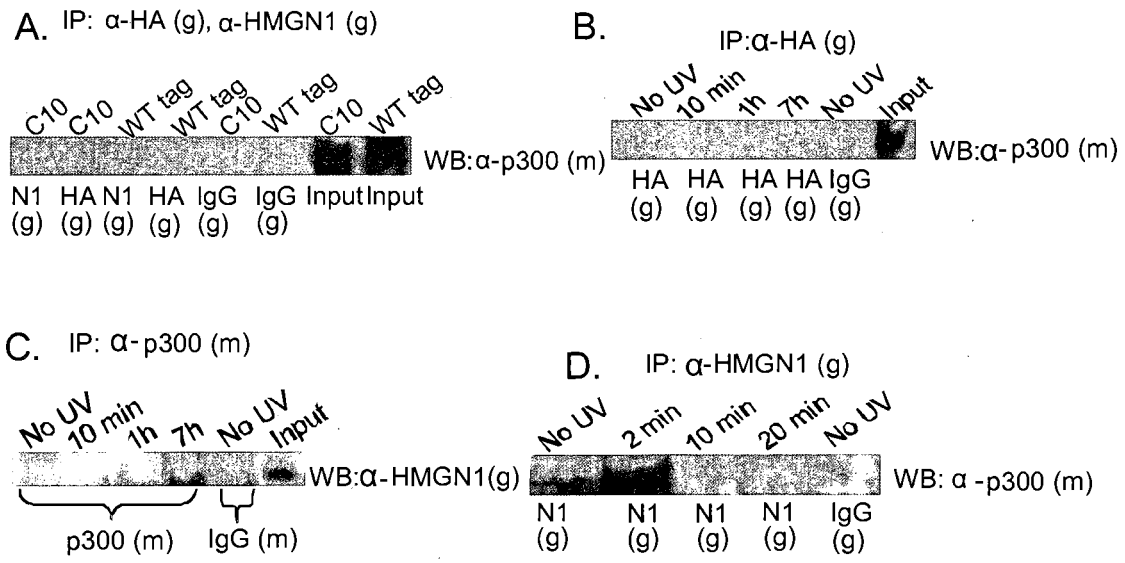

Figure 22. p300 and HMGN1 are associated with each other before and after UV irradiation in HeLa cells. (A) Immunoprecipitation with extracts from non-irradiated HMGN1- tag overexpressing cell-lines or HeLa wild-type tag cells, with anti-HMGN1 or anti-HA tag and detecting with anti-p300 antibody on the Western blot does not show any association. The proteins were resolved on a 5% SDS-PAGE. (B) Immunoprecipitation with extracts from UV irradiated and non-irradiated HMGN1- tag overexpressing cell-lines with anti-HA and detecting anti-p300, shows no association. The proteins were resolved on a 5% SDS-PAGE. (C) The reciprocal experiment of the above two experiments (Figure 22, A and B), where immunoprecipitation with extracts from HMGN1- tag overexpressing HeLa cells with anti-p300 antibody and detecting HMGN1 on Western blot did not show any association. The proteins were resolved on 18% SDS-PAGE. (D) Association between p300 and HMGN1 was observed before UV irradiation and 2 minutes after UV irradiation when immunoprecipitating with anti-HMGN1 antibody and Western blotting against p300. The proteins were resolved on a 5% SDS-PAGE.

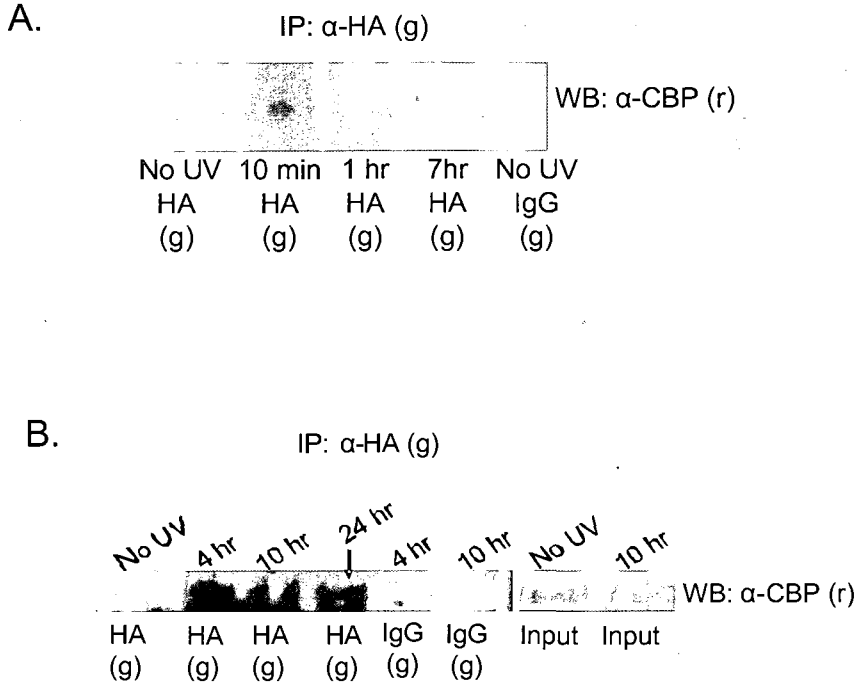

Figure 23. CBP and HMGN1 are associated with each other after UV irradiation in HeLa cells. (A) Association between CBP and HMGN1 was observed 10 minutes after UV irradiation when immunoprecipitating with goat-anti-HA antibody and Western blotting against CBP. The proteins were resolved on a 5% SDS-PAGE. (B) Association between HMGN1 and CBP was observed 24 hours after UV irradiation when immunoprecipitating with goat-anti-HA antibody and Western blotting against CBP. The proteins were resolved on a 5% SDS-PAGE.

A.

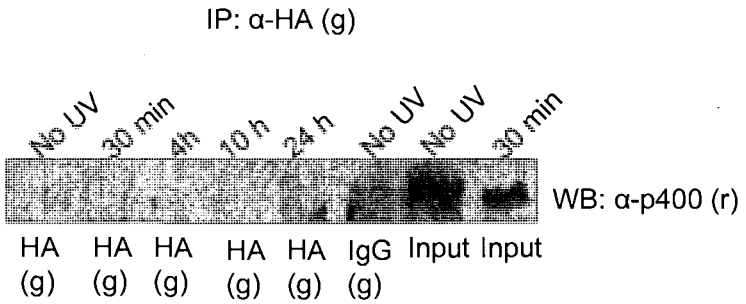

B.

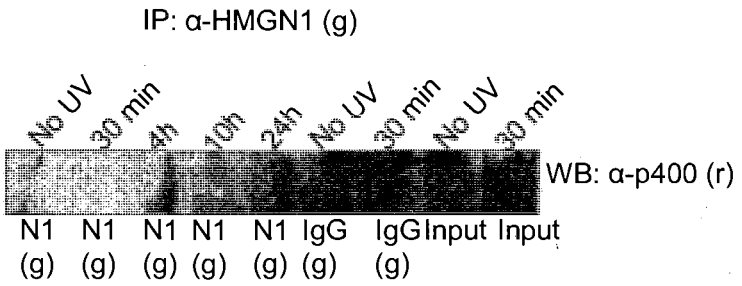

Figure 24. p400 and HMGN1 do not associate with each other before or after UV irradiation. (A) This figure shows no association between HMGN1 and p400 before UV irradiation or at various time intervals after UV irradiation, when HeLa whole cell protein extracts were immunoprecipitated with anti-HA antibody and anti-p400 was used for the Western blot. The proteins were resolved on a 5% SDS-PAGE. (B) This figure shows no association between HMGN1 and p400 before UV irradiation or at various time intervals after UV irradiation, when overexpressing HMGN1-tag whole cell protein extracts were immunoprecipitated with anti-HMGN1 antibody and anti-p400 was used for the Western blot. The proteins were resolved on a 5% SDS-PAGE.

Experiment 12: HMGN Null Cells Remove CPDs From DNA in a HAT-Independent Manner

So far we have shown that 24 hours following UV irradiation there was an increase in the acetylation of H3K9 and K14 and H4K5 in HeLa cells (see Figure 18). We have also shown that 48 h and 72 h following UV irradiation, there was a significant increase in the acetylation of histones H3 and H4 in the chicken wild-type cells as compared to the HMGN null chicken cells (see Figures 13–15). In addition, we have shown that HMGN1 immunoprecipitates a very significant HAT activity before UV irradiation and 10 and 24 hours after UV irradiation (see Figure 20B and Table 6). By co-immunoprecipitation assay, we have not only shown that before UV irradiation and 2 minutes after UV irradiation, HMGN1 associates with p300 (see Figure 22D) but also 10 minutes and 24 hours following UV irradiation HMGN1 associates with CBP (see Figure 23, A and B). The above experiments suggest that HMGNs repair function following UV irradiation, may need the association of HAT proteins. Therefore, we wanted to test whether HMGNs require HAT activity to enhance the DNA repair. If so, the lack of HMGNs in the cells and the consequent lower HAT activity and impaired DNA repair would be possibly rescued by addition of an HDAC inhibitor that will increase the level of acetylation after UV irradiation of HMGN null cells.

For this end we treated chicken DT40 cells and Nh43 (HMGN1a-/-; N2-/-) with trichostatin A (TSA) and tested if they would repair the UV-induced DNA damage more efficiently as compared to the untreated cells. The chicken cells

were treated with 2 μM TSA for 15 hours. The cells, at a concentration of 0.88 x 10^6 cells/ml, were plated in 260 mm petridishes and irradiated at 12 J/m^2. DNA was purified immediately after UV irradiation (time 0), and 7 h and 20 h after UV irradiation. The DNA was slot blotted onto nylon membrane and probed with antibodies directed against CPDs. To measure the amount of DNA loaded, the nylon membrane was stained with ethidium bromide.

Following UV irradiation there was a gradual decrease in the CPD content of the DNA of all the cells, an indication of active repair of the damaged DNA (Figure 25). The wild-type untreated cells showed a robust repair as compared with HMGN1a-/-; N2-/- cells. In the wild-type cells, 70% CPDs were removed from the chromatin 7 hours following UV irradiation in comparison with the double null cells, where only 10% CPDs were removed. This indicates that HMGNs are indeed required for the repair of the damaged DNA post-UV irradiation.

However, the TSA treated wild-type cells did not remove the CPDs as efficiently as compared to the untreated wild-type cells. Only 50% of the damage was removed, 7 hours following UV irradiation in comparison with the untreated wild-type cells (Figure 25) (Wilcoxon-Signed Ranks test, two tailed, $p > 0.1$). The DNA repair removal rate, 7 hours following UV irradiation remained the same in both treated and untreated double null cells (Figure 25) (Wilcoxon-Signed Ranks test, two tailed, $p > 0.1$).

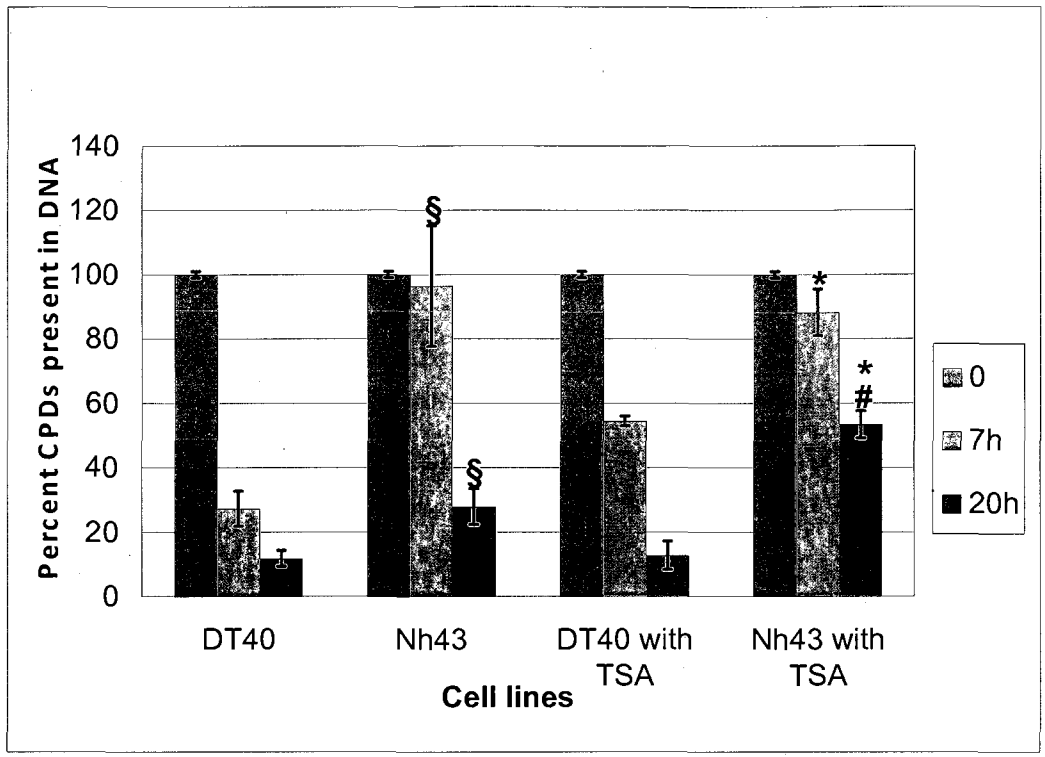

Figure 25. TSA treated HMGN null chicken cells show slow DNA repair rate similar to the untreated cells. Shown is southwestern analysis of the CPD removal rates in cells lacking both HMGN2 and HMGN1a (Nh43) compared to that of wild-type DT40 cells. DNA was extracted from cells at 0, 7 and 20 hours after UVC irradiated with a dose of 12 J/m^2 (see Materials and Methods). The CPD values were normalized against the DNA levels by staining the membranes with ethidium bromide. The CPD/DNA ratio was determined using spot densitometry of the CPD blot. The bar graph represents the kinetics of removal of photoproducts. The percent CPD is calculated based on the ratio of CPD levels at the given time interval after UV irradiation relatively to the levels of CPDs after 0 h. The graph represents the means and standard error bars from three independent experiments.

Note: *, § – Nh43 cell lines have a significantly slower CPD removal rate, 7 h and 20 h after UV irradiation as compared to DT40 cells, when treated or untreated with TSA by Mann-Whitney U test (two tailed, $p \leq 0.1$); Kruskal-Wallis test (two tailed, $p \leq 0.1$).

–TSA treated Nh43 cells have a significantly slower CPD removal rate as compared to untreated Nh43 cells, 20 h following UV irradiation by Wilcoxon-Signed Rank test (two tailed, $p \leq 0.1$).

However, TSA treated Nh43 cells have a significantly slower CPD removal rate as compared to untreated Nh43 cells, 20 h following UV irradiation (Figure 25) (Wilcoxon-Signed Rank test two tailed, $p \leq 0.1$). Following TSA treatment, Nh43 cell lines showed a significantly slower CPD removal rate, 7 h and 20 h after UV irradiation as compared to DT40 cells (Mann-Whitney U test, two tailed, $p \leq 0.1$). In conclusion, there was no significant increase in the DNA repair rate in the TSA treated wild-type cells. Moreover, the cells lacking both the HMGN variants did not show any effect on the DNA repair rate upon TSA treatment. Therefore, based on this experiment we suggest that HMGNs repair the UV-induced DNA damage independent of their interaction with HATs, at specific time intervals after UV irradiation.

CHAPTER IV

DISCUSSION

Our major goal in this work was to determine the role and molecular mechanism of HMGNs involvement in the UV response of vertebrate cells. We found that the nucleosomal binding proteins HMGNs are involved in the NER-GGR subpathway. By analyzing HMGN null cells, we have shown that HMGNs are important in UV-induced DNA damage response and are needed for efficient removal of the CPDs from the chromatin template. It was previously shown that DNA repair is associated with increasing acetylation at the damage site (Smerdon *et al.*, 1982). Recently several publications found that HMGNs are involved in modulating post-translational modifications of core histones (Postnikov *et al.*, 2006; Ueda *et al.*, 2006; Zhang and Wang, 2008). Therefore, we hypothesized that the mechanism by which HMGNs facilitate DNA repair is by modulating the post-translational modification of histones after UV irradiation. We further hypothesized that the association of HMGNs with HAT protein is the mechanism by which these proteins modulate the PTMs of histones and consequently facilitate the repair. The post-translational modification studies were conducted in chicken HMGN null cells and human HeLa cells by Western blot analysis at various time intervals after UV irradiation. These studies led us to

an unexpected finding — the levels of core histone acetylation actually decreased following UV irradiation, and they only increased 4 -10 hours after UV irradiation. We demonstrated, though, that HMGNs are playing a role in the post-UV irradiation increase of the core histone acetylation levels. Previous studies have identified the independent involvement of HMGN1 and p300 in the NER-TCR process (Fousteri *et al.*, 2006). We discovered an association of HMGNs with p300 before UV irradiation and immediately after UV irradiation. We also demonstrated an association of HMGNs with CBP 10 minutes and 24 hours after UV irradiation. Further support for the association of HMGNs with HATs came from demonstrating that HMGN1 immunoprecipitated HAT activity. On the other hand, the DNA repair capacity contributed by HMGNs is not related to their association with HATs since the DNA-repair rate in HMGN null cells treated with the HDAC inhibitor TSA does not increase.

Our results indicate that HMGN1 is involved in NER-GGR, but the association of HMGNs with p300/CBP and the HAT-activity do not correlate with the peak of the CPD removal. Thus, HMGNs are involved in NER-GGR by a HAT-dependent and by a HAT-independent pathway.

HMGN1a and HMGN2 are in the Same Pathway in UV-induced DNA Damage Response

Since cells lacking HMGNs had a lower survival after UV irradiation (Figure 4, Table 1), we concluded that HMGN proteins are important for the cells' response to UV. The double knockout HMGN cells did not show any major

additive or synergistic effect. These results indicated that for the most part HMGN1a and HMGN2 function in the different stages of the same pathway in conferring UV-resistance to cells. In other words, disrupting each of the HMGN genes alone was sufficient to reduce the UV tolerance to almost the same level as disrupting both the genes. However, these results could not rule out a partial redundancy between HMGN2 and HMGN1a which could possibly contribute to a minor additive effect.

We assessed if the UV hypersensitivity of HMGN null cells was due to growth rate advantage of the wild-type cells relatively to the HMGN null cells. This investigation was performed by the growth curve studies of the wild-type DT40 cell and HMGN null cells. Similar work was conducted by Schreiber and colleagues studying growth rate in UV-sensitive c-*fos* null cells (Schreiber *et al.*, 1995) and they did find a higher growth rate of the wild-type cells in comparison to the c-*fos* null cells. Previous work by Dr. Jerry Dodgson and others did not show significant growth rate differences in the HMGN null cell lines (Li *et al.*, 1997). In our study, we showed that, overall, there were no significant differences observed between the wild-type DT40 cells and the HMGN null cells (Tables 2 and 3). However, the saturation density and growth rate of cells disrupted for HMGN1a alone or disrupted for HMGN1a first followed by disrupting HMGN2 (Nh43) were higher and faster than the cells disrupted for HMGN2 first followed by HMGN1a (Bp5) or cells disrupted for HMGN2 (Figure 5, Tables 2 and 3).

The different growth patterns among these cells could be because of DNA imprinting or other epigenetic changes differentially induced by HMGN1a or HMGN2. Cells lacking HMGNs may have an irregular epigenetic steady state that contributes to the deregulated growth curve pattern. The growth pattern differences, however, did not correlate with the UV-sensitivity of the HMGN null cells and therefore, they did not appear to confer an advantage to the wild-type cells over the null cells.

HMGN1a/N2 are Involved in Global Genome Repair

Although the hypersensitivity of HMGN null cells could not be attributed to the growth rate of the cells, it could be explained by a slow DNA repair rate. Based on Southwestern blot analysis, we showed that HMGNs affect the repair rate of CPDs in the context of chromatin (Figure 6). Therefore, we concluded that the HMGN null cells hypersensitivity to UV irradiation is because of slower DNA repair rate. The increased rate of mortality in UV irradiated cells is linked to the activation of the apoptotic pathway (Martin and Cotter, 1991; Assefa *et al.*, 2003). Indeed, HMGN null cells showed higher apoptosis rate following UV irradiation (Figure 7). Cells lacking HMGN proteins also activated the apoptotic pathway faster, and therefore moved faster from early to late apoptosis (Figure 7, Table 4).

HMGN null cells had also a higher G_2/M population following UV irradiation (Figure 8, A and B). This increase in the G_2/M population indicated an

activation of either the G_2/M checkpoint arrest, or a mitotic checkpoint arrest, or both. In order to distinguish between these possibilities, we conducted a Western blot analysis with two antibodies, which served as specific markers for G_2/M arrest and mitotic arrest. Interestingly, the HMGN1a-/-; N2-/- cells, Nh43, had both an extended G_2-M checkpoint arrest and a significant mitotic arrest (Figures 9 and 11). In contrast, the null HMGN2-/- cells, D108-1, had mainly extended G_2-M arrest (Figures 9 and 10). A possible explanation might be that in the HMGN1a-/-; N2-/- cells there is a leakage of cells with DNA-damage through the G_2-M checkpoint to the mitosis phase, and it follows by their arrest in the mitotic checkpoints. This leakage is indicative of a possible role of HMGN1a in the activation of the G_2-M checkpoint. Evidence for the role of HMGN1 in the G_2-M checkpoint arrest was previously found in mice cells. In response to gamma irradiation, *Hmgn1-/-* mouse embryonic fibroblasts did not show a decrease in the mitotic population as opposed to the wild-type cells (Birger *et al.*, 2005). Therefore, the authors concluded the involvement of HMGN1 in G_2-M arrest (Birger *et al.*, 2005).

It is important to note that the differences between the null cell lines, D108-1 and Nh43, and the wild-type DT40 cells cannot be attributed to random mutations that may have accumulated in these cells, but only to the lack of HMGN proteins. The reason for excluding this possibility is that the two null cell lines were independently derived from DT40; Nh43 cells were first disrupted for

HMGN1a alleles and then for the two *HMGN2* alleles, so they were not derived from the D108-1 (HMGN2-/-) cells (Li and Dodgson, 1995; Li *et al.*, 1997). The higher apoptosis rate and increased checkpoint arrest of HMGN2-/- and HMGN1a-/-; N2-/- cells can be attributed to the lower removal rate of CPDs from chromatin (Figure 6).

A previous paper analyzing *Hmgn1* null mice cells indicated the involvement of these proteins in NER-TCR (Birger *et al.*, 2005). Another group indicated the participation of HMGN1 in TCR process in a specific complex associated with CSB protein in human fibroblast cells (Fousteri *et al.*, 2006). The former study conducted in mice could not demonstrate the role of HMGNs in NER-GGR since mice lack an efficient GGR subpathway. The latter group did not study the NER-GGR subpathway.

Our research shows for the first time the involvement of HMGN proteins in GGR. This is also the first time a higher apoptosis and a cell cycle arrest in HMGN null cells were observed following UV irradiation.

HMGNs Modulate PTMs After UV irradiation

HMGNs are known to modulate the PTMs of the histones, when bound to the nucleosomes (Lim *et al.*, 2005). Previous studies showed that loss of HMGN1 elevated the steady-state levels of H2AS1p throughout the cell cycle (Postnikov *et al.*, 2006). HMGNs affect also the phosphorylation of H3S10 and H3S28; acetylation of H3K14, and H3K9; methylation of H3K9 and modifications of H2A

(Ueda *et al.*, 2006). Thus, the interaction of HMGN with chromatin affects the levels of several types of modifications in the tails of the core histones (Ueda *et al.*, 2006). Lim and others showed that HMGN1 increases the levels of acetylation of nucleosomal but not free H3K14, a modification that has been linked to transcriptional activation and gene expression (Lim *et al.*, 2005).

Other reports link the involvement of HMGN proteins in stress response and their ability to modulate core histone PTMs. Cells with HMGN responded better to ionizing radiation (IR) in comparison to cells lacking HMGN1 because HMGN caused a higher basal level of acetylation of H3K14 and a higher activation of ATM. Treatment of *Hmgn1-/-* mouse embryonic fibroblasts (MEFs) with histone deacetylase inhibitors bypassed the HMGN1 requirement for efficient ATM activation (Kim *et al.*, 2009). Belova and colleagues showed that HMGN1 affects the acetylation of H3K14ac in response to heat shock stress (Belova *et al.*, 2008). Other studies suggested the involvement of other types of HMG proteins in UV stress response. Mammalian cells lacking HMGB1 proteins are hypersensitive to DNA damage induced by psoralen plus UVA irradiation (PUVA) or UVC radiation, showing less survival and increased mutagenesis (Lange *et al.*, 2008). In addition, the study revealed by immunoblotting, that cells lacking HMGB1 showed no histone acetylation upon DNA damage, in contrast to HMGB1 proficient cells (Lange *et al.*, 2008).

Our research, employing the chicken HMGN null cells gave us a unique insight into the role of HMGN proteins in modulation of histone acetylation upon UV irradiation and induction of NER-GGR. Post-translational modification studies in chicken HMGN null cells showed no increase in the acetylation of H3K9, H3K14 and H4K5, 48 hours and 72 hours, following UV irradiation (Figures 12–15). This may indicate that HMGNs have a role in maintaining the chromatin architecture after the removal of the photoproducts. For example, H4K5ac is known to mark new histones to be assembled in the chromatin during the last stage of repair (Benson *et al.*, 2007). Previous work by Bustin and others showed that HMGN1 modulates the levels of H3K14ac and H3K9ac (Lim *et al.*, 2005; Ueda *et al.*, 2006). However, there is no published data about the effect of HMGNs on the acetylation of H4K5. Our research contributes to the study of the effect of HMGNs following UV irradiation on this novel site of histone H4K5ac.

The trimethylation of H3K9 is known to code for suppression of transcription and this mark is associated with heterochromatin regions (Fischle *et al.*, 2003; Gonzalez-Gomez *et al.*, 2003; Lachner *et al.*, 2003). H3K9me3 is also known to serve as a mark for the binding of heterochromatin protein-1 (HP-1) which upon binding to these nucleosomes initiate heterochromatinization of the pericentric portion of the chromosome (Jacobs and Khorasanizadeh, 2002; Freitag *et al.*, 2004). Some reports showed that the acetylation of H3K9 and its trimethylation are mutually exclusive (Lachner *et al.*, 2004). However, based on

our research, despite the effect of HMGNs on increasing H3K9ac there is no effect on the trimethylation of H3K9 in chicken HMGN null cells and the wild-type cells (Figure 16). Thus, the trimethylation of H3K9 maintains its epigenetic state in the chromatin, independent of HMGNs. This finding indicated that HMGNs affect a different population of nucleosomes for the increase in H3K9ac rather than the nucleosome population which are marked by H3K9me3.

The PTM studies in chicken cells revealed that the phenomenon of returning to the pre-UV acetylation steady state levels was observed only in DT40 wild-type chicken cells but was lacking in HMGN null cells. HMGN null chicken cells demonstrated a significantly slower recovery of the acetylation levels of histones H3 and H4 after UV irradiation. We therefore suggested that HMGNs may be involved in recruiting HATs to chromatin following UV irradiation. Since most commercially available antibodies are directed against human proteins, we decided to test our hypothesis in human HeLa cell line. To further our study we wanted to first observe if human cells showed similar kinetics of PTMs to chicken cells following UV irradiation.

Previous studies showed hyperacetylation of H3K9 and H3K14 following UV irradiation in yeast at the repressed *MFA2* promoter (Yu *et al.*, 2005). These events occurred 30 minutes immediately after UV irradiation and the level of histone hyperacetylation diminished gradually as repair proceeded (Yu *et al.*, 2005). Yu and others emphasized that UV radiation triggers genome wide

hyperacetylation of both histones H3 and H4 in yeast (Yu *et al.*, 2005). Another study by Lange and colleagues showed increase in acetylation levels with time in MEF cells. The peak of acetylation of histone H4 was observed 30 minutes after UV irradiation and continued till 60 minutes (Lange *et al.*, 2008). The former group performed their experiments in yeast and was observing changes in acetylation levels at a specific gene following UV irradiation. The latter group irradiated the MEFs at 100 J/m^2 which could induce a massive apoptosis and thereby increase in acetylation levels. Moreover, they observed acetylation changes of histone H4 at large in shorter time intervals (1 minute to 60 minutes), and not at specific lysine residues of histone H4.

On the contrary, our results showed a wave of global deacetylation 4 hours after UV irradiation in both human and chicken cells (Figures 13–18). In agreement with our results, Tjeertes and others showed global deacetylation of histones H3K9 and H3K56 in response to UV irradiation and other stresses (Tjeertes *et al.*, 2009). The global wave of deacetylation in histones that was observed in our research is a result of UV-induced stress response. Several reasons could explain this wave of deacetylation:

(1) it could be part of compaction of chromatin to protect the chromatin from further molecular insult by UV irradiation; (2) it could be related to silencing of transcriptionally active genes to facilitate the repair in the following manner: a) to shut down transcription of active genes and direct some of the transcription

factors to repair or b) to channel the energy resources of the cells from gene transcription to repair. Recent studies from Tjeertes and others showed that H3K9Ac and H3K56Ac become diminished at promoter regions of both cell-cycle responsive and active genes in response to DNA damage (Tjeertes *et al.*, 2009); (3) it may be a completely unknown event.

HMGN1 Associates With HAT Proteins

The increased acetylation after UV irradiation in wild-type cells but not in HMGN null cells suggested the possibility of increased HMGN-dependent HAT activity in both chicken and human cells. Therefore we decided to explore if HMGN1 immunoprecipitates any HAT activity, which could indicate HMGN1-HAT association.

The *in vitro* assay showed that HMGN1 immunoprecipitated a significant HAT activity before UV irradiation and 4, 10 and 24 hours following UV irradiation in histone H4K5 (Figure 20B, Table 6). But the highest levels of HAT activity (2 folds or higher) were before UV irradiation and 10 and 24 hours after UV irradiation. The timing of highest HAT activity in HMGN1 immunoprecipitates coincided with the kinetics of the acetylation of H4K5, H3K9 and H3K14 in chicken and HeLa cells (Figures 13–18). This correlation could indicate that HMGNs were indeed involved in recruitment of HATs to chromatin after UV irradiation. This led us to further investigation to identify the specific HAT associated with HMGN1, using co-immunoprecipitation assay. Previous studies

have shown the involvement of p300 in DNA repair (Hasan *et al.*, 2001). P300 was also shown to acetylate HMGN (Bergel *et al.*, 2000). In addition, p300 was found to associate with several of its substrates such as p53 (Iyer *et al.*, 2004). We therefore hypothesized that p300 not only acetylates HMGN1 but also associates with it. Consequently, we chose antibodies against p300, CBP (homologue of p300) and p400 (belonging to the family of p300) for the co-immunoprecipitations. HMGN1 can unfold chromatin by competing with linker histones H1, by directly interacting with the N-terminal tails of core histones H3 and H2A, and by modulating the levels of PTMs (Bustin and Reeves, 1996; Bustin, 1999; Bustin, 2001). Based on previous theories the way HMGNs modulate the PTMs is by steric hindrance, but our work revealed another mechanism for post-translational modification regulation by HMGNs include the association with HAT proteins. By co-immunoprecipitation assays, p300 was shown to be associated with HMGN1 before UV irradiation and 2 minutes after UV irradiation (Figure 22D). Moreover, CBP was shown to associate with HMGN1 10 minutes and 24 hours following UV irradiation (Figure 23, A and B). This is the first time to the best of our knowledge that HMGN proteins are found to be associated with HATs. There is a very limited number of reports about the interaction of HMGNs with other proteins. Lim and colleagues showed that in HeLa nuclei a large fraction of the HMGN chromosomal proteins is found in multiple, metastable macromolecular complexes (Lim *et al.*, 2002). In another

study, HMGN1 proteins have been shown to associate with 14.3.3 proteins which impede the reentry of the proteins into the nucleus until the end of telophase (Prymakowska-Bosak *et al.*, 2002). Hansen and others showed that HMGN1 interacts specifically with both, estrogen receptor α (ERα) and serum response factor (SRF), which regulate the responses of Trefoil factor 1 (*TFF1*) and *FOS* to estrogen respectively (Zhu and Hansen, 2007). The latter work demonstrated the role of HMGN1 in regulating the expression of particular genes via specific protein-protein interactions with transcription factors at target gene regulatory regions (Zhu and Hansen, 2007).

HMGN1 is Involved in NER-GGR in HAT- Independent Manner

We have observed that cells lacking HMGNs have a lower HAT activity tethered to the HMGN proteins. If the association of HMGN1 and HAT proteins is needed for their DNA repair mechanism, by increasing the acetylation levels in HMGN null cells, we should be able to rescue the repair deficiency of cells. The increase in acetylation of histones can be achieved by HDAC inhibitors, such as TSA. Based on our results, TSA treated chicken HMGN null cells showed no difference or even slower (20 hour point) removal of CPDs in comparison to untreated HMGN null cells, indicating that HMGNs do not require HAT protein to enhance the repair rate (Figure 25). A previous study has shown that treatment with an HDAC inhibitor such as sodium butyrate improved DNA repair rate (Smerdon *et al.*, 1982). This study focused on measuring the DNA repair

synthesis and not on the CPD removal rate. However, the use of sodium butyrate in millimolar concentrations could have triggered other mechanisms, in addition to hyperacetylation of core histones which could affect the DNA repair synthesis.

The lack of increase in the DNA repair rates after HDAC treatment is in agreement with the fact that the acetylation of core histones increased after the peak of repair rate. These results could lead to a working model by which HMGN1 is participating in NER-GGR by both HAT-dependent and HAT-independent pathways as summarized below.

Mechanism of HMGN1 Involvement in NER-GGR

- Before UV irradiation, p300 is associated with HMGN1 (for details see Figure 26).
- Immediately after UV irradiation, CBP replaces p300 in associating HMGN1. We propose that CBP is acetylating HMGN1, thereby inducing its dissociation from active genes an event which facilitates directing it to the damage site.
- Four hours after UV irradiation, which is the peak of DNA repair, HMGN1's interaction with HATs is minimal. We predict that HMGN1 is still present in the vicinity of the damage site, suggesting that HMGN modulate DNA repair rate by unfolding the chromatin, but without interacting with HATs. This time point also marks the nadir of acetylation observed in both, human and chicken cells. At this time the chromatin may go through a

global compaction and heterochromatinization which is consistent with the timing of the decreased acetylation and HMGN-HAT interaction. The damage site may stay unfolded due to an increased HMGN and ATP dependent modeling complexes activity.

- Twenty four hours after UV irradiation, the CBP reassociates with HMGN1 an event which we believe is involved in reestablishing the pre-UV chromatin architecture. The cyclicity of the core histone acetylation status during the repair process observed by us marks as we believe, the cyclicity in the chromatin architecture as the repair process proceeds and eventually returns to the pre-UV steady state structure. This part of our model is also in agreement with Fousteri and others that suggested the involvement of HMGN1 in reestablishing the chromatin architecture after the damage removal in NER-TCR (Fousteri *et al.*, 2006).

This model is described in Figure 26, where we integrate the events following UV irradiation with the involvement of HMGN1 in the UV-induced DNA damage repair.

Our proposed model incorporates the fact that HMGN1 does not have to be associated with HAT protein through all the process, and therefore we hypothesize that HMGN1 is involved in NER-GGR by both HAT-dependent and HAT-independent pathways.

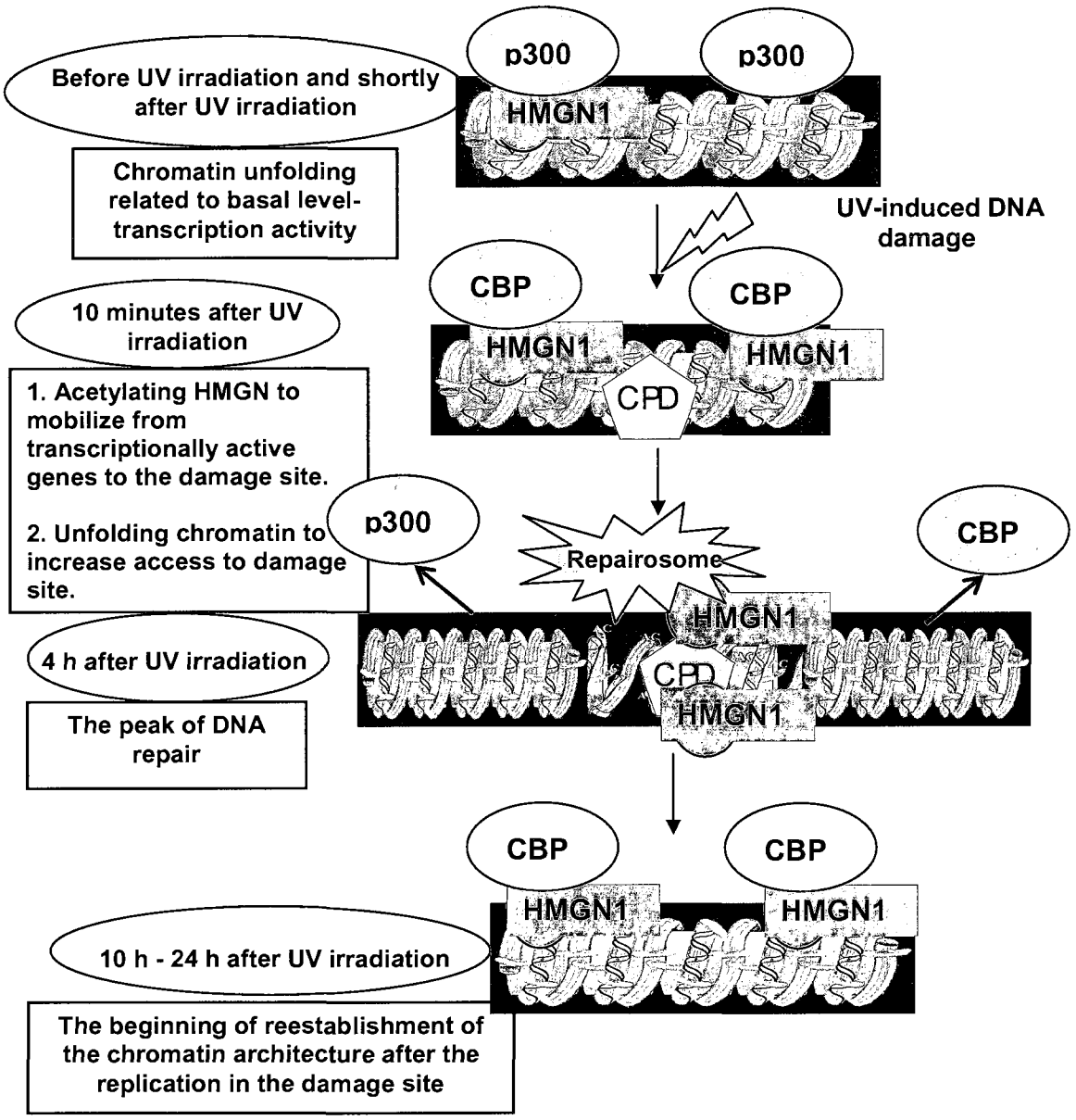

Figure 26. Proposed model for HMGN1's involvement in NER-GGR.

REFERENCES

Aboussekhra, A., and Thoma, F. (1999). TATA-binding protein promotes the selective formation of UV-induced (6-4)-photoproducts and modulates DNA repair in the TATA box. The EMBO journal *18*, 433-443.

Aboussekhra, A., Biggerstaff, M., Shivji, M.K., Vilpo, J.A., Moncollin, V., Podust, V.N., Protic, M., Hubscher, U., Egly, J.M., and Wood, R.D. (1995). Mammalian DNA nucleotide excision repair reconstituted with purified protein components. Cell *80*, 859-868.

Adair, J.E., Kwon, Y., Dement, G.A., Smerdon, M.J., and Reeves, R. (2005). Inhibition of nucleotide excision repair by high mobility group protein HMGA1. The Journal of biological chemistry *280*, 32184-32192.

Allison, S.J., and Milner, J. (2003). Loss of p53 has site-specific effects on histone H3 modification, including serine 10 phosphorylation important for maintenance of ploidy. Cancer research *63*, 6674-6679.

Ames, B.N., Shigenaga, M.K., and Hagen, T.M. (1993). Oxidants, antioxidants, and the degenerative diseases of aging. Proceedings of the National Academy of Sciences of the United States of America *90*, 7915-7922.

Assefa, Z., Garmyn, M., Vantieghem, A., Declercq, W., Vandenabeele, P., Vandenheede, J.R., and Agostinis, P. (2003). Ultraviolet B radiation-induced apoptosis in human keratinocytes: cytosolic activation of procaspase-8 and the role of Bcl-2. FEBS letters *540*, 125-132.

Belova, G.I., Postnikov, Y.V., Furusawa, T., Birger, Y., and Bustin, M. (2008). Chromosomal protein HMGN1 enhances the heat shock-induced remodeling of Hsp70 chromatin. The Journal of biological chemistry *283*, 8080-8088.

Benson, L.J., Phillips, J.A., Gu, Y., Parthun, M.R., Hoffman, C.S., and Annunziato, A.T. (2007). Properties of the type B histone acetyltransferase Hat1: H4 tail interaction, site preference, and involvement in DNA repair. The Journal of biological chemistry *282*, 836-842.

Bergel, M., Herrera, J.E., Thatcher, B.J., Prymakowska-Bosak, M., Vassilev, A., Nakatani, Y., Martin, B., and Bustin, M. (2000). Acetylation of novel sites in the nucleosomal binding domain of chromosomal protein HMG-14 by p300 alters its interaction with nucleosomes. The Journal of biological chemistry *275*, 11514-11520.

Bhakat, K.K., Hazra, T.K., and Mitra, S. (2004). Acetylation of the human DNA glycosylase NEIL2 and inhibition of its activity. Nucleic acids research *32*, 3033-3039.

Bhakat, K.K., Mokkapati, S.K., Boldogh, I., Hazra, T.K., and Mitra, S. (2006). Acetylation of human 8-oxoguanine-DNA glycosylase by p300 and its role in 8-oxoguanine repair *in vivo*. Molecular and cellular biology *26*, 1654-1665.

Bird, A.W., Yu, D.Y., Pray-Grant, M.G., Qiu, Q., Harmon, K.E., Megee, P.C., Grant, P.A., Smith, M.M., and Christman, M.F. (2002). Acetylation of histone H4 by Esa1 is required for DNA double-strand break repair. Nature *419*, 411-415.

Birger, Y., Catez, F., Furusawa, T., Lim, J.H., Prymakowska-Bosak, M., West, K.L., Postnikov, Y.V., Haines, D.C., and Bustin, M. (2005). Increased tumorigenicity and sensitivity to ionizing radiation upon loss of chromosomal protein HMGN1. Cancer research *65*, 6711-6718.

Birger, Y., Ito, Y., West, K.L., Landsman, D., and Bustin, M. (2001). HMGN4, a newly discovered nucleosome-binding protein encoded by an intronless gene. DNA and cell biology *20*, 257-264.

Birger, Y., West, K.L., Postnikov, Y.V., Lim, J.H., Furusawa, T., Wagner, J.P., Laufer, C.S., Kraemer, K.H., and Bustin, M. (2003). Chromosomal protein HMGN1 enhances the rate of DNA repair in chromatin. The EMBO journal *22*, 1665-1675.

Bustin, M. (1999). Regulation of DNA-dependent activities by the functional motifs of the high-mobility-group chromosomal proteins. Molecular and cellular biology *19*, 5237-5246.

Bustin, M. (2001). Chromatin unfolding and activation by HMGN(*) chromosomal proteins. Trends in biochemical sciences *26*, 431-437.

Bustin, M., and Reeves, R. (1996). High-mobility-group chromosomal proteins: architectural components that facilitate chromatin function. Progress in nucleic acid research and molecular biology *54*, 35-100.

Chen, Q., Dowhan, D.H., Liang, D., Moore, D.D., and Overbeek, P.A. (2002). CREB-binding protein/p300 co-activation of crystallin gene expression. The Journal of biological chemistry *277*, 24081-24089.

Coward, W.R., Watts, K., Feghali-Bostwick, C.A., Knox, A., and Pang, L. (2009). Defective histone acetylation is responsible for the diminished expression of cyclooxygenase 2 in idiopathic pulmonary fibrosis. Molecular and cellular biology *29*, 4325-4339.

Datta, A., Bagchi, S., Nag, A., Shiyanov, P., Adami, G.R., Yoon, T., and Raychaudhuri, P. (2001). The p48 subunit of the damaged-DNA binding protein DDB associates with the CBP/p300 family of histone acetyltransferase. Mutation research *486*, 89-97.

Devary, Y., Gottlieb, R.A., Smeal, T., and Karin, M. (1992). The mammalian ultraviolet response is triggered by activation of Src tyrosine kinases. Cell *71*, 1081-1091.

Ding, H.F., Bustin, M., and Hansen, U. (1997). Alleviation of histone H1-mediated transcriptional repression and chromatin compaction by the acidic activation region in chromosomal protein HMG-14. Molecular and cellular biology *17*, 5843-5855.

Ding, H.F., Rimsky, S., Batson, S.C., Bustin, M., and Hansen, U. (1994). Stimulation of RNA polymerase II elongation by chromosomal protein HMG-14. Science (New York, N.Y.) *265*, 796-799.

Ehrenhofer-Murray, A.E. (2004). Chromatin dynamics at DNA replication, transcription and repair. European journal of biochemistry / FEBS *271*, 2335-2349.

Ellis, N.A. (1997). DNA helicases in inherited human disorders. Current opinion in genetics & development *7*, 354-363.

Engelberg, D., Klein, C., Martinetto, H., Struhl, K., and Karin, M. (1994). The UV response involving the Ras signaling pathway and AP-1 transcription factors is conserved between yeast and mammals. Cell *77*, 381-390.

Espinosa, J.M., and Emerson, B.M. (2001). Transcriptional regulation by p53 through intrinsic DNA/chromatin binding and site-directed cofactor recruitment. Molecular cell *8*, 57-69.

Evans, E., Fellows, J., Coffer, A., and Wood, R.D. (1997a). Open complex formation around a lesion during nucleotide excision repair provides a structure for cleavage by human XPG protein. The EMBO journal *16*, 625-638.

Evans, E., Moggs, J.G., Hwang, J.R., Egly, J.M., and Wood, R.D. (1997b). Mechanism of open complex and dual incision formation by human nucleotide excision repair factors. The EMBO journal *16*, 6559-6573.

Fernandez-Capetillo, O., and Nussenzweig, A. (2004). Linking histone deacetylation with the repair of DNA breaks. Proceedings of the National Academy of Sciences of the United States of America *101*, 1427-1428.

Fernandez-Capetillo, O., Lee, A., Nussenzweig, M., and Nussenzweig, A. (2004). H2AX: the histone guardian of the genome. DNA repair *3*, 959-967.

Fischle, W., Wang, Y., Jacobs, S.A., Kim, Y., Allis, C.D., and Khorasanizadeh, S. (2003). Molecular basis for the discrimination of repressive methyl-lysine marks in histone H3 by Polycomb and HP1 chromodomains. Genes & development *17*, 1870-1881.

Fousteri, M., and Mullenders, L.H. (2008). Transcription-coupled nucleotide excision repair in mammalian cells: molecular mechanisms and biological effects. Cell research *18*, 73-84.

Fousteri, M., Vermeulen, W., van Zeeland, A.A., and Mullenders, L.H. (2006). Cockayne syndrome A and B proteins differentially regulate recruitment of chromatin remodeling and repair factors to stalled RNA polymerase II *in vivo*. Molecular cell *23*, 471-482.

Freitag, M., Hickey, P.C., Khlafallah, T.K., Read, N.D., and Selker, E.U. (2004). HP1 is essential for DNA methylation in neurospora. Molecular cell *13*, 427-434.

Gale, J.M., Nissen, K.A., and Smerdon, M.J. (1987). UV-induced formation of pyrimidine dimers in nucleosome core DNA is strongly modulated with a period of 10.3 bases. Proceedings of the National Academy of Sciences of the United States of America *84*, 6644-6648.

Galiova, G., Bartova, E., Raska, I., Krejci, J., and Kozubek, S. (2008). Chromatin changes induced by lamin A/C deficiency and the histone deacetylase inhibitor trichostatin A. European journal of cell biology *87*, 291-303.

Gonzalez-Gomez, P., Bello, M.J., Arjona, D., Lomas, J., Alonso, M.E., De Campos, J.M., Vaquero, J., Isla, A., Gutierrez, M., and Rey, J.A. (2003). Promoter hypermethylation of multiple genes in astrocytic gliomas. International journal of oncology *22*, 601-608.

Gray, S.G., and Teh, B.T. (2001). Histone acetylation/deacetylation and cancer: an "open" and "shut" case? Current molecular medicine *1*, 401-429.
Green, C.M., and Almouzni, G. (2002). When repair meets chromatin. First in series on chromatin dynamics. EMBO reports *3*, 28-33.

Hara, R., Mo, J., and Sancar, A. (2000). DNA damage in the nucleosome core is refractory to repair by human excision nuclease. Molecular and cellular biology *20*, 9173-9181.

Harvey Lodish, A.B., Chris A. Kaiser, Monty Krieger, Matthew P. Scott, Anthony Bretscher, Hidde Ploegh, Paul Matsudaira (2007). Molecular Cell Biology. W. H. Freeman; 6th edition.

Hasan, S., Hassa, P.O., Imhof, R., and Hottiger, M.O. (2001). Transcription coactivator p300 binds PCNA and may have a role in DNA repair synthesis. Nature *410*, 387-391.

Herrera, J.E., Sakaguchi, K., Bergel, M., Trieschmann, L., Nakatani, Y., and Bustin, M. (1999). Specific acetylation of chromosomal protein HMG-17 by PCAF alters its interaction with nucleosomes. Molecular and cellular biology *19*, 3466-3473.

Herrlich, P., Ponta, H., and Rahmsdorf, H.J. (1992). DNA damage-induced gene expression: signal transduction and relation to growth factor signaling. Reviews of physiology, biochemistry and pharmacology *119*, 187-223.

Hill, D.A., Peterson, C.L., and Imbalzano, A.N. (2005). Effects of HMGN1 on chromatin structure and SWI/SNF-mediated chromatin remodeling. The Journal of biological chemistry *280*, 41777-41783.

Iyer, N.G., Chin, S.F., Ozdag, H., Daigo, Y., Hu, D.E., Cariati, M., Brindle, K., Aparicio, S., and Caldas, C. (2004). p300 regulates p53-dependent apoptosis after DNA damage in colorectal cancer cells by modulation of PUMA/p21 levels. Proceedings of the National Academy of Sciences of the United States of America *101*, 7386-7391.

Jacobs, S.A., and Khorasanizadeh, S. (2002). Structure of HP1 chromodomain bound to a lysine 9-methylated histone H3 tail. Science (New York, N.Y.) *295*, 2080-2083.

James D. Watson, T.A.B., Stephen P. Bell, Alexander A. F. Gann, Michael Levine, Richard M. Losick. (2007). Molecular Biology of the Gene. Benjamin Cummings; 6th edition.

Kawamura, T., Ono, K., Morimoto, T., Wada, H., Hirai, M., Hidaka, K., Morisaki, T., Heike, T., Nakahata, T., Kita, T., and Hasegawa, K. (2005). Acetylation of GATA-4 is involved in the differentiation of embryonic stem cells into cardiac myocytes. The Journal of biological chemistry *280*, 19682-19688.

Kim, J.K., and Choi, B.S. (1995). The solution structure of DNA duplex-decamer containing the (6-4) photoproduct of thymidylyl(3'-->5')thymidine by NMR and relaxation matrix refinement. European journal of biochemistry / FEBS *228*, 849-854.

Kim, Y.C., Gerlitz, G., Furusawa, T., Catez, F., Nussenzweig, A., Oh, K.S., Kraemer, K.H., Shiloh, Y., and Bustin, M. (2009). Activation of ATM depends on chromatin interactions occurring before induction of DNA damage. Nature cell biology *11*, 92-96.

Lachner, M., O'Sullivan, R.J., and Jenuwein, T. (2003). An epigenetic road map for histone lysine methylation. Journal of cell science *116*, 2117-2124.

Lachner, M., Sengupta, R., Schotta, G., and Jenuwein, T. (2004). Trilogies of histone lysine methylation as epigenetic landmarks of the eukaryotic genome. Cold Spring Harbor symposia on quantitative biology *69*, 209-218.

Lange, S.S., Mitchell, D.L., and Vasquez, K.M. (2008). High mobility group protein B1 enhances DNA repair and chromatin modification after DNA damage. Proceedings of the National Academy of Sciences of the United States of America *105*, 10320-10325.

Li, Y., and Dodgson, J.B. (1995). The chicken HMG-17 gene is dispensable for cell growth *in vitro*. Molecular and cellular biology *15*, 5516-5523.

Li, Y., Strahler, J.R., and Dodgson, J.B. (1997). Neither HMG-14a nor HMG-17 gene function is required for growth of chicken DT40 cells or maintenance of DNaseI-hypersensitive sites. Nucleic acids research *25*, 283-288.

Lim, J.H., Bustin, M., Ogryzko, V.V., and Postnikov, Y.V. (2002). Metastable macromolecular complexes containing high mobility group nucleosome-binding chromosomal proteins in HeLa nuclei. The Journal of biological chemistry *277*, 20774-20782.

Lim, J.H., West, K.L., Rubinstein, Y., Bergel, M., Postnikov, Y.V., and Bustin, M. (2005). Chromosomal protein HMGN1 enhances the acetylation of lysine 14 in histone H3. The EMBO journal *24*, 3038-3048.

Liu, X., Mann, D.B., Suquet, C., Springer, D.L., and Smerdon, M.J. (2000). Ultraviolet damage and nucleosome folding of the 5S ribosomal RNA gene. Biochemistry *39*, 557-566.

Luger, K., Mader, A.W., Richmond, R.K., Sargent, D.F., and Richmond, T.J. (1997). Crystal structure of the nucleosome core particle at 2.8 A resolution. Nature *389*, 251-260.

Martin, S.J., and Cotter, T.G. (1991). Ultraviolet B irradiation of human leukemia HL-60 cells *in vitro* induces apoptosis. International journal of radiation biology *59*, 1001-1016.

Martinez, E., Palhan, V.B., Tjernberg, A., Lymar, E.S., Gamper, A.M., Kundu, T.K., Chait, B.T., and Roeder, R.G. (2001). Human STAGA complex is a chromatin-acetylating transcription coactivator that interacts with pre-mRNA splicing and DNA damage-binding factors *in vivo*. Molecular and cellular biology *21*, 6782-6795.

Mitchell, D.L., Nguyen, T.D., and Cleaver, J.E. (1990). Nonrandom induction of pyrimidine-pyrimidone (6-4) photoproducts in ultraviolet-irradiated human chromatin. The Journal of biological chemistry *265*, 5353-5356.

Nakamura, Y. (2004). Isolation of p53-target genes and their functional analysis. Cancer science *95*, 7-11.

Niida, H., and Nakanishi, M. (2006). DNA damage checkpoints in mammals. Mutagenesis *21*, 3-9.

Nishi, R., Okuda, Y., Watanabe, E., Mori, T., Iwai, S., Masutani, C., Sugasawa, K., and Hanaoka, F. (2005). Centrin 2 stimulates nucleotide excision repair by interacting with xeroderma pigmentosum group C protein. Molecular and cellular biology *25*, 5664-5674.

O'Donovan, A., Davies, A.A., Moggs, J.G., West, S.C., and Wood, R.D. (1994). XPG endonuclease makes the 3' incision in human DNA nucleotide excision repair. Nature *371*, 432-435.

Ogryzko, V.V., Kotani, T., Zhang, X., Schiltz, R.L., Howard, T., Yang, X.J., Howard, B.H., Qin, J., and Nakatani, Y. (1998). Histone-like TAFs within the PCAF histone acetylase complex. Cell *94*, 35-44.

Pannetier, M., Julien, E., Schotta, G., Tardat, M., Sardet, C., Jenuwein, T., and Feil, R. (2008). PR-SET7 and SUV4-20H regulate H4 lysine-20 methylation at imprinting control regions in the mouse. EMBO reports *9*, 998-1005.

Paranjape, S.M., Krumm, A., and Kadonaga, J.T. (1995). HMG17 is a chromatin-specific transcriptional coactivator that increases the efficiency of transcription initiation. Genes & development *9*, 1978-1991.

Park, C.H., Bessho, T., Matsunaga, T., and Sancar, A. (1995). Purification and characterization of the XPF-ERCC1 complex of human DNA repair excision nuclease. The Journal of biological chemistry *270*, 22657-22660.

Pehrson, J.R. (1995). Probing the conformation of nucleosome linker DNA *in situ* with pyrimidine dimer formation. The Journal of biological chemistry *270*, 22440-22444.

Peterson, C.L., and Cote, J. (2004). Cellular machineries for chromosomal DNA repair. Genes & development *18*, 602-616.

Pfeifer, G.P. (1997). Formation and processing of UV photoproducts: effects of DNA sequence and chromatin environment. Photochemistry and photobiology *65*, 270-283.

Postnikov, Y.V., Belova, G.I., Lim, J.H., and Bustin, M. (2006). Chromosomal protein HMGN1 modulates the phosphorylation of serine 1 in histone H2A. Biochemistry *45*, 15092-15099.

Prymakowska-Bosak, M., Hock, R., Catez, F., Lim, J.H., Birger, Y., Shirakawa, H., Lee, K., and Bustin, M. (2002). Mitotic phosphorylation of chromosomal protein HMGN1 inhibits nuclear import and promotes interaction with 14.3.3 proteins. Molecular and cellular biology *22*, 6809-6819.

Qin, S., and Parthun, M.R. (2002). Histone H3 and the histone acetyltransferase Hat1p contribute to DNA double-strand break repair. Molecular and cellular biology *22*, 8353-8365.

Ramanathan, B., and Smerdon, M.J. (1989). Enhanced DNA repair synthesis in hyperacetylated nucleosomes. The Journal of biological chemistry *264*, 11026-11034.

Rapic-Otrin, V., McLenigan, M.P., Bisi, D.C., Gonzalez, M., and Levine, A.S. (2002). Sequential binding of UV DNA damage binding factor and degradation of the p48 subunit as early events after UV irradiation. Nucleic acids research *30*, 2588-2598.

Riedl, T., Hanaoka, F., and Egly, J.M. (2003). The comings and goings of nucleotide excision repair factors on damaged DNA. The EMBO journal *22*, 5293-5303.

Rochman, M., Postnikov, Y., Correll, S., Malicet, C., Wincovitch, S., Karpova, T.S., McNally, J.G., Wu, X., Bubunenko, N.A., Grigoryev, S., and Bustin, M. (2009). The interaction of NSBP1/HMGN5 with nucleosomes in euchromatin counteracts linker histone-mediated chromatin compaction and modulates transcription. Molecular cell *35*, 642-656.

Ronai, Z.A., Lambert, M.E., and Weinstein, I.B. (1990). Inducible cellular responses to ultraviolet light irradiation and other mediators of DNA damage in mammalian cells. Cell biology and toxicology *6*, 105-126.

Rubbi, C.P., and Milner, J. (2003). p53 is a chromatin accessibility factor for nucleotide excision repair of DNA damage. The EMBO journal *22*, 975-986.

Saka, Y., Esashi, F., Matsusaka, T., Mochida, S., and Yanagida, M. (1997). Damage and replication checkpoint control in fission yeast is ensured by interactions of Crb2, a protein with BRCT motif, with Cut5 and Chk1. Genes & development *11*, 3387-3400.

Sancar, A., Lindsey-Boltz, L.A., Unsal-Kacmaz, K., and Linn, S. (2004). Molecular mechanisms of mammalian DNA repair and the DNA damage checkpoints. Annual review of biochemistry *73*, 39-85.

Schreiber, M., Baumann, B., Cotten, M., Angel, P., and Wagner, E.F. (1995). Fos is an essential component of the mammalian UV response. The EMBO journal *14*, 5338-5349.

Sijbers, A.M., de Laat, W.L., Ariza, R.R., Biggerstaff, M., Wei, Y.F., Moggs, J.G., Carter, K.C., Shell, B.K., Evans, E., de Jong, M.C., Rademakers, S., de Rooij, J., Jaspers, N.G., Hoeijmakers, J.H., and Wood, R.D. (1996). Xeroderma pigmentosum group F caused by a defect in a structure-specific DNA repair endonuclease. Cell *86*, 811-822.

Smerdon, M.J., and Lieberman, M.W. (1978). Nucleosome rearrangement in human chromatin during UV-induced DNA- repair synthesis. Proceedings of the National Academy of Sciences of the United States of America *75*, 4238-4241.

Smerdon, M.J., Lan, S.Y., Calza, R.E., and Reeves, R. (1982). Sodium butyrate stimulates DNA repair in UV irradiated normal and xeroderma pigmentosum human fibroblasts. The Journal of biological chemistry *257*, 13441-13447.

Subramanian, M., Gonzalez, R.W., Patil, H., Ueda, T., Lim, J.H., Kraemer, K.H., Bustin, M., and Bergel, M. (2009). The nucleosome-binding protein HMGN2 modulates global genome repair. The FEBS journal.

Sugasawa, K., Ng, J.M., Masutani, C., Iwai, S., van der Spek, P.J., Eker, A.P., Hanaoka, F., Bootsma, D., and Hoeijmakers, J.H. (1998). Xeroderma pigmentosum group C protein complex is the initiator of global genome nucleotide excision repair. Molecular cell *2*, 223-232.

Sullivan, B.A., and Karpen, G.H. (2004). Centromeric chromatin exhibits a histone modification pattern that is distinct from both euchromatin and heterochromatin. Nature structural & molecular biology *11*, 1076-1083.

Suquet, C., and Smerdon, M.J. (1993). UV damage to DNA strongly influences its rotational setting on the histone surface of reconstituted nucleosomes. The Journal of biological chemistry *268*, 23755-23757.

Szyf, M. (2005). DNA methylation and demethylation as targets for anticancer therapy. Biochemistry (Mosc) *70*, 533-549.

Tjeertes, J.V., Miller, K.M., and Jackson, S.P. (2009). Screen for DNA-damage-responsive histone modifications identifies H3K9Ac and H3K56Ac in human cells. The EMBO journal *28*, 1878-1889.

Tornaletti, S., and Hanawalt, P.C. (1999). Effect of DNA lesions on transcription elongation. Biochimie *81*, 139-146.

Trievel, R.C. (2004). Structure and function of histone methyltransferases. Critical reviews in eukaryotic gene expression *14*, 147-169.

Ueda, T., Postnikov, Y.V., and Bustin, M. (2006). Distinct domains in high mobility group N variants modulate specific chromatin modifications. The Journal of biological chemistry *281*, 10182-10187.

Ura, K., and Hayes, J.J. (2002). Nucleotide excision repair and chromatin remodeling. European journal of biochemistry / FEBS *269*, 2288-2293.

Ura, K., Araki, M., Saeki, H., Masutani, C., Ito, T., Iwai, S., Mizukoshi, T., Kaneda, Y., and Hanaoka, F. (2001). ATP-dependent chromatin remodeling facilitates nucleotide excision repair of UV-induced DNA lesions in synthetic dinucleosomes. The EMBO journal *20*, 2004-2014.

van Hoffen, A., Venema, J., Meschini, R., van Zeeland, A.A., and Mullenders, L.H. (1995). Transcription-coupled repair removes both cyclobutane pyrimidine dimers and 6-4 photoproducts with equal efficiency and in a sequential way from transcribed DNA in xeroderma pigmentosum group C fibroblasts. The EMBO journal *14*, 360-367.

van Steeg, H., and Kraemer, K.H. (1999). Xeroderma pigmentosum and the role of UV-induced DNA damage in skin cancer. Molecular medicine today *5*, 86-94.

Volker, M., Mone, M.J., Karmakar, P., van Hoffen, A., Schul, W., Vermeulen, W., Hoeijmakers, J.H., van Driel, R., van Zeeland, A.A., and Mullenders, L.H. (2001). Sequential assembly of the nucleotide excision repair factors *in vivo*. Molecular cell *8*, 213-224.

Yajima, H., Lee, K.J., Zhang, S., Kobayashi, J., and Chen, B.P. (2009). DNA double-strand break formation upon UV-induced replication stress activates ATM and DNA-PKcs kinases. Journal of molecular biology *385*, 800-810.

Yu, Y., Teng, Y., Liu, H., Reed, S.H., and Waters, R. (2005). UV irradiation stimulates histone acetylation and chromatin remodeling at a repressed yeast locus. Proceedings of the National Academy of Sciences of the United States of America *102*, 8650-8655.

Zhang, Q., and Wang, Y. (2008). High mobility group proteins and their post-translational modifications. Biochimica et biophysica acta *1784*, 1159-1166.

Zhu, N., and Hansen, U. (2007). HMGN1 modulates estrogen-mediated transcriptional activation through interactions with specific DNA-binding transcription factors. Molecular and cellular biology *27*, 8859-8873.

APPENDIX
(LIST OF ABBREVIATIONS)

LIST OF ABBREVIATIONS

6-4 PPs – photoproducts

8-oxo-G – 7,8-dihydro-8-oxoguanine

AAF – amide 2-acetylaminofluorene

Ac – acetyl

Ac-CoA – acetyl coenzyme A

ACF – ATP-dependent chromatin remodeling factor

AT- hook – Adenine-Thymidine hook

ATM – ataxia telangiectasia-mutated

ATP– Adenosine tri phosphate

ATR – ATM and Rad3-related

BrdU – bromodeoxyuridine

BRM – brahma, encodes ATPase subunit

CAF-1– chromatin assembly factor

cAMP– cyclic adenosine monophosphate

CBP – CREB-binding protein

Cdc-25A – cell division cycle

Cdk – cyclin dependent kinase

CENP-A – centromere Protein A

CHD – chromo-helicase/ATPase DNA binding

Chk1/Chk2 – cell cycle checkpoint kinase 1/ 2

CHRAC – chromatin accessibility complex

Co-IP – co-immunoprecipitation

COX-2 – cyclooxygenase 2

CPDs – cyclobutane pyrimidine dimers

CREB – cAMP-response element–binding protein

CS – Cockyane Syndrome

CUL4-DDB-ROC1 – ubiquitin ligase

DDB 1/2 – damaged DNA binding complex

DSB – double strand break repair

DUB – deubiquitinating enzyme

ERCC1 – Excision repair cross complementing protein 1

FACS – fluorescent activated cell sorter

FITC – fluorescein isothiocyanate

GADD45 – growth arrest and DNA-damage-inducible

GCN5 – general control of amino acid synthesis 5 (histone acetyl transferase)

GGR – global genome repair

H1– linker histone

H2/H3/H4 – core histones

H2A.Z – histone 2 variant

H_2O_2 – hydrogen peroxide

H3K14ac – acetylation of histone H3 lysine 14

H3K9ac – acetylation of histone H3 lysine 9

H3K9me3 – trimethylation of histone H3 on lysine 9

H3S10p – phosphorylation of H3 Ser 10

H4K5ac – acetylation of histone H4 lysine 5

HA tag – hemagglutinin tag

HAT – histone acetyl transferase

HDAC – histone deacetylases

hHR23B – human homologue of the yeast protein RAD23B

HMGA – high mobility group AT-hook protein

HMGB – high mobility group box protein

HMGN – high mobility group nucleosomal binding proteins

HMTases – histone methyl tranferases

Hybond N^+ – positively charged nylon membrane

IgG – Immunoglobulin G

IgG (g) – goat Immunoglobulin G

IgG (m) – mouse Immunoglobulin G

IgG (r) – rabbit Immunoglobulin G

IP – immunoprecipitation

I-SWI – Imitation SWItch

LD_{50} – lethal dose

MFA2 – mating pheromone a-factor

Mi-2 – is a part of NURD complex, ATP-dependent chromatin remodeler

N.S. – non significant

NEIL –Nei like-2 protein, a DNA glycosylase/AP lyase specific

for oxidatively damaged bases.

NER – nucleotide excision repair

NHEJ – non-homologous end joining repair

N-terminal – amino terminal

NURD – nucleosome remodeling and deacetylating complex

NURF – nucleosome-remodeling factor

$O_2^{\cdot -}$ – oxygen radical

OGG1 – 8-oxoguanine-DNA glycosylase 1

$OH^{\cdot}$ – hydroxyl radical

P127 – tumor suppressor protein

P21 – cyclin-dependent kinase inhibitor

P300 – E1A binding protein p300

P400 – E1A binding protein p400

P53 – tumor suppressor protein

P53R2 – p53 ribonucleotide reductase-repair protein

PAGE – polyacrylamide gel electrophoresis

PCAF – p300/CBP Associated Factor

PCNA – proliferating cell nuclear antigen

PHD – plant homeo domain

PI – propidium iodide

PK – protein kinase

PTM – post translational modification

RAD 23 – gene of *Saccharomyces cerevisiae* is required

for excision-repair of UV damaged DNA

RNA-Pol II – ribonucleic acid polymerase II

ROS – reactive oxygen species

RPA – replication protein A

Rpd3p – histone deacetylase (yeast)

RSC – ATP-dependent chromatin-remodeling complex (yeast)

SD – standard deviation

SE – standard error

SDS – sodium dodecyl sulfate

SNF – sucrose nonfermenting (yeast)

SRF – serum response factor

STAGA – SPT3-TAF_{II}31-GCN5L acetylase

Suv 39 – histone methyl transferase (murine)

SWI – switching (yeast)

TCR – transcription coupled repair

TF IIH – transcription factor

TFF1 – trefoil factor 1

TLS – translesion DNA synthesis

TSA – trichostatin A(an HDAC inhibitor)

TTD – trichothiodystrophy

USP 1 – ubiquitin specific protease 1

UV– ultraviolet rays

UVC – ultraviolet subtype C

XP – xeroderma pigmentosum

XPA, B, C, D, E, F, G, H – xeroderma pigmentosum protein

GroupA-H-human homolog

ylSWI – yeast Imitation SWItch

Mangalam Subramanian

417 Withers street
Apt # 3
Denton, TX-76201

smangalam_in@yahoo.com

Objective:

- Entry-level position in research/project planning leading to a supervisory position. Long term objective is to qualify for senior management position.

Education:

- Ph. D., Molecular biology, Texas Woman's University. Dissertation title - The role and molecular mechanism of HMGN proteins in global genome repair after UV irradiation (under guidance of Dr. Michael Bergel) — Graduation in **December 2009**

- M. Sc., Microbiology, University of Mumbai, India. Title of thesis - "Synergistic action of aminoglycosides and cephalosporins against multidrug resistant enterobacteria and *Pseudomonas aeruginosa*" — **April 2003**

- B. Sc., Microbiology, University of Mumbai, India — **May 2001**

Papers:

- **Mangalam Subramanian**, Rhiannon W. Gonzalez, Hemangi Patil, Takahiro Ueda, Jae-Hwan Lim, Kenneth H. Kraemer, Michael Bustin and Michael Bergel. The Nucleosome Binding Protein HMGN2 Modulates Global Genome Repair. **FEBS J. — October 2009**

- **M. Subramanian**, R.M. Wold-Gonzalez, L. BeCoats, S. John and M. Bergel. HMGN1 and HMGN2 modulate global histone H3 acetylation post UV irradiation. Manuscript in preparation.

- L. Lawrence, **M. Subramanian** and M. Bergel. High mobility group nucleosomal protein 1 is involved in nucleotide excision repair in human cells. Manuscript in preparation.

- Patil H, Gonzalez R.M, **Subramanian M**, and Bergel M. HDAC-3 and histone H1.3 complex is involved in mitotic regulation. Manuscript in preparation.

Posters/Platform Presentation:

- **M. Subramanian**, S. John, L. BeCoats and M. Bergel: HMGN1/N2 nucleosomal binding proteins are involved in the NER-global genome repair subpathway by both histone acetylation-dependent and histone acetylation-independent pathways. 58th Annual Montagna Symposium of the Biology of Skin: The Genetic-Epigenetic Basis of Skin Disease, Oregon — Platform and poster presented, **October 2009**

- **M. Subramanian**, R. W. Gonzalez, L. Lawrence, S. John, L. BeCoats and M. Bergel: HMGN1/N2 nucleosome binding proteins modulate early and late UV-induced responses. FASEB Summer Research Conference: Epigenetics, Chromatin & Transcription, Snowmass Village, Colorado — Poster presented, **July 2009**

- **M. Subramanian**. HMGN proteins affect global histone post-translational modifications and levels of H1 variants following UV irradiation. TWU Student Creative Arts and Research Symposium — Poster presented, **April 2008**

- **M. Subramanian**. Global chromatin acetylation and deacetylation in response to ultraviolet irradiation of cells. TWU 10th Annual Research and Creative Arts Symposium — Platform presentation, **April 2007**

- **M. Subramanian**, H. Patil and M. Bergel. Cells lacking chromosomal proteins HMGN1a and HMGN2 show increased sensitivity to UV irradiation. Texas Genetics Society, Texas Scottish Rite Hospital for Children, Dallas — Poster presented, **April 2005**

- **M. Subramanian**, H. Patil and M. Bergel. Cells lacking chromosomal proteins HMGN1a and HMGN2 show increased sensitivity to UV irradiation. TWU 8th Annual Research and Creative Arts Symposium — Poster presented, **April 2005**

- **M. Subramanian**, K. Girard, R. Bernal, A. Niv, B. Odhiambo, K. Marsh-West, M. Bustin and M. Bergel. Cells lacking the chromosomal protein HMGN2 or both HMGN1 and HMGN2 demonstrate irregular growth patterns, impaired stress response and deregulated gene expression. TWU 7th Annual Research and Creative Arts Symposium — Poster presented, **April 2004**

Laboratory skills:

Western blotting, Southwestern blot, UV-irradiation of cells, tissue culture, FACS (Fluorescent Activated Cell Sorter analysis), co-immunoprecipitation assay, HDAC assay, HAT assay, preparation of nucleosomes and core histones, worked with radioactive isotope (^{14}C), ChIP assay, DNA cloning techniques, running SDS-PAGE gels (from 5% to 18% gels and running Criterion gels) and agarose gels.

Honors/ Awards/ Scholarships:

- Full member of **Phi Kappa Phi honor** society — **November 2009**

- **Eugene M. Farber Travel Award** for Young Investigators from Society of Investigative Dermatology — **October 2009**

- Nominated and chosen as **"Who's Who among Students in American Universities & Colleges" — November 2005, November 2006, March 2007, March 2009**

- Awarded the **Virginia Chandler Dykes scholarship** for academic excellence and outstanding leadership skills, the College of Arts & Sciences, TWU — **May 2008**

- Awarded the **"Golden Girls Scholarship"** by Former Students Association, TWU — **September 2006**

- Full member of **TriBeta Biological Honor Society — August 2004 onwards**

- **Graduate Assistant** at Department of Biology, TWU: (Teaching assistant for BACT 1001, BACT 3111, BIOL 1021 and study sessions for MOL BIOL 4813) — from **August 2003 to Spring 2009**

Service for the Department/ University/ Community:

- **September 2006 - April 2007** — Member of **TWU Graduate Council** (representative for Doctoral students).

- **September 2006 - May 2007** — Assisted the staff of **Former Student's Association (FSA)** to recruit TWU graduates as members for the FSA.

- **April 2006** — Invited speaker for the **Minority Biomedical Research Support (MBRS)** students, "Graduate school in TWU"

- **October 2005 - May 2006 -** Secretary of Student Health Advisory Committee **(SHAC)**, TWU.

- **April 2005** — Planted trees as a part of **"Keep Denton Beautiful",** a non-profit community organization in Denton, TX.

- **August 2004** — Invited speaker for the **TriBeta Biological Honor Society,** "The life of a Graduate (International) student at TWU".

- Trained undergraduate and graduate students in laboratory skills.

- **February 2004, February 2006, and February 2008 -** Volunteered for **American Association of University Women (AAUW)** "Expanding your horizons" Conference for Middle School Girls at TWU.